TRANSPORT MECHANISM OF METHIONINE IN THE INTESTINAL TRACT OF RAINBOW TROUT (*Oncorhynchus mykiss*)

A Thesis Submitted to the College of
Graduate and Postdoctoral Studies
In Partial Fulfillment of the Requirements
For the Degree of Doctor of Philosophy
In the Department of Veterinary Biomedical Sciences
University of Saskatchewan
Saskatoon

By
Van Pham Thi Ha To

Permission to use

In presenting this thesis in partial fulfillment of the requirements for a Postgraduate degree from the University of Saskatchewan, I agree that the Libraries of this University may make it freely available for inspection. I further agree that permission for copying of this thesis in any manner, in whole or in part, for scholarly purposes may be granted by the professor or professors who supervised my thesis work or, in their absence, by the Head of the Department or the Dean of the College in which my thesis work was done. It is understood that any copying or publication or use of this thesis or parts thereof for financial gain shall not be allowed without my written permission. It is also understood that due recognition shall be given to me and to the University of Saskatchewan in any scholarly use which may be made of any material in my thesis.

Requests for permission to copy or to make other uses of materials in this thesis in whole or part should be addressed to: Head of the Department of Veterinary Biomedical Sciences University of Saskatchewan, Saskatoon, Saskatchewan, S7N 5B4, Canada

OR

College of Graduate and Postdoctoral Studies University of Saskatchewan, 116 Thorvaldson Building, 110 Science Place Saskatoon, Saskatchewan, S7N 5C9, Canada

Abstract

DL-Methionine (DL-Met) and its corresponding hydroxy analogue (DL-MHA) have been increasingly used in animal feeds. In mammalian and avian species, DL-Met is known to be transported by amino acid transporters, while DL-MHA is transported by monocarboxylate transporters. However, the characterization of transporters responsible for transport of these Met products in the fish intestine has not been studied. Therefore, this thesis focuses on understanding the transport mechanism of DL-Met and DL-MHA in different intestinal segments of rainbow trout (*Oncorhynchus mykiss*) using radiolabeled substrates and gene expression.

Firstly, both sodium-dependent and independent DL-Met transport were characterized in Ussing chambers at low (µM) and high concentrations (mM) in triploid and diploid trout intestine at pyloric caeca (PC), midgut (MG), and hindgut (HG) regions. DL-[^{14}C]Met radiolabeled isotope fluxes demonstrated a Na^+-dependent high-affinity (K_m in µM ranges) and low-affinity (K_m in mM ranges) transport mechanism across the intestine, associated with apical ASCT2 and B^0AT1-like transporters at low and high concentrations, respectively. Gene expression detected the presence of transporters y^+LAT1 and LAT4, which might play a role in facilitating re-influx/efflux Met from the basolateral side of intestinal epithelial cells. Secondly, the dependence of DL-MHA transport was investigated in both sodium and proton conditions. The results indicated that there was intestinal segmental segregation of DL-[^{14}C]MHA flux, revealing different transport mechanisms along trout intestine. Specifically, the apical DL-MHA influx was mediated by sodium-requiring systems in all regions, which associated with SMCTs. Basolateral efflux in PC and MG regions seemed to be proton-independent, but basolateral efflux in HG tended to be proton-dependent, which associated with MCT9 and MCT1, respectively. Thirdly, the transport rates of radioisotopic DL-Met and DL-MHA were compared to partially explain the effectiveness

of the use of these Met sources in animal feeds. The comparison showed that DL-Met flux rates were significantly higher than DL-MHA throughout the intestinal segments at both low and high concentrations in physiological conditions. This probably has economic implications in selecting a suitable Met form to supplement in fish diets.

Overall, DL-Met and DL-MHA transport in trout intestine followed different pathways along the intestinal tract. Similar to mammals, the transport of both Met substrates were dependent on sodium. In addition, DL-Met transport was more efficient than DL-MHA. These findings are of importance from both a physiological and nutritional perspective.

Acknowledgments

The completion of this thesis would not be possible in four years without the guidance and support of many individuals. It is my great pleasure to thank and acknowledge those who have contributed to this thesis.

First of all, I would like to express my sincere thanks to my supervisor, Dr. Matthew Loewen, for giving me the opportunity to do research in his lab and his valuable advice throughout my Ph.D. program. I value his mentorship and necessary suggestions to overcome challenges throughout the course of my research project. I have learned a lot about his positive attitude. His constant support and patience mean a great deal to me.

I want to extend my gratitude to my committee members. I greatly appreciate Dr. Lynn Weber and Dr. Denise Beaulieu, for their intellectual comments and recommendations to improve my thesis. Their academic credentials and sincerity have deeply inspired me. I wish to thank Dr. George Forsyth for his brilliant thoughts and questions to better this study during his time in the advisory committee. My heartfelt gratitude to Dr. Adelaine Leung for her timely participation in the advisory committee helping me to finish thesis. I'd also like to extend my appreciation to my graduate chairs Dr. Suraj Unniappan and Dr. Ali Honaramooz, for always making themselves available whenever I need help and information.

A special thanks to Dr. Marina Subramaniam, Dr. Khanh Luu, and Dr. Cole Enns, who teach me the methodology to conduct experiments and the way to present data as clear as possible. I also want to thank other lab members Brandon Keith, Gagan Kolimadu, Nitin Challa, and Akarin Asavajaru. They have given me a lot of assistance during the course of my study.

Finally, thank my family and Randell and Nina Goodman for their endless love and spiritual supports. I am thankful for their constant prayers every step of the way.

Table of contents

List of tables

List of figures

List of abbreviations

BBMV	brush border membrane vesicle
BCH	bicyclo[2.2.1]heptane-2-carboxylic acid
BCKDC	branched-chain alpha-keto acid dehydrogenase complex
Caco-2	colon adenocarcinoma cells
CBS	cystathionine β-synthase
cDNA	complementary deoxyribonucleic acid
CFU	colony forming units
CGL	cystathionine- ɤ -lase
cRNA	complementary ribonucleic acid
D-AAOX	D-amino acid oxidase
DBDS	4,4′-dibenzamidostilbene-2,2′-disulphonate
dc-SAM	decarboxylated S-adenosylmethionine
D-HADH	D-2 hydroxy acid dehydrogenase
DIDS	4,4′-diisothiocyanostilbene-2,2′-disulphonate
EAA	essential amino acid
EFα1	elongation factor 1 alpha
GI	gastrointestinal
HG	hindgut
HPLC	high-performance liquid chromatography
IBMX	3-isobutyl-1-methylxanthine
I_{sc}	short circuit current
J_{max}	maximal flux rate
J_{ms}	mucosal to serosal flux
K_m	half-saturation constant
KMB	2-keto 4-methylthiobutanoic acid
L-HAOX	L-2 hydroxy acid oxidase
MAT	methionine adenosyltransferase
MCM	methylmalonyl-CoA mutase
MCT	monocarboxylate transporter

MeAIB	2-(methylamino) isobutyric acid
Met	methionine
MG	midgut
MHA	methionine hydroxy analogue
mRNA	messenger ribonucleic acid
Mtase	methyltransferase
NCBI	national center for biotechnology information
NEM	N-ethylmaleimide
PC	pyloric caeca
PCC	propionyl-CoA carboxylase
pCMBS	*p*-chloromercuribenzene sulphonate
RT-qPCR	reverse transcription quantitative polymerase chain reaction
SAHH	S-adenosylhomocysteine hydrolase
SAM DC	S-adenosylmethionine decarboxylase
SAM	S-adenosylmethionine
SCFA	short chain fatty acid
SMCT	sodium monocarboxylate transporter
TCA	tricarboxylic acid cycle
THF	tetrahydrofolate
V_{max}	maximal current rate

CHAPTER I
INTRODUCTION

1.1. Rationale

Fisheries and aquaculture are important components of food security. Since the 1980s, wild capture fisheries production has remained relatively steady, while aquaculture production has increased tremendously over the past few decades contributing more than half of the global seafood supply (109). Commercial feed plays a critical role in the success of modern aquaculture. Traditionally, the fish feed industry heavily relies on fish meal as the major protein source, an expensive and not sustainable protein ingredient. Thus, terrestrial plant-derived ingredients have been increasingly used in aquafeeds to reduce the aquaculture industry's reliance on fishmeal. The challenge of this approach is that plant-based proteins typically do not have a balanced amino acid profile. As one of the first limiting essential amino acids (EAAs) in plant-based diets, methionine (Met) is often supplemented to ensure the adequate nutritional requirement of fish. Met supplementation is typically achieved using DL-Methionine (DL-Met) or DL-Methionine Hydroxy Analogue (DL-MHA). The relative bioefficacy between these two Met sources has been compared in a wide range of species. *In vivo* studies in poultry (99, 172, 209, 300, 390), pigs (113, 194, 288, 448) and fish (192, 319, 332) have demonstrated that bioefficacy of DL-Met is considerably higher than that of DL-MHA. However, there are several studies indicating that DL-MHA is as effective as DL-Met (136, 201, 325). A possible reason for the varying results in effectiveness between DL-Met and DL-MHA is that each species may have different transport pathways associated with these Met sources in the gastrointestinal (GI) tract, which may be altered under different experimental conditions. In mammals, it has been reported that DL-Met transport in the GI tract could be facilitated by both sodium-dependent and sodium-independent transport

systems, which involves multiple transporters (39, 367, 393, 445). However, a proton-dependent monocarboxylate transporter (MCT) is predicted to be responsible for DL-MHA absorption since the chemical structure of DL-MHA is relatively similar to monocarboxylate compounds or short-chain fatty acids (SCFAs) (245, 445). Such understandings in fish are largely lacking. Therefore, understanding the mechanism behind the intestinal transport of DL-Met and DL-MHA in fish will likely make it possible to explain the differences in bioefficacy between two products, which also contributes to the current knowledge in fish nutrition and physiology. The overall objective of this thesis is to characterize the transport pathways of DL-Met and DL-MHA in rainbow trout intestine using radioactive isotopes under *ex-vivo* conditions.

1.2. Objectives

1. Characterize sodium-dependent DL-Met transport in the intestinal tract of rainbow trout using Ussing chamber and gene expression analysis.
2. Characterize proton-dependent DL-MHA transport in the intestinal tract of rainbow trout using Ussing chamber and gene expression analysis.
3. Compare the transport kinetics between DL-Met and DL-MHA by reanalyzing data obtained from the mentioned objectives.

1.3. Hypotheses

1. DL-Met transport is sodium-dependent, and there are segmental differences in DL-Met transport along the intestinal tract of rainbow trout.
2. DL-MHA transport is proton-dependent, and there are segmental differences in DL-MHA transport along the intestinal tract of rainbow trout.
3. DL-Met is transported with higher affinity and rate than DL-MHA in rainbow trout intestine.

CHAPTER II

LITERATURE REVIEW

2.1. Aquaculture and methionine supplementation in plant-based diets

2.1.1. Aquaculture and the use of plant-based diets

Aquaculture is one of the most rapidly growing sectors of the food industry. FAO (107, 108) estimates that global food fish aquaculture production increased from 32.4 million tons in 2000 to 80 million tonnes in 2016. The rapid increase of fish production is mainly due to the expansion of intensive farming systems in which commercial feeds are fed as the major nutrient source for cultured animals. High dependence on commercially formulated feed in intensive farming models generates economic and environmental concerns. Economically, feed typically accounts for more than 50% of the total production cost, which is the primary factor in determining the profitability of farm operation. Environmentally, aquaculture is often criticized due to the inefficient uses of fishmeal. Therefore, a cost-effective and sustainable aquaculture industry is highly desirable. In order to reduce the cost per protein unit, studies have focused on substituting fishmeal with alternative protein sources. Plant-origin protein sources such as soybean meal (SBM) have feasibly shown to replacing the inclusion of fishmeal to great extents. However, the deficiency of essential amino acids (EAAs) and the presence of anti-nutritional factors are the major constraints that limit the full replacement of plant-based protein ingredients in practical diets. The adverse influences of high dietary inclusion of SBM have been reported in several studies: increasing mortality and reducing growth performance (335); lower feed intake, weight gain and protein efficiency ratio (447); decreasing nutrient digestibility and AA uptakes due to shorter microvilli of the brush border membrane (8, 53) and reduction in digestive enzymes, carrier-mediated transporters and ability to reabsorb the endogenous digestive secretion (81, 204,

281). These may imply that although dietary changes could be adapted over time, carnivorous fish are still inherently more capable of digesting protein and absorbing AAs than digesting carbohydrate and absorbing glucose. Thus, supplementation of synthetic AAs in plant-based diets is widely practiced to ensure nutrient balance when shifting from animal-based diets to plant-based diets in carnivorous fish.

2.1.2. Supplementation of different types of methionine sources in plant-based diets

Methionine (Met) is an essential amino acid (EAAs) that donates a methyl group for numerous activities of cellular metabolism and protein synthesis, which ensures normal growth and physiological functions (50, 223, 258). It is also one of the first limiting EAAs in plant-based protein ingredients (11, 23, 319). The dietary Met requirement for rainbow trout is about 0.59-0.67% (7), or between 0.8-1.1% of diets when expressed as total sulfur amino acid (TSAA: methionine + cysteine) (283). The formation of cataracts is one of the unique indicators in rainbow trout fed Met-deficient diets (318, 421). Imbalance of dietary Met has been shown to influence feed intake, transcriptional gene regulation, protein turnover, growth performance and mortality in several fish species (20, 79, 103, 260, 360, 397). Thus, Met is often supplemented in plant-based diets to ensure the normal development of fish. Commercially, dietary Met supplementation is commonly obtained using chemically synthesized DL-methionine (DL-Met) or DL- 2-Hydroxy-4-methylthiobutanoic acid (DL-MHA) in which an amino group (NH_2) is replaced with a hydroxyl group (OH) (10). A large number of studies have compared the bioefficacy between the two products. However, disagreements still remain within and among species. For instance, the bioefficacy of DL-MHA was reported to be only about 57-69% on the product-product (wt/wt) basis (83, 172, 236, 300, 405) in poultry, and 64-71% in swine (194, 288, 358) in comparison to DL-Met. Similar conclusions were also made in different fish species (191, 192, 317, 319, 331).

Conversely a few studies indicate that DL-MHA could equally support animal growth (136, 201, 325), causing controversy. The differences in bioefficacy between DL-Met and DL-MHA could be due to the dissimilarity in metabolism pathway and transport system involved in these two Met sources.

2.2. General background of methionine

2.2.1. Methionine metabolism pathways

Methionine (Met) is a non-polar, sulfur-containing AA (CH_3-S-CH_2-CH_2-CH(NH_2)-COOH) that was originally discovered from casein in 1922 by Mueller (416); its chemical formula was described as ɤ-methylthiol-α-aminobutyric acid in 1928 by Barger and Coyne (416). Despite its late discovery, Met has received great attention since it serves as the initiating AA for nearly all eukaryotic protein synthesis (44, 370). This EAA participates in several fundamental biological processes, including protein biosynthesis, methyl donor, formation of polyamines, cysteine synthesis and other important metabolites (116).

Met metabolism (Figure 2.1) is a complex process that involves several metabolic and synthetic pathways of Met and its intermediate metabolites. The Met metabolism cycle includes four main steps, which are briefly described as follows: (I) Met metabolism begins with the conversion of L-Met into S-adenosylmethionine (SAM, aka AdoMet and SAMe) by using ATP and methionine adenosyltransferase (MAT) enzymes, creating a high energy molecule which energetically favors the transfer of a methyl group on to other molecules. Three separate forms of MAT (MAT-I, MAT-II, MAT-III) have been identified in mammalians, which differ in kinetic properties and tissues distribution although all forms could catalyze the same reaction (116). MAT-III (high K_m isoenzyme) is exclusively found in the liver which may allow this organ to adapt rapidly to excess Met supply (116). In transmethylation, SAM donates a methyl group for a wide

range of receptors such as nucleic acids, phospholipids, and protein; subsequently used for over 100 methylation reactions (248). For example, SAM offers the methyl group not only in the production of essential bio-molecules such as carnitine (fatty acid oxidation), epinephrine (neurotransmitter and hormone), melatonin (circadian rhythm regulator), phosphatidylcholine (membrane function); but also in epigenetic modulations of DNA methylation and gene expression (361, 438, 443). Additionally, SAM is also involved in the biosynthesis of polyamines. The synthesis process is achieved by converting SAM into decarboxylated *S*-adenosylmethionine (dc-SAM) by SAM decarboxylase. The aminopropyl groups of dc-SAM is then catalyzed to form polyamines such as spermine and spermidine which play an essential role in the activity of ion channels, the structure of nucleic acids and cell proliferation (301, 302). The concentration of dc-SAM in mammalian tissues is about 1-5% of the total available SAM (168, 248). (II) SAM is then converted into S-adenosylhomocysteine (SAH) via methyltransferase reactions. (III) S-adenosylhomocysteine hydrolase (SAHH, aka AHCY) enzyme hydrolyzes SAH into homocysteine. (IV) At this point, homocysteine can be then either remethylated to form Met or entered transsulfuration pathway to form cystathionine.

In the remethylation cycle, homocysteine could be converted back to Met using methionine synthase (MS, also called methylfolate-homocysteine methyltransferase (MFMT)) and betaine-homocysteine methyltransferase (BHMT). The MS enzyme uses N^5-methyl-Tetrahydrofolate (N^5-methyl-THF) as the methyl donor and requires vitamin B12 (in the form of methylcobalamin) as a cofactor, which occurs in all mammalian tissues; whereas BHMT enzyme employs betaine as the methyl donor and is mainly present in the liver (117, 118). In case of B12 deficiency or starvation, folate will become “trapped” at N^5-methyl-THF. The level of N^5-N^{10} methylene-THF is reduced, which causes hyperhomocysteinemia and decreases nucleic acid synthesis since Met is

preserved for methyl transfers of essential metabolic molecules to maintain life (9, 173). For transsulfuration, homocysteine is metabolized to form cystathionine using cystathionine β-synthase (CBS) enzyme and in the presence of vitamin B6 as an obligate cofactor and serine. Cystathionine, in turn, is converted to α-ketobutyrate and cysteine by cystathionine-ɤ-lase enzyme (CGL) (118, 248). Once α-ketobutyrate enters the mitochondrial matrix, branched-chain alpha-keto acid dehydrogenase complex (BCKDC) transforms α-ketobutyrate to propionyl-CoA which is catalyzed into methylmalonyl-CoA through carboxylation by propionyl-CoA carboxylase (PCC) (49, 430). Through methylmalonic acid production using methylmalonyl-CoA mutase (MCM-a vitamin B12-dependent enzyme), methylmalonyl-CoA is then transformed to succinyl-CoA to be further used in the TCA cycle producing energy and AAs (381, 433). Finally, cysteine can be used for protein synthesis. It is also an important precursor for synthesizing other AAs and metabolites such as taurine, glutathione and inorganic sulfates (329, 346)

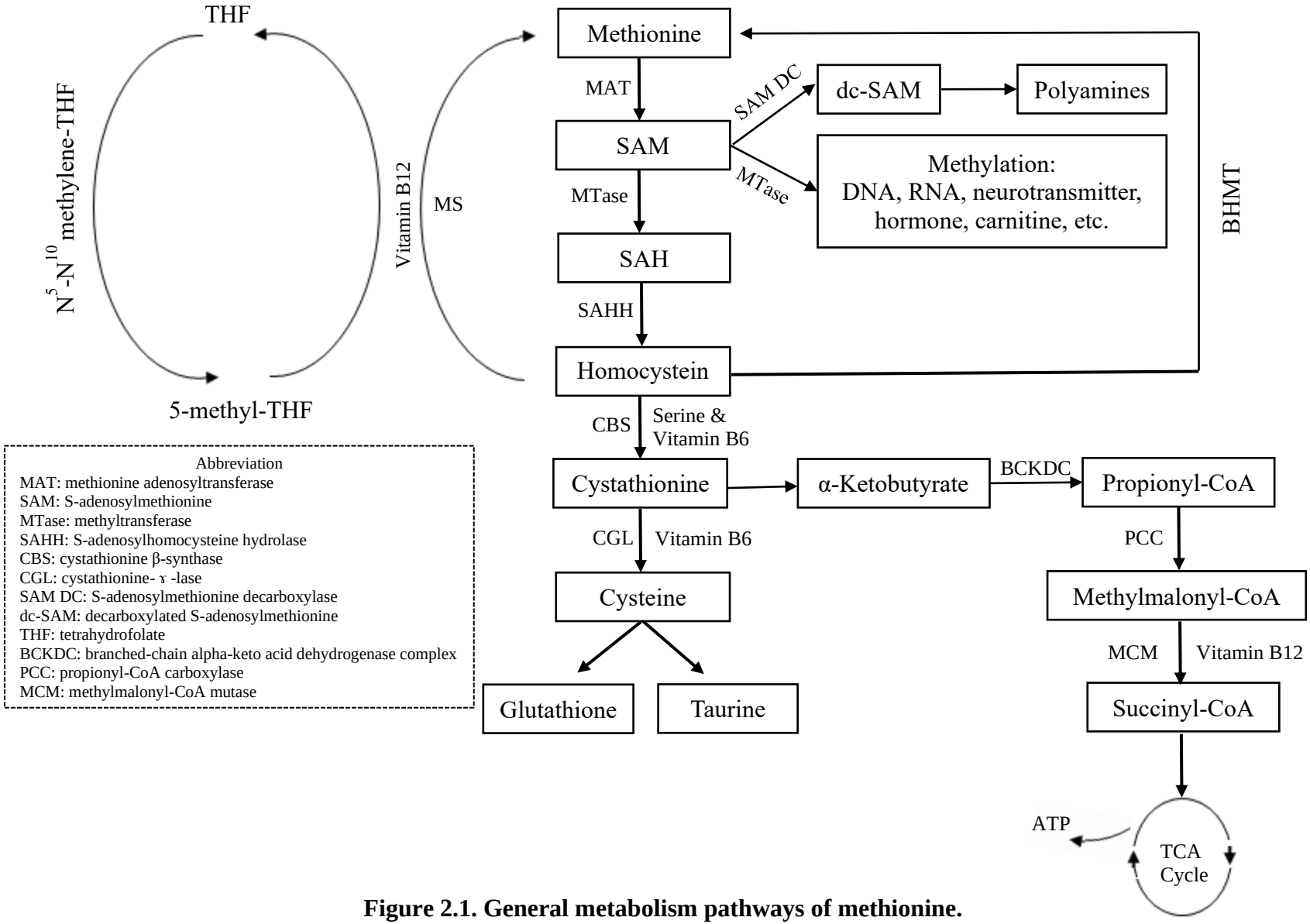

Figure 2.1. General metabolism pathways of methionine.

2.2.2. Metabolism pathways of DL-Met and DL-MHA and intestinal microbial metabolism

Once absorbed, the active form L-Met can be directly incorporated into protein, while D-Met or DL-MHA needs to be converted into L-Met in a two-step process with different enzymes required (90) (Figure 2.2). The first step involves in the conversion of D-Met or DL-MHA into 2-keto 4-methylthiobutanoic acid (KMB): D-amino acid oxidase (D-AAOX) is needed for D-Met, while D-2 hydroxy acid dehydrogenase (D-HADH) and L-2 hydroxy acid oxidase (L-HAOX) are needed for D- and L- MHA, respectively. The second step is the attachment of an amine group to form L-Met via transamination.

Microflora is made of a diverse and large number of microbial species in the GI tract of animals. The composition and metabolic activities of intestinal microflora have been increasingly studied because of its important influences on nutrient metabolism and immune functions of host animals (66, 120, 175). Although gut microbes may support digestion and benefit the immune system, they may compete with the hosts for nutrients and/or potentially convert nutrients into non-absorbable products. The level of crude protein, protein sources and AA composition of protein sources are essential elements in determining the quantity and quality of the intestinal microbial community by providing preferential substrates for microflora (94, 170). Several studies have shown that Met could be used by microbes which tend to prefer DL-MHA to L-Met and DL-Met. For example, Yokota and Coates (439) reported that the absorption of L-[^{3}H]-Met per gram intestinal tissue was higher in germ-free than in conventional and monoassociated chicks. Malik (234) found that the lactobacilli population was significantly greater in digesta for the pigs fed DL-MHA (6.22 CFU/g) compared to the DL-Met group (5.63 CFU/g). This means the longer DL-MHA remains in the intestinal tract, the more it is exposed to microbial degradation and/or being converted into non-absorbable compounds. Maenz and Engele-Schaan (231) showed that about

12% of DL-MHA was converted into non-absorbable by-products in the chicken intestine, which was likely attributed to microbial activity. Likewise, Drew and co-workers (95) demonstrated that the residual ^{3}H-labeled-DL-MHA activity remained in the distal ileum of conventional broilers (10.2%) was greater than that of germ-free broilers (4.7%), whereas no significant difference in ^{3}H-labeled-L-Met between germ-free and conventional broilers.

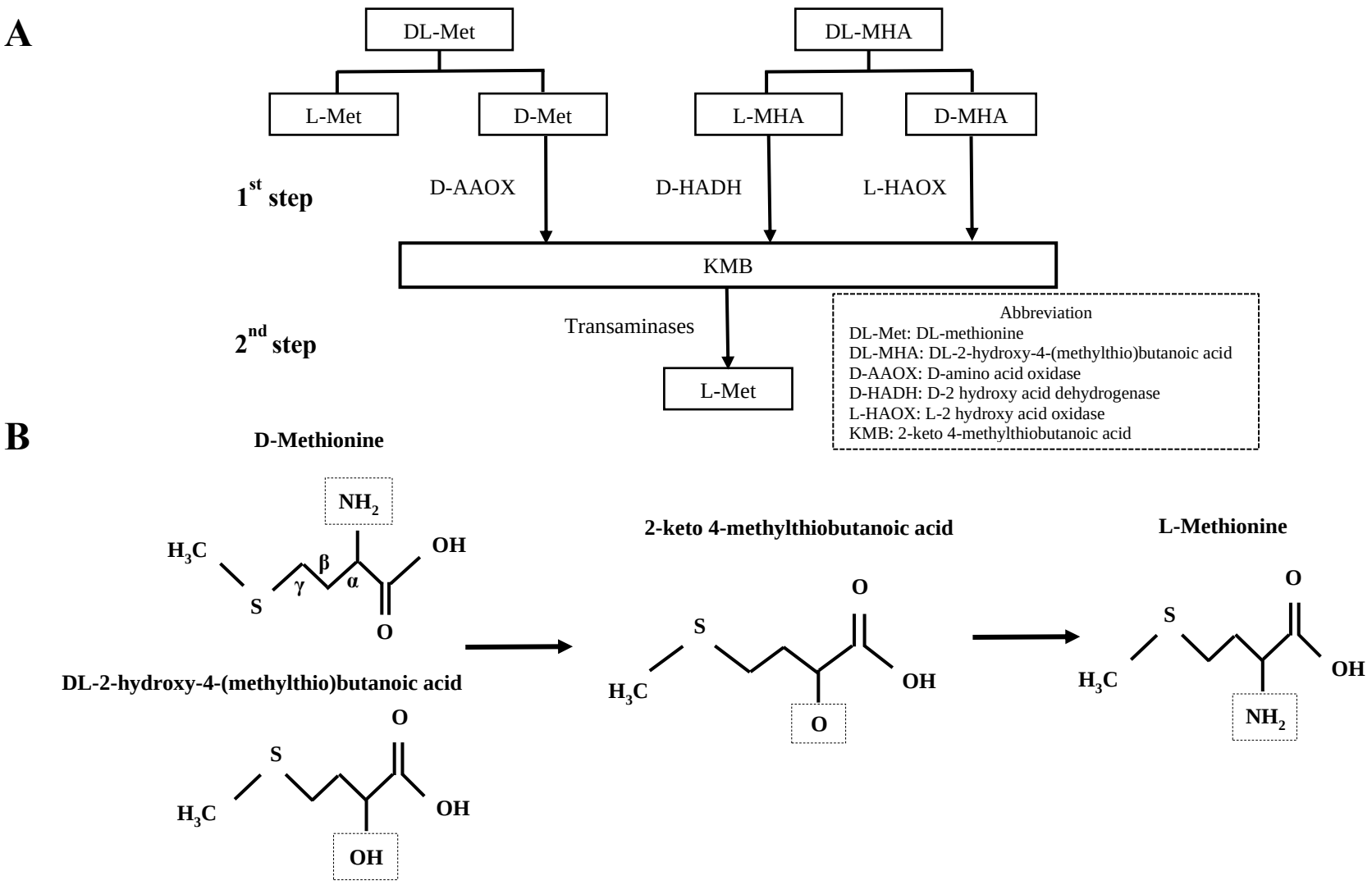

Figure 2.2. Metabolism pathways of DL-Met and DL-MHA

A) Two-step conversion of D-Met and D- or L-MHA to L-Met and **B)** their chemical structures.

2.3. Common *in vitro*/*in situ*/*ex vivo* methods to study nutrient transport

2.3.1. *In vitro* methods

Using *in vitro* techniques to study intestinal transport has some advantages such as less expensive, less labor-intensive, no animal ethical concern and more controllable environment than *in vivo* techniques. The common limitation of *in vitro* methods is that physiological factors such as blood vessels, enzymes, pH, and intestinal transit rates are not included in data interpretation.

2.3.1.1. *Xenopus laevis* oocyte

Oocytes are widely used as a tool for injecting genetic material and defining the functional transport properties of expressed proteins. It is considered a standard method to study the kinetic functions of a transporter. The general protocol includes: (i) isolating mRNA, (ii) generating cDNA library, (iii) converting cDNA pools into cRNA pools, (iv) injecting cRNA pools into oocyte cytoplasm for translating into protein, (v) confirming expression of the protein with immunofluorescence microscopy, and (vi) studying functional transport of proteins by measuring the activity of radioactive isotopes, or electrophysiological changes (242, 261). Detail of measuring transport of radiolabeled substrates using oocytes are described by Baltz et al. (15). In brief, oocytes are incubated with media containing the radiolabeled compounds that are substrates for transmembrane transporters for a precise period. The labelled compound outside of the cell is carefully washed out. The intracellular amount of the labelled compound is quantified using scintillation counting, followed by determining transport kinetics and characteristics. To study electrophysiological properties, oocytes membrane potential induced by ionic movements could be observed using several techniques such as single electrode recording, whole-cell voltage clamping with two electrodes, and macro-patch recording (46, 137).

2.3.1.2. Cellular model

Human-derived intestinal cell lines are valuable tools to examine nutrient absorption and pharmacokinetics. Similar to intestinal columnar absorptive cells, human colon adenocarcinoma cells (Caco-2) are widely used as an *in vitro* model to define the transport characteristics of substances since it possesses several valuable morphological and functional properties including tight junctions, presence of brush border enzymes and nutrient transporters (169, 314). In general, Caco-2 cells are cultured in Transwell filter insert (polycarbonate membrane) for about 20 days (259). After reaching confluence, the mature enterocytes form a distinct apical and basolateral membrane and tight junctions. Before performing a transport study, transepithelial electrical resistance (TEER) is measured to ensure the formation of tight junctions and the integrity of cell monolayers. The Transwell inserts are then placed into the transport medium. The transport studies are initiated by replacing the transport medium in the apical (or basal) side with the radioactively-labelled substrate dissolved in the identical transport medium. Samples are withdrawn from the basal (or apical) side. The absence of mucus is one of the limitations of the Caco-2 monolayer model. Therefore, co-cultures of Caco-2 with mucus-secreting cells HT29-MTX have been developed. Caco-2 and HT29-MTX cells are mixed and cultured with a specific ratio. The culture conditions and permeability study performed are similar to Caco-2 cell monolayers.

2.3.1.3. Brush border membrane vesicles (BBMV)

The epithelial cells are made of apical and basolateral membranes. The apical membrane (aka brush border membrane, BBM) is covered with microvilli of epithelial cells. Under well-controlled *in vitro* conditions, isolation of vesicles derived from the apical and basolateral plasma membranes makes it possible to characterize some transport systems. In an effort to overcome drawbacks in studying intestinal transport using isolated intestinal cells, the use of BBMV was

introduced in the early 1960s. With pure BBMV, transport properties could be investigated without the interference of the transport from the lateral-basolateral membrane (176). The method used to isolate intestinal BBMV is based upon the principle of divalent cation precipitation which results in the coalescence of cytoplasmic organelles (61). The success of isolation procedure could be evaluated by comparing the enrichment level of BBM marker enzymes (e.g. alkaline phosphatase, sucrase) and the contamination level of the basolateral membrane (e.g. Na^+/K^+-ATPase) in final vesicle suspension and the original homogenate. After confirming the purity, BBMV could be used for tracer flux measurement with rapid filtration technique, which is described in detail by Turner (399). Briefly, the technique involves three main steps: 1) the vesicles are incubated in a medium containing a radioactively-labelled tracer and other components as required, 2) a "stop solution" is added at a specific time interval, and 3) the vesicles are collected on a filter, washed and counted for radioactivity.

2.3.2. *In situ* methods

In situ approaches overcome several physiological limitations of *in vitro* approaches since blood vessels, endocrine enzymes and membrane integrity are preserved.

2.3.2.1. Intestinal perfusion

Since the 1950s-1960s, intestinal absorption of water, electrolytes and nutrients has been estimated using perfusion methods (80, 144, 342). The technique is also widely used to study intestinal drug permeability in rodents, which has been introduced and studied with various modifications, including single-pass perfusion (225), recirculating perfusion (341), oscillating perfusion (348), and the closed-loop Doluisio perfusion (92). Although models are slightly different from each other, the general experimental procedure is similar and described in previous studies (82, 105, 224). Firstly, fasted animals are anesthetized and isolated intestinal segments are

rinsed with an appropriate buffer. Secondly, the perfusion solution containing a known concentration of a drug or a substance of interest is perfused into the intestine at the desired rate controlled by a peristaltic pump. To evaluate the viability of intestinal segments during the experiment, non-absorbable inert markers (e.g. phenol red or ^{14}C-labeled PEG-4000), glucose and antipyrine are included in the perfusion solution for later assessment of water flux, active transport and passive transport, respectively. The perfusate is then collected at predefined time intervals for calculation of the effective permeability coefficient (P_{eff}).

Although the *in situ* technique is the nearest to the *in vivo* system, it still has some limitations. For example, the absorption rate can be greatly decreased due to the reduction of intestinal blood flow caused by anesthesia and intestinal surgery (400). The central principle of the perfusion method is that the substance concentration of interest in the perfusion solution reduces over time when passing through the intestinal tract, which is attributed to intestinal absorption. The technique relies on the disappearance of test substances from the intestinal lumen as an indicator of absorption rather than the appearance of test substances in the serosal side (13). However, measuring the reduction of substance concentration in the perfusate does not always reflect the accurate arrival of the substance in the vessels, particularly for substances that undergo pre-systemic or intracellular intestinal metabolism (19).

2.3.2.2. Intestinal perfusion with the mesenteric blood sampling method

As introduced earlier, the intestinal perfusion technique allows us to measure the disappearance of the test compound from the perfusion solution (effective permeability). However, the prediction of the amount that appears in the blood circulation could be misleading due to intestinal metabolism or non-specific binding of the test compound to the isolated intestinal segments. Therefore, intestinal perfusion along with mesenteric blood sampling makes it possible

to measure the appearance of the test substance in the blood (apparent permeability), which results in better insights about the drug/nutrition absorption mechanism. Along with the basic experimental set-up of classical intestinal perfusion, mesenteric vein or portal vein near the liver may be cannulated, and blood samples are collected at fix time intervals for calculating the apparent permeability (373).

2.3.3. *Ex-vivo* methods

Ex-vivo methods imply experiments that are performed on tissues in an artificial milieu with minimum modification of natural conditions of animals. In comparison, studying nutrient transport using the *ex-vivo* method involves in advantages of both *in vitro* and *in situ* approaches.

2.3.3.1. Everted intestinal sac

The intestinal sac method was originally developed by Wilson and Wiseman (428). The preparation is simple and effective to study nutrient and drug absorption. In brief, excised intestine segments are placed over a glass/stainless steel rod and everted. The everted intestinal are tied off with thread ligatures to form sacs. The sac is filled with the appropriate buffer. The empty sac and filled sac are weighed, and the increase in weight is considered the initial volume. The filled sac is transferred into the incubation buffer containing a test substrate or drug. At the end of experiment, the final volume in the sac is determined by weighing the sac before and after draining the fluid. The differences between the initial and final volume will be used to determine the transference direction of the test substance: positive transference values indicate the transport of the substance from mucosal to serosal side, while negative values indicate the transport from serosal to mucosal (428). The major advantages of using everted intestinal sac are: 1) the transport across the apical and basolateral membrane could be independently evaluated, (2) buffer inside and outside sacs could be removed/changed at ease (219). However, the technique still has some

limitations such as tissue viability and high passive diffusion. The histological evaluation shows that 50-75% of the normal epithelium has disappeared after 30 min incubation at 37^0 C (210).

2.3.3.2. Ussing chamber

The method was first introduced by Hans H. Ussing and Zerahn in 1951 when measuring active sodium transport across the frog skin (401). The principle idea is to study the transport properties of ions, nutrients and drugs across intestinal epithelium between Lucite half-chambers (Figure 2.3). There are two major applications of the technique including measurement of total ionic currents across the epithelium (short-circuit current, I_{sc}) and radioactively-labelled substrate flux. The basic protocol is described as follows. Excised intestinal tissues are mounted as a flat sheet between the buffer-filled chambers. The physiological buffer could be modified depending on species. The buffer is oxygenated, and temperature is maintained with a heating water jacket attached around the chamber.

In a classic experiment of I_{sc} measurement, the bathing buffer is identical in both chamber reservoirs, resulting in the same electrical potential. The spontaneous potential difference between the two sides could be eliminated with a computer-controlled voltage-clamp apparatus. The change in I_{sc} (net active ions transports, measured as $\mu A/cm^2$) is continuously recorded by voltage/current Ag-$AgCl_2$ electrodes via 3M KCl agar bridges. In a general setting, a movement of a cation (anion) from the mucosal to the serosal direction or an anion (cation) from the serosal to the mucosal direction would result in positive (negative) changes in I_{sc}.

Isotopic flux measurement is the other important application of Ussing chamber. The basic set up is similar as described earlier. However, using radioisotopic tracers to measure the electrolytes or substrates across the epithelium requires some additional steps. After tissues are loaded into the chambers, about 0.5-1.0 μCi/ml isotopes are added to the “source” side, aka “hot

or donor" side. 30-60 min equilibration is necessary to allow isotopic flux to get stead-state. Flux period is carried out by sampling the "sink" side, aka "cold or receiver" side. An identical volume of fresh bathing buffer is replaced after each sampling. Radioactivity could be determined using Geiger counters, scintillation counters, and solid-state detectors depending on isotope used.

After considering the advantages and limitations of each of the different methods, the use of Ussing chamber, an *ex-vivo* method, is chosen as an effective approach to study methionine transport in the current thesis.

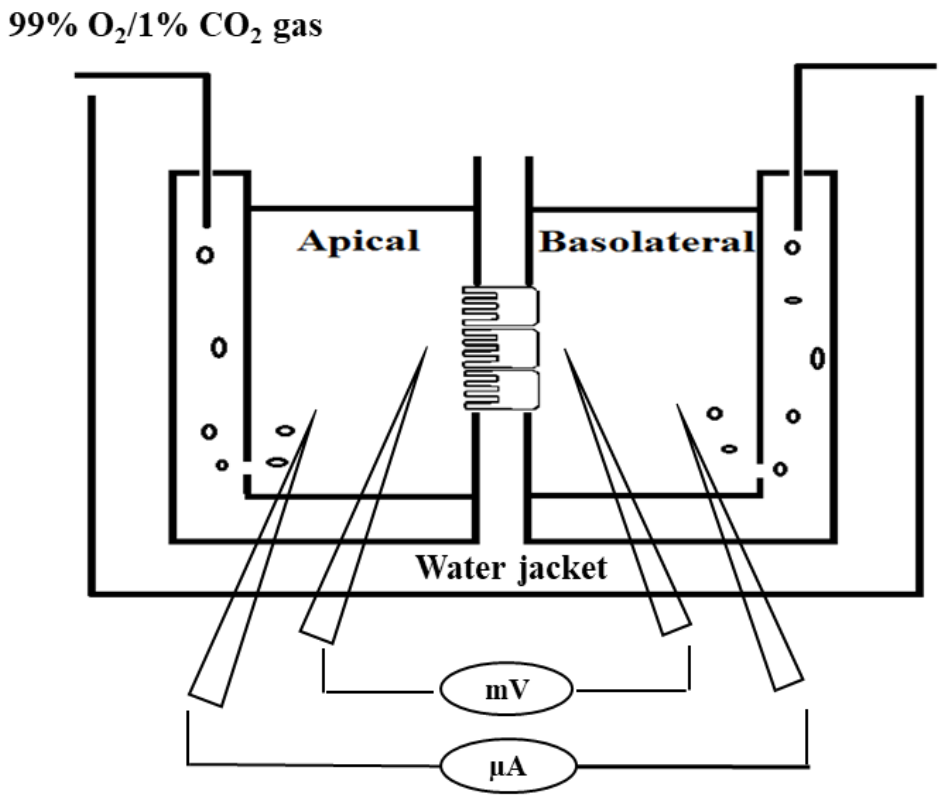

Figure 2.3. Measurement of nutrient transport across intestine using Ussing chamber.

2.4. Nutrient transport in the gastrointestinal tract

2.4.1. Structure of fish gastrointestinal tract

Structural and functional characteristics of the fish GI tract are vastly diverse among species due to the diversity of habitats and feeding habits. Structurally, the intestine is divided into three different segments: proximal intestine, mid and distal intestine (hindgut). In several fish species, there are finger-like projections that extend from the proximal intestine, called pyloric caeca or intestinal caeca (Figure 2.4). Original thoughts suggested that the function of pyloric caeca was to store and ferment food, but its role has more recently been correctly identified as important for nutrient absorption and osmoregulation (47, 77, 411). According to Ferraris and Ahearn (115), the length of fish intestine is shorter in carnivores (meat-eaters) than in herbivores (plant-eaters) and omnivores (flexible eaters). This divergence probably results from the differences in nutrient density and digestibility of food groups. While meat is rich in energy and highly digestible, most plant-based food contains a high percentage of difficult-to-digest materials such as fibre and cellulose. Hence, the longer intestine may allow the digesta to stay longer in the GI tract, which could improve the digestion and absorption in herbivorous fish. Whereas, increasing the absorptive surface area of pyloric caeca is an effective strategy to enhance nutrient absorption in carnivorous fish with shorter intestine (48).

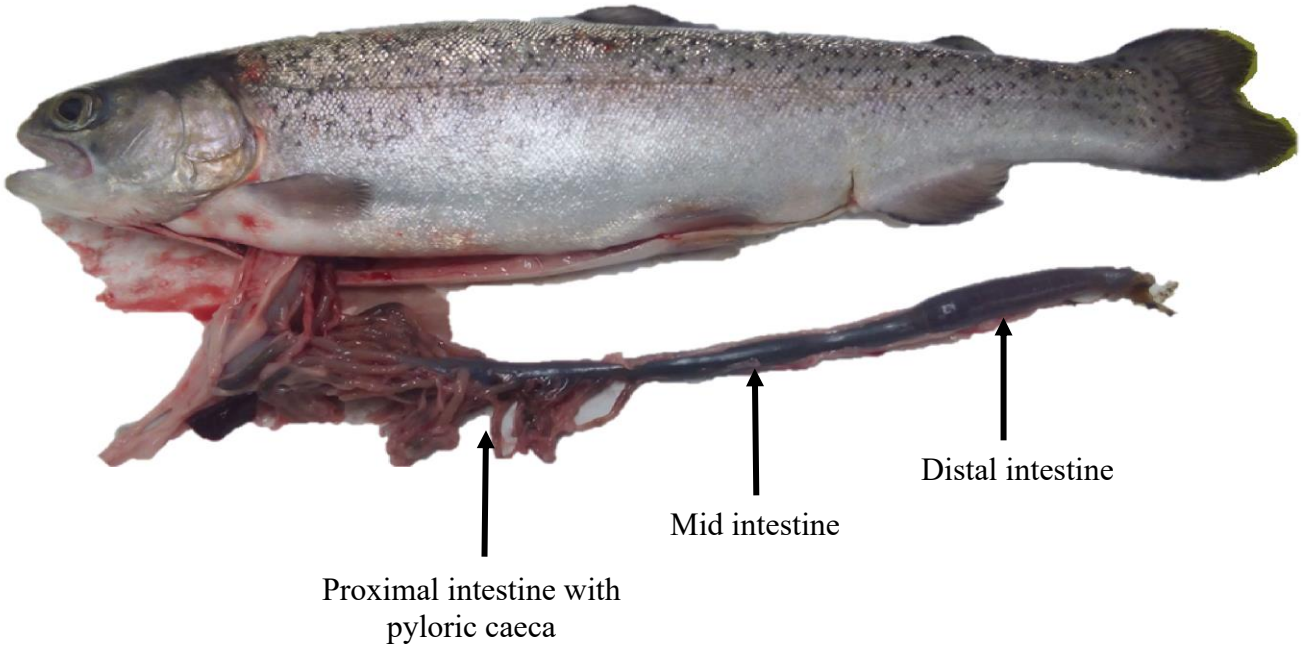

Figure 2.4. Intestinal segments of rainbow trout.

Intestinal histology of teleost fish has been described in several species including *Esox Zucius L*. Pike (45), *Prochilodus scrofu* (272), *Danio rerio* zebrafish (420), *Oncorhynchus mykiss* rainbow trout (193), topmouth culter *Culter alburnus* (56), and *Schizodon knerii* (338). Basically, the intestinal wall is composed of three main layers: mucosa (including epithelium and connective tissue lamina propria), muscularis (including circular and longitudinal smooth muscle), and serosa. The mucosa is an important layer for several physiological functions such as nutrients transport, osmoregulation and barrier against external toxicity (26, 146). Compared to mammals, similar types of intestinal epithelial cells are found in fish mucosa including enterocytes (absorptive cells), goblet cells (mucus - secreting cells) and enteroendocrine cells (hormone - secreting cells); while Paneth cells (antimicrobial peptides - secreting cells) and M cells (gatekeepers of luminal antigens) haven not been reported in the fish intestine. According to Van der Flier and Clevers (403), enterocytes account for more than 80% of total epithelial cells and are mainly responsible for nutrient absorption. The cells are highly polarized and characteristically possess an apical (facing lumen) and basolateral membrane domains (facing capillary), which are separated by intercellular junctional complexes (aka tight junction). The transporting properties of enterocytes are determined by the presence of the transporters and ion channels located in apical and basolateral membranes.

2.4.2. Modes of nutrient transport across intestinal epithelial cells

Once ingested, nutrients are broken down into absorbable molecules. Generally, solutes could be transported either between the enterocytes (paracellular transport) or across the cellular membranes (transcellular transport) (Figure 2.5A). The transport achieved by the former route in healthy cells is negligible due to the tight junction. The transport achieved by the the latter route is composed of two different processes (Figure 2.5B): passive transport process (down a

concentration gradient - no energy ATP required) and active transport process (against a concentration gradient - ATP needed).

The passive transport process includes simple diffusion and facilitated diffusion which includes channel or carrier (aka passive channel/carrier-mediated transports). Substances that could move via simple diffusion pathway are typically small molecules such as steroid hormones and non-polar gases (e.g. O_2, CO_2 and N_2) (436). When plotting the diffusion rate versus substrate concentration, the rate of simple diffusion increases linearly with substrate concentration and obeys Fick's law (295). Unlike, large and charged molecules such as inorganic ions (Na^+, K^+, Cl^-, etc.) and AAs are transported via facilitated diffusion pathway using channel or uniporter carrier (267, 349). The rate of facilitated diffusion will reach maximum (V_{max} or J_{max}) when a carrier is saturated, which could be described by the Michaelis-Menten equation (2). The transport rate achieved by facilitated diffusion is typically faster than that of simple diffusion, but the capacity is determined by the number of the carriers.

In the active transport process, molecules move across a membrane from low to high concentration at the expense of biological energy adenosine triphosphate (ATP). There are two types of active transport processes: primary and secondary. In primary active transport, the carrier protein pumps a solute against its concentration gradient by direct use of energy derived from ATP hydrolysis, which thus is referred to as a pump (or ATPase). A protein pump could transport one type of ion (e.g. H^+ ATPase, Ca^{2+} ATPase) or two different types of ion (e.g. Na^+/K^+ ATPase) (111). In secondary active transport, the energy stored in ion gradient (known as coupling ions/or driving ions such as Na^+ or H^+) that is originally established from primary active transport is used to drag a second molecule (driven molecule) across a membrane. A symporter moves two types of molecules in one direction (e.g. sodium/glucose cotransporter, sodium/amino acid cotransporter);

whereas an antiporter (exchanger) moves two types of molecule in opposite directions (e.g. Na^+/H^+ exchanger) (111, 295).

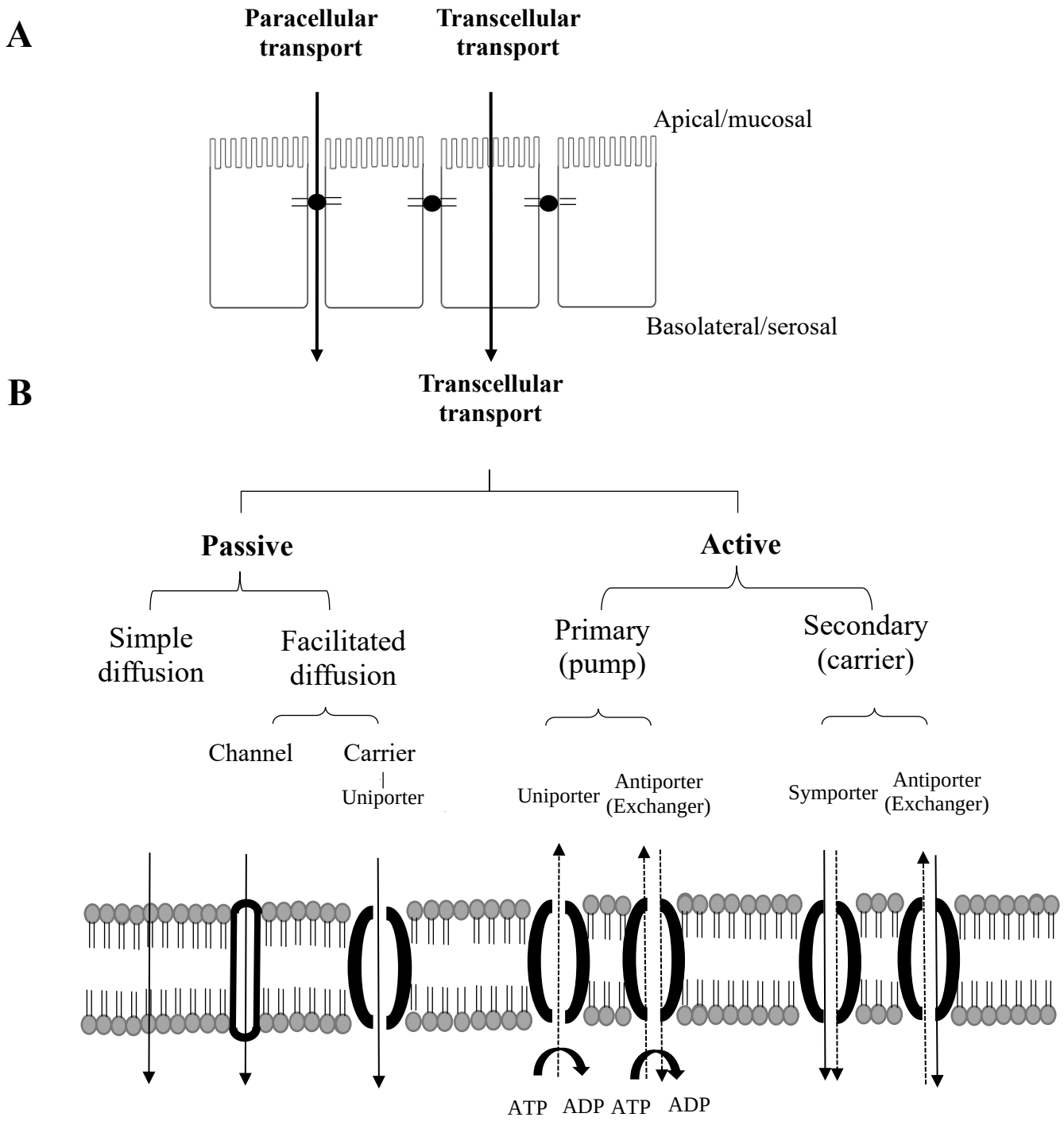

Figure 2.5. Schematic model of molecule transport

A) Paracellular and transcellular transport. **B)** Types of transcellular transport routes. Regular arrows indicate molecules moving down concentration gradient. Broken line arrows indicate molecules moving against concentration gradient.

2.4.3. General transport pathways of amino acid across the intestine

The nutrient transport mechanisms in fish are greatly unknown, and most of the literature on the transport processes comes from mammalian studies. AA uptake in the intestine is a complex process, and an individual AA usually could be transported by multiple systems. In order to classify transport routes, AAs are structurally grouped into non-polar and polar AAs. The latter is divided into three subgroups: neutral, negatively (anion), and positively (cation) charged side chains (18). As a neutral AA, Met could be transported by multiple routes including sodium-dependent (system A, system ASC, system B^0, system $B^{0,+}$, system IMINO and system y^+L) and sodium-independent pathways (system $b^{0,+}$-like, system y^+-like, and system L) (39, 202, 247, 367). Putative transporters that are responsible for methionine transport are described in figure 2.6 as well as summarized in table 2.1. To characterize AA transport systems, carrier kinetics and inhibitors associated with the transport systems are the principal criteria (190) which include: 1) dependence on Na^+, Cl^- or H^+, 2) kinetic parameters K_m and J_{max} (V_{max}), 3) competition between AAs for a transporter, 4) sensitivity to some inhibitors such as bicyclo[2.2.1]heptane-2-carboxylic acid (BCH), N-ethylmaleimide (NEM) and 2-(methylamino) isobutyric acid (MeAIB).

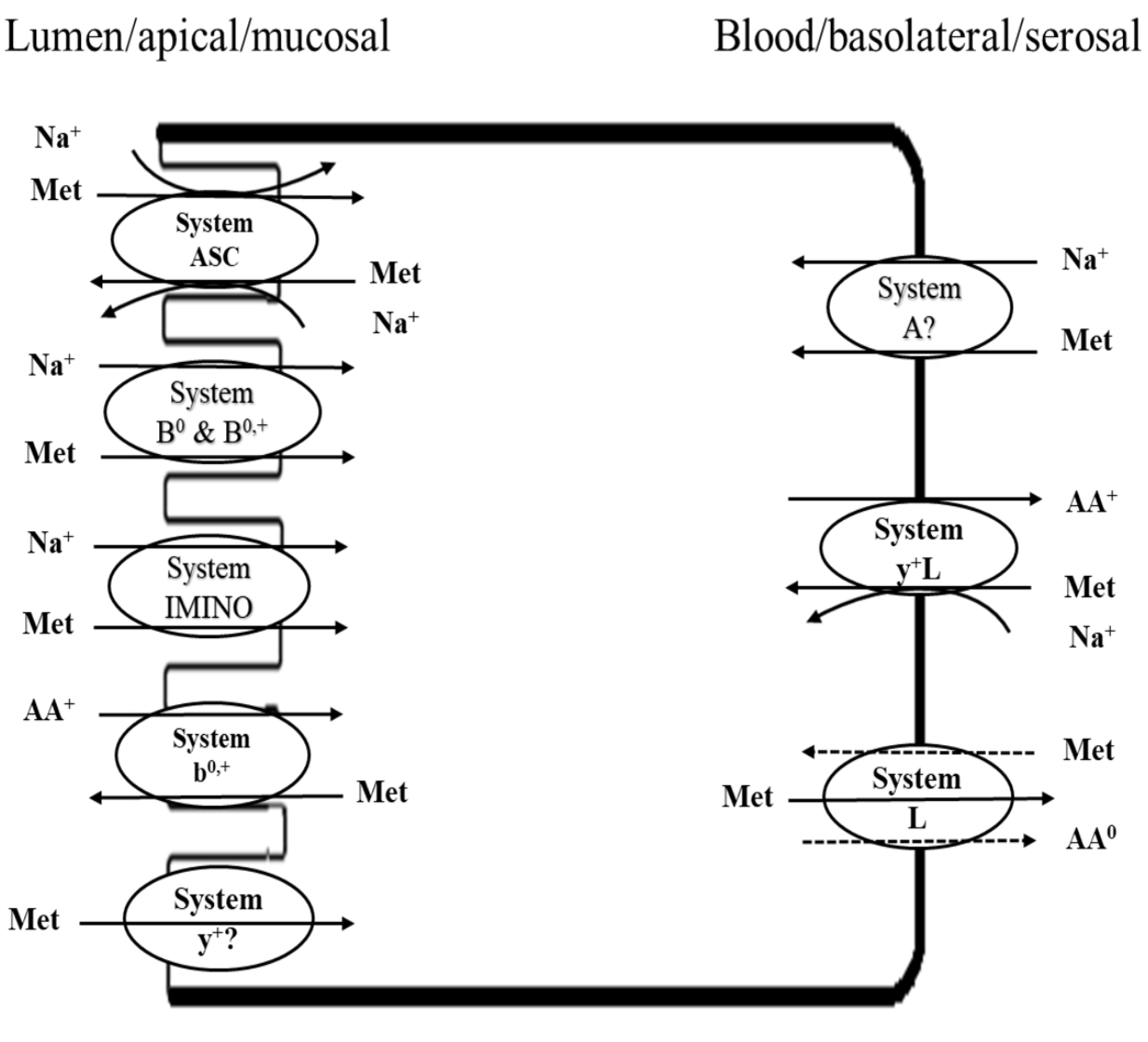

Figure 2.6. Hypothetical model of Met transport in the intestine of mammals and avian.

Table 2.1. Putative transporters mediate Met transport in the intestine of mammals and avian.

	System	Gene name	SLC[1]	Affinity[2]	Mechanism[3]	Location[4]
Sodium-dependent	A	SNAT1	SLC38A1	Medium?	S	BM
		SNAT2	SLC38A2	Medium?	S	BM
		SNAT4	SLC38A4	Medium?	S	BM
	ASC	ASCT1	SLC1A4	High	A	BM
		ASCT2	SLC1A5	High	A	AM
	B^0	B^0AT1	SLC6A19	Low	S	AM
		B^0AT2	SLC6A15	High	S	AM
	$B^{0,+}$	$ATB^{0,+}$	SLC6A14	High	S	AM
	IMINO	IMINO	SLC6A20	Low	S	AM
	y^+L	$4F2hc/y^+LAT1$	SLC3A2/SLC7A7	High	A	BM
		$4F2hc/y^+LAT2$	SLC3A2/SLC7A6	Medium	A	BM
Sodium-independent	$b^{0,+}$	$rBAT/b^{0,+}AT$	SLC3A1/SLC7A9	High	A	AM
	y^+	CAT1	SLC7A1	Low?	U	AM
		CAT2	SLC7A2	Low?	U	AM
		CAT3	SLC7A3	Low?	U	AM
	L	4F2hc/LAT1	SLC3A2/SLC7A5	High	A	BM
		4F2hc/LAT2	SLC3A2/SLC7A8	Medium	A	BM
		4F2hc/LAT3	SLC43A1	Low	U	BM
		4F2hc/LAT4	SLC43A2	Low	U	BM

1-Solute carrier. 2-Affinity (high, < 100 μM; medium, 100 μM – 1 mM; low, > 1 mM). 3-Mechanism (A: antiport, S: symport, U: uniport). 4-Location (AM: apical membrane, BM: basolateral membrane).

2.5. DL-Met transport across the gastrointestinal tract by AA transporters

Amino acid transporters are defined as solute carrier transporter (SLC) that could be classified into some families based on substrate selectivity and sodium-dependence/independence.

2.5.1. Sodium-dependent AA transport systems

2.5.1.1. System A

System A encoded by the SLC38 gene family is the sodium-coupled neutral AA transporter (SNAT) (227). This system is present in almost all cell types, which transport most of the aliphatic AAs with Na^+ ions (251). System A activity has been found in both the apical and basal membrane of the placenta (282), but is generally associated with the basolateral side in the intestine (247, 445). The system is recognizably different from several AA transport systems by the fact that it could also transport N-methylated AAs like MeAIB (68). This system is shown to be pH-sensitive (98, 251). Three cDNAs that encode proteins for system A activity have been identified and recently renamed by Mackenzie and Erickson (227) as follows: SNAT1 (previously known as ATA1, GlnT, SA2, SAT1, or NAT2), SNAT2 (previously ATA2, SA1, or SAT2) and SNAT4 (previously ATA3, NAT3, or SAT3).

SNAT1 (SLC38A1) mediates neutral AA/Na^+ cotransport with a stoichiometry of 1:1 and exhibits a preference for glutamine, asparagine, methionine, alanine, cysteine, serine, histidine, etc. (1, 228). Glutamine is the principal substrate of SNAT1 in the brain, which is transported with K_m value of ~ 300 μM (228). In *X.* oocytes expressing SNAT1, pH could change the affinity of Na^+ (K_m for Na^+ increases from 3.5 mM at pH 7.4 to 31 mM at pH 6.0), which likely causes an allosteric site effect on the transporter (1). SNAT1 is dominantly expressed in the brain, placenta, and heart (408, 422). Although SNAT1 is predicted to transport methionine from the basolateral

side of the intestine (445), its protein expression in rat intestine has been shown to reduce shortly after birth (426).

SNAT2 (SLC38A2) has been suggested to operate by a similar mechanism as SNAT1, including substrate specificity, 1:1 stoichiometry of sodium/AA and pH-sensitive. Alanine appears to be a preferred substrate for SNAT2 transporter with K_m ~ 0.5 mM, as well as MeAIB with K_m between 0-2-0.5 mM (377, 437). Glutamine is also transported by SNAT2, although with lower affinity (K_m ~ 1.6 mM) (437). Competition experiments reveal that methionine is one of the effective neutral AAs that competes with [^{14}C]MeAIB for the transport process mediated by SNAT2 expressed in *X. laevis* oocytes (165, 377). Although mRNA expression SNAT2 has not been found in the human intestine (165), SNAT2 protein is found in all duodenum, jejunum and ileum during the suckling period (211).

Although SNAT4 (SLC38A4) performs comparable transport characteristics with other isoforms of system A, it has some striking differences from SNAT1 and SNAT2. Firstly, common substrates of system A are transported by SNAT4 with significantly lower affinity: K_m values are 3.5-4.2 mM for alanine (147, 378) and 6.7 mM for MeAIB (164). Secondly, while SNAT1 and SNAT2 do not interact with cationic AAs such as arginine and lysine (422, 437), evidence shows that SNAT4 recognizes these AAs as good substrates (164). Thirdly, SNAT4 is expressed dominantly in the liver and lower extent in other tissues like muscle, kidney, and pancreas (147, 164, 378).

2.5.1.2. System ASC

System ASC's preferred substrates are alanine, serine and cysteine. Thus, the initial letters of these AAs were originally used by Christensen and co-workers to describe the substrate specificity of this Na^+-requiring system (71). The transport properties of these AAs are then studied

in many cell lines to represent common neutral AAs (133, 357, 441). The system ASC has been found to express in a wide variety of cell types (135, 313, 402), and it consists of two isoforms, including ASCT1 and ASCT2.

ASCT1 (SLC1A4) termed by Arriza et al. (5), or named as SATT by Shafqat et al. (355), is a Na^+-dependent neutral AA transporter. The K_m values for L-alanine, L-serine, and L-cysteine transport by ASCT1-expressing oocytes are between 29-88 μM (5). ASCT1-mediated transport is reported to be an electrogenic process that is sensitive to the reduction of intracellular Na^+ concentration (5). However, Zerangue and Kavanaugh (442) argued that the electrical currents detected during an AA flux could be attributed to the activation of an uncoupled negative charged of chloride movement through ASCT1; and the transporter mediates an electroneutral AA exchange rather than the net flux of AA. The transporter has been abundantly found in the brain and non-neuronal peripheral tissues (162, 178, 355). In the intestine, ASCT1 is described as a transporter localized on the basolateral membrane (162, 179).

ASCT2 (SLC1A5) is generally known as a Na^+-dependent exchanger in the apical membrane (39). It mediates the transport of L-alanine, L-serine, L-cysteine, L-threonine, L-glutamine with high affinity (K_m between 18-24 μM), whereas L-methionine, L-glycine, L-leucine and L-valine are transported with slightly lower affinity (K_m between 300-500 μM) (402). While there is the suggestion that D-Met is a better substrate for ASCT2, D-serine appears to be transported by ASCT2 with lower affinity (135) than L-serine (402). This is interesting because generally AA transporters favour L over D-isomers (27, 34, 54). However, there is little information about the impact of D and L transport in a mixture. It is suspected that the affinity of DL-Met mixture would be between D-Met and L-Met. The electrical property generated by ASCT2 is not uniformly observed. Some studies describe the transport process mediated by

ASCT2 is electroneutral (33, 402), along with the ability to display substrate-gated anion conductance (37). In the GI tract, it is first believed that ASCT2 is only present in the large intestine (402). However, later studies show that it also resides in the small intestine (97) and stomach (199).

2.5.1.3. System B^0

Characterization of neutral AA transporters was performed early in rabbit BBMV (343), bovine renal epithelial cell line NBL-1 (93), and Caco-2 cells (368). These studies suggest that the transport system is sodium-dependent and chloride-independent and denoted as neutral brush-border (NBB). The system was later renamed as system B to indicate the broad substrate specificities and is finally preferred as B^0 to reveal the zero net charge on the substrate molecules. There are two members of system B^0, including B^0AT1 and B^0AT2.

B^0AT1 (SLC6A19) mediates the apical Na^+-AA cotransport with a stoichiometry of 1:1 (29). The transporter is mainly expressed in intestine and kidney, which accepts all neutral AAs with different affinities and is considered as a methionine-preferring transporter (35, 39). B^0AT1 transports neutral AA with affinities from approximately 1-10 mM and shows a preference for carbon-sulfur side chains (e.g. methionine) and branched-chain AAs (e.g. leucine and valine) (29, 39). *X. laevis* oocytes expressing mouse B^0AT1 reveals that K_m value for methionine is approximately 0.67 mM (276). A recent electrophysiological study on sea bass and salmon indicates that the functional properties of B^0AT1 expressed in *X.* oocytes are similar to mammalian transporter (240, 241). However, it appears that salmon B^0AT1 needs to co-express with accessory protein collectrin in order to perform its functions appropriately (240).

B^0AT2, aka SBAT1 (SLC6A15), is a neuron-specific neutral AA transporter. Its function has been exclusively studied in the brain (150, 324). B^0AT2 transports several large zwitterionic AAs, with a preference for the branched-chain AAs, methionine and proline (K_m ~ 40-200 μM)

(36, 382). It also accepts glutamine, phenylalanine and alanine with lower affinities (K_m ~ 0.6-5.3 mM) (36).

2.5.1.4. System $B^{0,+}$

System $B^{0,+}$ is a sodium- and chloride-dependent system that could transport both neutral (0) and basic (+) AAs. According to Sloan and Mager (362), human $ATB^{0,+}$ (SLC6A14) is responsible for the activity of system $B^{0,+}$ and it transports AAs with high affinity (K_m for methionine ~ 14 μM). The AA uptake via $ATB^{0,+}$ is driven by transmembrane gradients of Na^+ and Cl^- ions with a stoichiometry of 2 or 3 Na^+:1 Cl^-:1 AA (275, 362). Although the expression of the transporter is mainly found in the lung, trachea, and salivary gland, it may still contribute to the absorption of AAs in the GI tract since it is detected in the stomach and colon of mammalians (128, 163, 362).

2.5.1.5. System IMINO

System IMINO (SLC6A20) (aka sodium/imino-acid transporter 1 (SIT1)) is the major Na^+-dependent transporter for the absorption of proline and hydroxyl-proline in the intestine and kidney (383). At physiological sodium concentration, proline is transported by IMINO with a consistent affinity (K_m between 0.2-0.3 mM) in intestinal BBMV and in oocytes (375, 383). It also appears to transport N-methylated AAs (K_m = 3.2 mM for sarcosine) (383) and methionine with lower affinity (K_m = 6.9 mM) (276). The transporter is obviously shown to be sodium-dependent, most likely transporting one to two Na^+ with one substrate (374, 375, 383). Unlike sodium, a noticeable discrepancy in dependent (270) or not completely dependent on chloride (383) for IMINO carrier has been observed, which proposes inconclusive electrogenicity of the transporter.

2.5.1.6. System y^+L

System y^+L is a unique system that has characteristics of both system y^+ and system L which more information is presented in the next sections. The capability of this system in transporting both neutral and basic AAs was originally identified and described in the erythrocyte plasma membrane (88). Specifically, this system could transport neutral AAs in the presence of sodium and is also capable of transporting basic AAs in the absence of sodium (4, 87, 88). The system y^+L is composed of a heavy subunit (4F2hc) and light subunits: y^+LAT1 and y^+LAT2.

4F2hc/y^+LAT1 (SLC3A2/SLC7A7) was originally identified as a member of the family that is homologous to the yeast high-affinity methionine permease MUP1 (396). It is highly expressed in the basolateral membrane of the kidney and intestine, which involves the efflux of basic AAs and the influx of neutral AAs (4, 64). The transport of basic AAs such as arginine and lysine is not affected when replacing Na^+ by K^+, while the transport of neutral AAs such as methionine and leucine is highly Na^+-dependent (88, 307). In physiological Na^+ conditions, the transporter functions as an obligatory antiporter with affinity for neutral AAs that tends to be higher than basic AAs. It is suggested that the transporter mediates the cellular efflux of basic AAs in exchange for a cellular influx of neutral AAs, plus a cellular influx of Na^+, which overall process is electroneutral (307). Thus, y^+LAT1 potentially facilitates the re-enter of Met and to support the exit of intracellular basic AAs from the basolateral membrane of enterocytes.

4F2hc/y^+LAT2 (SLC3A2/SLC7A6) is abundantly present in several tissues and functions similarly with y^+LAT1. However, its substrate specificity tends to be narrower than y^+LAT1, and it may play an important role in the release of arginine in tissues or cell types that have low transport capacity (38). It has further been suggested that y^+LAT2 activity may be suppressed by mutations of y^+LAT1 (369).

2.5.2. Sodium-independent AA transport systems

2.5.2.1. System $b^{0,+}$

System $b^{0,+}$ was originally studied in mouse blastocysts as a Na^+-independent transport system with broad specificity for neutral (0) and cationic (+) AAs and cystine (406). The system $b^{0,+}$ is composed of two different protein subunits: a heavy chain rBAT (approximately 90 kDa) and a light chain $b^{0,+}$AT (roughly 40 kDa) (297). rBAT/$b^{0,+}$AT (SLC3A1/SLC7A9) is mainly expressed in the apical membrane of the small intestine and the nephron epithelial cells (127, 310). In oocytes and opossum kidney (OK) cells, the transporter demonstrates as an obligatory exchanger that mediates the influx of cationic AAs and efflux of neutral AAs with 1:1 stoichiometry (64). Substrates are transported with high affinity, and K_m values are between 71-130 μM for methionine (276, 296). rBAT/$b^{0,+}$AT is also known as cystine transporter due to the critical role in the reabsorption of cystine in the kidney. In chicken BBMV, Soriano-García and co-workers (367) indicates that L-Met could be transported by a carrier-mediated mechanism that is described as $b^{0,+}$-like with high affinity Michaelis constant ($K_m \sim 2.2$ μM) and low capacity ($V_{max} \sim 0.13$ pmol (mg protein)$^{-1}$ (2 s)$^{-1}$).

2.5.2.2. System y^+

System y^+ is known as a Na^+-independent lysine-accepting system (system L^+) that was originally described in Ehrlich cells by Christensen (67). In later research, Christensen and Liang (70) showed that cationic AAs could be transported by two pathways, including lysine-accepting system L^+ and lysine-preferring agency known as Ly^+; which the former could be partially inhibited by phenylalanine, while the latter is resistant to the inhibition of phenylalanine. However, a further investigation performed in rabbit reticulocytes does not result in strong inhibitory effects of neutral AAs such as leucine, phenylalanine, and methionine on lysine uptakes (69). Therefore,

the authors concluded that there is only one system transporting cationic AAs. The system was then renamed as y^+ since it does not accept lysine exclusively, but also recognizes arginine, homoarginine, ornithine, and other cationic analogs in human skin fibroblasts (427). Investigation on intestinal transport of Met, Soriano-García and co-authors (367) found that Met could be transported by a system that was similar to system y^+ and named as y^+m with K_m about 3 mM in chicken BBMV. However, this has not been confirmed in heterologous expression systems. System y^+ is assembled by four main cationic AA transporters genes (CAT1-4) which have assigned to the gene names as SLC7A1-4 (415).

CAT1 (SLC7A1) is likely to be the major Na^+-independent transporter of system y^+ in most of the cells. It was originally identified as a receptor for murine ecotropic leukemia viruses. CAT1 expression has been found in all tissues with the exception of the liver (87), which its expression levels markedly vary among types of tissues and are controlled by different factors such as growth factors, hormones, nutrients, etc. (166). Cationic AAs such as L-arginine, L-ornithine, and L-lysine are transported with high-affinity (70-100 μM) by CAT1 expressed in oocytes, while D-isomers are transported by lower affinity (K_m in mM ranges) (197, 423). In addition, neutral AAs (e.g. cysteine) are also transported at high concentrations, but only with the condition of sodium (197).

CAT2 (SLC7A2) with two isoforms (CAT2A and CAT2B) is structurally similar to CAT1, but different in substrate affinity and tissue distribution. CAT2A is abundantly expressed in the liver (229) and exhibits low-affinity with cationic substrates (K_m ~ 2-5 mM), while CAT2B could be found in a variety of cells, and K_m ranges between 0.3-0.7 mM (75). CAT3 (SLC7A3) expression is restricted to the brain in rodents and displays high-affinity when transporting L-arginine (K_m ~ 40-103 μM) and L-lysine (K_m ~ 115-165 μM) (177, 183). Whereas, CAT4 (SLC7A4) has not been functionally studied.

2.5.2.3. System L

System L was originally defined in the Ehrlich ascites tumor cell and named as the leucine-preferring site because of its high transport rate with leucine (293). It is an important basolateral Na^+-independent system that transports large neutral, branched or aromatic AAs, and could be inhibited by BCH. A study in Chang liver cells proposes that an imposed proton gradient across the membrane could increase the affinity of the transport system for leucine (263). There are four members of system L including LAT1-4. LAT1 and LAT2 belong to the SLC7 family and are heterodimeric proteins that require a heavy chain subunit 4F2hc to elicit transport activity. In contrast, LAT3 and LAT4 belong to the SLC43 family and are not heterodimeric transporters, so no co-expression with 4F2hc is required.

4F2hc/LAT1 (SLC3A2/SLC7A5) and 4F2hc/LAT2 (SLC3A2/SLC7A8) are expressed in varieties of cell. In the intestine, LAT1 is abundantly found in the colon, while LAT2 is homogenously present throughout the intestinal tract (124). LAT1 and LAT2 are identified as AA exchangers with a 1:1 stoichiometry (414). This means that the transporters transfer one AA out of the cell and simultaneously one AA into the cell, resulting in neither a net influx nor efflux. Thus, their roles are likely to equilibrate the AA concentration across the membrane rather than to contribute to a net flux of AA (252). Both LAT1 and LAT2 could transport substrate AAs with high affinity. For instance, human LAT1 transports large neutral AAs with high-affinity (K_m ~ 15-50 µM) including L-Met with the affinity of 20 µM and is equally capable of accepting D-isomers (434). Compared to LAT1, LAT2 exhibits a broader substrate selectivity including large and small neutral AAs, but with lower affinities (K_m ~ 30-300 µM), plus L-Met with the affinity of 204 µM (351). It appears that pH-dependence is the primary criterion to differentiate between LAT1 and

LAT2. The transport mediated by the former is not influenced by proton concentration (321), while the latter could be stimulated by low pH (351).

LAT3 (SLC43A1) and LAT4 (SLC43A2) are Na^+-, Cl^-, and H^+- independent transporters that have narrow substrate specificity including leucine, isoleucine, methionine, and phenylalanine (6, 27). LAT3 mRNA is mainly expressed in the pancreas, liver and skeletal muscle (6), whereas LAT4 mRNA is highly distributed in the placenta, kidney and intestine (27). Unlike antiporters LAT1 and LAT2, LAT3 and LAT4 play an important role in facilitating a net efflux of AAs across the membrane (73). An earlier study in Caco-2 cell proposed that the rate-limiting of Met transport is largely determined by basolateral efflux (62). A recent study in knock-out mice has confirmed the role of uniporter LAT4 in controlling (re)absorption of essential AAs, especially phenylalanine and methionine in basolateral sides of the small intestine and kidney (148). Experiments in oocytes demonstrates that LAT4 transports phenylalanine with low affinity from 4-5 mM (27, 148).

2.6. DL-MHA transport across the gastrointestinal tract by monocarboxylate transporters

The chemical structure of Met includes an amine group (NH_2), a carboxyl group (COOH), a hydrogen atom and a R group (C_3SH_7). In the MHA molecule, the amino group is substituted with a hydroxyl group (OH). Due to this substitution, MHA is closely similar to monocarboxylate rather than a true Met. As a result, DL-MHA is believed to be transported by a different mechanism that involves monocarboxylate transporters of the SLC16 family and/or sodium monocarboxylate transporters of SLC5 family (230, 245). The general description of transporters are presented in table 2.2

Table 2.2. Putative transporters mediate MHA transport in the intestine of mammals

	Gene name	SLC[1]	Affinity[2]	Mechanism[3]	Location[4]
Proton-dependent/independent	MCT1	SLC16A1	Low	H^+	AM/BM
	MCT2	SLC16A7	High-Medium	H^+	AM/BM
	MCT3	SLC16A8	Low	H^+	AM/BM
	MCT4	SLC16A3	Low	H^+	AM/BM
	MCT5	SLC16A4	?	?	?
	MCT6	SLC16A5	?	?	?
	MCT7	SLC16A6	?	?	?
	MCT8	SLC16A2	?	?	?
	MCT9	SLC16A9	?	?	BM?
	TAT1	SLC16A10	?	?	?
	MCT11	SLC16A11	?	?	?
	MCT12	SLC16A12	?	?	?
	MCT13	SLC16A13	?	?	?
	MCT14	SLC16A14	?	?	?
Sodium-dependent	SMCT1	SLC5A8	High-Medium-Low	Na^+	AM
	SMCT2	SLC5A12	Low	Na^+	AM

1-Solute carrier. 2-Affinity (high, < 100 μM; medium, 100 μM – 1 mM; low, > 1 mM). 3-Mechanism (H^+: proton-dependent, Na^+: sodium-dependent). 4-Location (AM: apical membrane, BM: basolateral membrane).

2.6.1. Monocarboxylate transporters

The monocarboxylate transporter (MCT) family consists of 14 members in which only MCT1-4 are well characterized and known as H^+-coupled transporters, while the functions of the remaining transporters have not fully understood.

MCT1 (SLC16A1) expression is found in almost all tissue and most pronounced in muscles, which directly link to the regulation of lactic acid production (12, 30, 188, 354). Findings of expression pattern along the intestine show that MCT1 mRNA and protein are richly expressed in the large intestine, including colon and cecum (132, 184, 330). The abundant expression of MCT1 in the distal intestine is logical with the dominant activity of bacterial fermentation producing SCFAs in this area (394). Initial studies on lactate transport were carried out in human red blood cells (86, 96) using radiolabeled substrates flux techniques, and in tumor cells by monitoring the substrate-induced decrease in intracellular pH using fluorescent H^+ indicator BCECF (57). Subsequently, MCT1 is expressed in *X. laevis* oocytes and its transport properties are studied using similar mentioned techniques (43, 237, 330). Recently, a new technique using hyperpolarized [^{13}C]-labeled substrates combined with nuclear magnetic resonance (NMR) was employed to study the transport kinetics of monocarboxylic acids (161). Regardless of methodologies used, these studies reveal that MCT1 accepts a wide range of SCFAs. C-2 (acetate, glyoxylate, oxamate, lycolate), C-3 (propionate, pyruvate, lactate, chloropropionate), and C4 (oxobutyrate, hydroxybutyrate, hydroxy-2-methylpropionate) are transported with affinity from 0.2-63 mM; whereas, C-1 (formate and bicarbonate) are poorly transported with affinity >100 mM (152). MCT1-mediated substrate transport is suggested to be an electroneutral process because of 1:1 H^+/monocarboxylate stoichiometry and the transport process is easily stimulated by decreasing the pH from 8 to 5.0 (181, 207, 233, 330). Although Martin-Venegas and co-workers suggest that

MCT1 mediates the transport of DL-MHA in Caco-2 cells with K_m around 13 mM (245), the authors could not observe the differences in DL-MHA uptakes between pH conditions (pH 5.5 versus 7.4). Whether or not MCT1 could regulate DL-MHA uptakes also depends on its location in the cell membrane, which has been inconsistently observed. Several studies have showed that MCT1 is mainly expressed in the apical membrane (55, 63, 273, 308). Some studies find its exclusive expression on the basolateral surface of epithelial cells (131, 132, 184), whereas the other studies find it on both apical and basolateral surfaces (243, 384). The identification of inhibitors is an essential part of characterizing transporters. According to Halestrap and Price (156), inhibitors of MCT1 could be grouped into four categories including: (1) substituted aromatic monocarboxylates such as α-cyano-4-hydroxycinnamate (CHC) and its analogs), (2) amphiphilic compounds such as phloretin, quercetin and 3-isobutyl-1-methylxanthine (IBMX), (3) organomercurial thiol reagents such as *p*-chloromercuribenzene sulphonate (pCMBS), and (4) stilbene disulphonates such as 4,4′-dibenzamidostilbene-2,2′-disulphonate (DBDS) and 4,4′-diisothiocyanostilbene-2,2′-disulphonate (DIDS). Since none of these inhibitors are specific for inhibiting MCT1, caution needs to be taken when analyzing data.

MCT2 (SLC16A7) is an H^+-dependent transporter. It is expressed in various animal tissues and tends to transport substrates with higher affinity than MCT1 (131, 214). Specifically, Garcia et al. (131) demonstrates that K_m values for [^{14}C] pyruvate uptake by hamster MCT2 and MCT1 expressed in insect Sf9 cells are 0.8 mM and 3.1 mM, respectively. A higher affinity for human MCT2-expressing in oocytes is also observed in the research of Lin et al. (214), which K_m values of 25 μM and 2.3 mM for pyruvate transported by MCT2 and MCT1, respectively. Likewise, a later experiment in oocytes conducted by Broer and co-workers (40) again concludes that K_m values generated by MCT2 are smaller than that by MCT1 for most of the substrates, including

pyruvate, L-lactate, acetoacetate, D,L-β-hydroxybutryate, 2-oxoisohexanoate, and 2-oxoisovalerate. It is reported that MCT2 is more sensitive than MCT1 to most of the inhibitors, including CHC, DIDS and DBDS (153). The main difference between MCT1 and MCT2 is that the former is inhibited by pCMBS, while the latter is resistant to the pCMBS (40, 131).

MCT3 (SLC16A8) distribution has been found in several tissues including retinal pigment, choroid plexus, skeletal muscle, heart, placenta, white blood cells, NBL1 cells, and COS cells (309, 429, 440). Wilson and his colleagues (429) performed transport kinetics of MCT3 in multiple cell lines derived from the bovine kidney (NBL1), monkey kidney COS and mouse tumor (ELT). The results show that K_m values are in millimolar ranges: L-lactate (6.4-10.1 mM) and D-lactate (12.6-46.6 mM) and pyruvate (0.9-2.1 mM). These authors also suggest that L-lactate transport is inhibited by CHC, DIDS, and phloretin. The location of MCT3 in the basolateral membrane of rat retinal pigment epithelium (RPE) is well demonstrated by Philp and co-workers (308). Subsequently, L-lactate is kinetically studied when MCT3 from chicken RPE is expressed in yeast. Although the results of affinity are compatible with previous research (K_m ~ 6 mM), MCT3 is greatly resistant to classical inhibitors such as CHC, pCMBS, and phloretin (145).

MCT4 (SLC16A3) is another major member of the MCTs family that plays an essential role in glycolytic metabolism. It is widely expressed in glycolytic tissues such as skeletal muscles (119, 311, 354), astrocytes (24) and white blood cells (256). MCT4 is similar to the other MCT isoforms in several aspects: specificity of substrate recognition, pH dependence, and inhibitory response to CHC, DIDS and phloretin. However, it could be distinguished from MCT1-3 by its low substrate affinity. The K_m for lactate transport is between 13-25 mM in rat sarcolemmal giant vesicles (mixed isoforms with MCT4 dominant) determined by monitoring intracellular pH response using fluorescent H^+ indicator BCECF (187). In oocytes experiment, rat MCT4 transports

lactate with K_m of 17 mM or 34 mM by measuring changes of the cytosolic pH with pH-sensitive microelectrodes or measuring flux with radioactive tracers, respectively (91).

The following are the remaining SLC16A family members with some defined functions, minimally characterized or not characterized at all. Despite being members of MCTs, several transporters below refuse to accept common monocarboxylic compounds.

MCT8 (SLC16A2) encoded by XPCT gene was initially cloned in 1994 and temporarily named as X-linked "PEST"-containing transporter since the domain region was rich in proline (P), glutamic acid (E), serine (S) and threonine (T) residues (206). However, its substrates and transport functions remained unknown until it was identified as a specific thyroid hormone transporter by Friesema and co-workers (126). Expression of MCT8 in *X. laevi*s oocytes shows that [^{125}I] labelled thyroxine (T4), 3,3',5-triiodothyronine (T3), and 3,3',5'-triiodothyronine (rT3) are transported with high affinity (apparent K_m values of 2-5 µM), whereas aromatic AAs such as phenylalanine, tyrosine, and tryptophan, and leucine are not transported. The authors also point out that the organic anion bromosulfophthalein (BSP) is a potent inhibitor along with T3 analogs where the α-NH_2 group is blocked (BrAcT3) or deleted (Triac). Data on expression is found on both protein and gene levels in various rat tissues including the brain, liver, kidney, teste, and heart (60, 126, 404).

TAT1 (SLC16A10) is known as T-type amino acid transporter 1 that mediates the transport of aromatic AAs, but not lactate and pyruvate. The transporter is primarily distributed in the kidney, skeletal muscle, intestine, liver and placenta (195, 196). Rat TAT1 expressed in *Xenopus* oocytes exhibits low-affinity transport of aromatic AAs with K_m of about 2-7 mM (195). Unlike MCT1-4, AAs uptakes mediated by TAT1 are Na^+ and H^+ independent. However, higher affinity (K_m in µM ranges) is observed when a similar experiment is performed in human TAT1 (196).

Both studies demonstrate the inhibitory effects of N-methyl and N-acetyl derivatives of aromatic AAs substrates on TAT1-mediated radiolabeled substrate uptakes.

MCT5-7 (SLC16A4-6) distribution has been performed in human tissues using Northern blots (323). Recent studies (203, 271) demonstrate that MCT6 (SLC16A5) facilitates drug uptakes with high affinities: K_m of 84 µM (bumetanide) and 46 µM (nateglinide), but does not accept common substrates of MCT (e.g. lactic acid and tryptophan). Although kinetic transports have not been studied, MCT7 (SLC16A6) is reported as an important factor regulating the secretion of ketone bodies in the liver during fasting (180). The information about the full substrate specificity of MCT9 (SLC16A9) has not been established. However, when expressed in *X.* oocytes, MCT9 has been identified as a pH-independent transporter that mediates unidirectional efflux of [^{3}H]-carnitine, suggesting its function in delivering substrates from basolateral membrane of absorptive epithelial cells into the blood (379). The functions of the remaining orphan MCT11-14 (SLCA11-14) have not been elucidated, although their distributions have been reviewed in a variety of tissues (154, 155).

2.6.2. Sodium monocarboxylate transporters

As mentioned previously, DL-MHA transport was proposed to be mediated by proton-dependent transporter MCT1 in Caco-2 cells by Martín-Venegas and co-authors (245). However, these authors fail to demonstrate the stimulation of DL-MHA transport by the imposed H^+-gradient. Likewise, the dependence of DL-MHA transport on sodium is inconsistently observed in a few studies. The transport of DL-MHA was not dependent on sodium when being studied in chick and rat intestinal BBMV (31, 32) as well as in *X.* oocytes injected with poly(A)$^+$ RNA that encode proteins capable of transporting DL-MHA isolated from chicken intestinal mucosa tissue (298). Whereas partial Na^+-dependence of DL-MHA uptake is detected in the chicken small

intestine using the everted sac method (244). The presence or absence of sodium dependence in these studies could be caused by the differences in techniques and/or animal species that are used. Hence, DL-MHA transport in the fish intestine could be sodium-dependent/independent, which requires the examination of sodium-linked monocarboxylate carriers. Evidence emerged many years ago that there are sodium/monocarboxylic acid cotransport pathway across renal brush border membranes. Uptake of L-lactate and pyruvate in BBMV was found to be stimulated by inwardly directed Na^+ gradient (16, 279) and no significant contribution of H^+/lactate co-transport is observed in the pH-dependent study (16). Analysis of transport properties shows that sodium: lactate stoichiometry is 2:1 (254), or 1:1 (17). K_m values are 0.4-4.3 mM for lactate (16, 253, 280) and 0.1-0.25 mM for pyruvate (279, 343). Thus, it is possible that DL-MHA could be transported by SLC5 sodium-coupled MCTs gene family (SMCTs) that includes two members: SMCT1 and SMCT2.

SMCT1 (SLC5A8) was originally cloned as a sodium iodide symporter (NIS) by Rodriguez et al. (333) and proposed as an important tumor suppressor in colon and gliomas cancer (174, 212). When expressed in *X.* oocytes, SMCT1 was shown to transport a broad range of SCFAs and drugs in a Na^+-dependent manner with high-affinity for L-lactate (159-235 µM), butyrate (72-81 µM), propionate (127-162 µM), pyruvate (387 µM), nicotinate (230-390 µM) ; and with low-affinity for acetate (2.5 mM), β-hydroxybutyrate (1.4-2.3 mM) and drugs such as benzoate and salicylate (1.1-1.5 mM) (76, 141, 246, 264, 299). In inhibitor studies, SMCT1 is strongly inhibited by probenecid or ibuprofen (76), but insensitive to CHC and phloretin which are the potent inhibitors for MCT1 (40, 42). Immunohistochemical findings in intestine indicate that SMCT1 and MCT1 have been primarily found in the apical and basolateral membrane, respectively, suggesting

the major role in luminal SCFA uptake of the former and the SCFA efflux towards bloodstream of the latter (184).

SMCT2 (SLC5A12) expression is primarily found in the kidney, intestine and skeletal muscle (371). In the intestine, SMCT2 is dominantly expressed in the proximal areas, while SMCT1 is expressed in distal areas (371). Similar findings in the kidney report that SMCT2 expression is extended throughout the whole length of the proximal tubule (S1/S2/S3 segments), whereas SMCT1 is confided in the final area (S3 segment) (142). In comparison, although the substrate specificity of SMCT2 is similar to that of SMCT1, SMCT2 interacts with its substrates with relatively lower affinity: butyrate (2.6-16 mM), nicotinate (3.7-9.5 mM), and lactate (16.9-49 mM) (142, 371). These observations in the distribution and affinity between two transporters lead to the suggestion that the uptake of SCFAs in proximal intestine/kidney is initiated by SMCT2 with low-affinity, whereas the presence of high-affinity SMCT1 will likely ensure complete absorption in the distal intestine/kidney (153). Another difference between SMCT1 and SMCT2 is in the electrophysiological nature of their transport processes. It is generally concluded that SMCT1 mediates electrogenic absorption of substrates with 2-4 sodium ions per one monocarboxylate (76, 129, 140). In contrast, there is no agreement about electrophysiological results generated by SMCT2, which the process could be electroneutral (142), electrogenic (371), or both (315).

2.7. Segmental differences in AA and SCFA transport in the gastrointestinal tract

The structure of the fish intestine is comprised of distinctive regions including proximal intestine with pyloric caeca, mid intestine (midgut) and distal intestine (hindgut). Pyloric caeca are finger-like pouches that protrude from the proximal intestine, whereas midgut and hindgut are long tubes with different thickness of circular and longitudinal muscle layers (52). Such anatomical

differences are expected to account for the existence of functional differences in nutrient transport in the intestine. In fact, several studies in fish have demonstrated that there are segmental differences in K_m and V_{max} of phenylalanine influx, activity of basolateral membrane Na^+/K^+ pump, electrical potential difference (PD) and short circuit current (I_{sc}) in gilthead seabream (3, 221, 222), the transepithelial influx of proline in coho salmon (77), and tissue permeability in rainbow trout (344). As introduced previously, intestinal nutrient transport is largely regulated by protein transporters. Distribution and mRNA expression of AA transporters in the intestine has been shown to be segmentally different. For example, study in pigs show that y^+ LAT1 is most abundant in the duodenum, while the highest expression of $b^{0,+}$AT and CAT2 are found in the ileum (112, 424, 446, 449). In rat small intestine, mRNA expression level of glutamate transporter (EAAC1) is apparently high in distal regions, proposing that it is an important region for transporting acidic AAs (102). Meanwhile, other studies in equine shows that $b^{0,+}$AT and LAT3 are highly expressed in large intestine, suggesting that this region could transport cationic and neutral AA as well (432). In fish, evidence has proven that segmental segregation of glucose transport kinetics highly associates with the gene expression pattern of glucose transporters along the intestinal tract of trout and tilapia (376). Hence, it would be interesting to explore the segmental-dependent DL-Met transport in rainbow trout intestine.

Regarding SCFAs, regional distribution of MCT1 is primarily expressed in the colon, corresponding to the segmental distribution of SCFAs production which are primarily produced from fibre fermentation in the large intestine of mammalian species (101, 134). The regional comparison has been performed in a limited amount within this segment. Unidirectional flux mucosal-serosal of acetate, butyrate and propionate are found to be higher in distal colon than in caecum and proximal colon of guinea pig (100). However, several studies have shown that the

small intestine is still capable of transporting SCFAs in mammalian animals (345, 366). This also holds true for teleost fish. Acetate concentration in the digesta determined by HPLC was shown to be similar in all three intestinal regions (upper, middle and lower) of tilapia (*Oreochromis mossambicus*) ranging from 14-18 mM (392). The transport of [^{3}H]acetate into BBMV from the proximal intestine of tilapia was found to obey Michaelis-Menten kinetics with K_m of 6.4 mM (392). These suggest that the entire intestinal tract may be able to transport SCFAs which are an important nutrient source for plant-eating fish. Interestingly, while caeca of mammals and birds often serve as fermentation chambers, pyloric caeca in carnivorous fish are known as an absorptive site of nutrients (47), which is typically reduced or absent in herbivorous fish (48). Therefore, the existence of segmental differences in transport of SCFAs in the intestine of rainbow trout, a carnivore, is possible and would be examined in the current thesis.

2.8. Triploid and diploid rainbow trout aquaculture

Salmonid species (salmon and trout) are one of the most important cultured finfish group and are primarily produced by Norway, Chile and several countries from Europe and North America. The use of triploid salmonids has been introduced in aquaculture as a strategy to mitigate the genetic threats caused by the interaction between escaped farmed and wild fish and to improve production. Genetically, triploid fish is not a genetic modified organism (GMO). Compared to normal diploid fish (2N), it has three sets of chromosomes (3N) which is produced by subjecting newly-fertilized eggs to a hydrostatic pressure, thermal or chemical shock to prevent the extrusion of a polar body during meiosis (21, 89, 216). Fundamentally, triploid fish are similar to diploid fish, with the exception of the inability to reproduce in the former. Therefore, scientists generally agree that negative consequences caused by interbreeding between wild fish population and escaped farmed triploid fish are prevented (78). On the other hand, whether triploid fish

outperforms diploid fish in growth performance and disease resistance is still the subject of debate. In salmonids, several authors suggest that the growth performance of diploids is better than (250, 385), or similar to triploids (284). In contrast, faster growth has been observed for triploid salmon and rainbow trout (289, 386), which agrees with work on other aquatic species including catfish, oyster, shrimp, and tilapia (110, 158, 316, 320). It is thought that triploid animals have superior growth, flesh quality and survival compared to diploid counterparts due to three main reasons: increased heterozygosity, the concept of gigantism, and sterility. Firstly, the genomic heterozygosity hypothesis states that meiosis I triploid is more heterozygous than diploid, suggesting that faster growth results from increased allelic diversity and/or numbers (167, 372, 425). Secondly, the hypothesis of gigantism in triploid suggests that the increased body size in triploid is due to the increased cell volume in order to compensate for a reduction in cell numbers (22, 106, 149). Thirdly, the reduced gonads could prevent the allocation of energy from somatic to gonadal development of female triploid fish during sexual maturation (160, 185, 215). Despite the economic and ecological potentials, there is a rising reluctance in commercial operation to produce triploid Atlantic salmon since triploid fish tend to be more susceptible to disease infection (294), less tolerant of suboptimal water conditions such as low oxygen and high temperature (159, 213, 412), and high occurrence of body deformities such as cataract, skeleton, jaw, and gill deformities (125, 208, 290, 305, 336, 380).

Although differences in growth and survival performances of 3N and 2N fish are not yet conclusive, morphological and physiological differences have been described for several species (249). The GI tract is an important site for nutrient absorption. Differences in relative gut length, pyloric caeca numbers and mass between diploid and triploid fish may be influential in digestive efficiency and nutrient utilization, which subsequently causes differences in growth (304, 407). In

an effort to understand the mechanisms, the effects on ploidy on gene expression have been studied to understand the dissimilarity in physiological performance between diploids and triploids. Cleveland and Weber (74) suggest that reduced expression of IGF binding proteins, altered expression of muscle regulatory factors (*mstn1a* and *mstn1b*); and altered tissue responsiveness to TGFbeta superfamily ligands possibly explain why 3N juvenile rainbow trout recovery from nutritional restriction is better than 2N counterparts. In studies about the changes in gene expression during sexual maturation, Manor et al. (238, 239) report that the expression of fatty acid synthesis-related genes increases in 3N triploid female liver and muscle, and expression of β-oxidation-related genes increases in 2N diploid muscle and adipose tissues. These indicate that the discrepancy in deposition and degradation of fatty acids in 3N and 2N fish during sexual maturation. Hence, understanding how nutrient is absorbed in the GI tract and how it correlates with genes involved in nutrient transport are potential approaches to explain phenotypic differences between 3N and 2N fish. Since knock-out models of genes that are capable of transporting methionine have not been developed in trout, triploid and diploid rainbow trout are used as a tool to exploit the potential differences in DL-Met transport and gene expression, which is performed in the 3rd chapter.

Transition

The following chapter focuses on addressing the 1st objective and the 1st hypothesis. It has been documented in mammalian species that DL-Met transport is mediated by sodium-dependent and sodium-independent transporters, and there is evidence of segmental differences in several amino acid transporters in the intestine. However, such understanding has not been confirmed in rainbow trout fish. This chapter has been published in Physiological Reports. The chapter has been reformatted from the original manuscript to fit the structure of the thesis.

Objective: Characterize sodium-dependent DL-Met transport in the intestinal tract of rainbow trout using Ussing chamber and gene expression analysis.

Hypothesis: DL-Met transport is sodium-dependent, and there are segmental differences in DL-Met transport along the intestinal tract of rainbow trout.

Manuscript: To, V.P.T.H.[1], Masagounder, K.[2], Loewen, M.E[1]. SLC transporters ASCT2, B^0AT1-like, y^+LAT1, and LAT4-like associate with methionine electrogenic and radio-isotope flux kinetics in rainbow trout intestine. Physiological reports 7, no. 21 (2019): e14274.

[1]Veterinary Biomedical Science, University of Saskatchewan, Saskatoon, SK, Canada
[2]Evonik Nutrition and Care GmbH Rodenbacher Chaussee 4D-63457 Hanau, Germany

Contribution: VT designed and performed experiments, analyzed data and interpreted data, prepared manuscript and revised manuscript. KM revised manuscript. ML received funding, designed experiments, interpreted data and revised manuscript.

CHAPTER III

DL-MET TRANSPORT IN THE INTESTINAL TRACT OF RAINBOW TROUT

3.1 Abstract

Methionine (Met) is an important building block and metabolite for protein biosynthesis. However, the mechanism behind its absorption in the fish gut has not been elucidated. Here we describe the fundamental properties of Met transport along trout gut at µM and mM concentration. Both electrogenic and unidirectional DL-[^{14}C]Met flux were employed to characterize Met transporters in Ussing chambers. Exploiting the differences in gene expression between diploid (2N) and triploid (3N) and intestinal segment as tools, allowed the association between gene and Met transport. Three intestinal segments: pyloric caeca (PC), midgut (MG) and hindgut (HG) were assessed. Results at 0-150 µM concentration demonstrated that DL-Met was most likely transported by apical transporter ASCT2 (SLC1A5) and recycled by basolateral transporter y^+LAT1 (SLC7A7) due to five lines of observation: (1) lack of Na^+-independent kinetics, (2) low expression of B^0AT2-like gene, (3) Na^+-dependent, high-affinity (K_m, µM ranges) kinetics in DL-[^{14}C]Met flux, (4) association mRNA expression with the high-affinity kinetics and (5) electrogenic currents induced by Met. Results at 0.2 - 20 mM concentration suggested that DL-Met is possibly transported by B^0AT1-like (SLC6A19-like). This observation is based on gene expression, Na^+-dependence, low-affinity kinetics (K_m, mM ranges), and cis inhibition. Similarly, genomic and gene expression analysis suggested the basolateral exit of DL-Met was primarily through LAT4-like transporter (SLC43A2-like). Conclusively, DL-Met uptake in trout gut was most likely governed by Na^+-dependent apical transporters ASCT2 and B^0AT1-like and released

through basolateral LAT4-like, with some recycling through y^+LAT1. This is a relatively simpler model than described in mammals.

3.2. Introduction

Methionine (Met) is a sulfur-containing essential amino acid (EAA) that plays an important role in numerous metabolic processes. Three primary functions of this EAA are protein biosynthesis, methyl donor and precursor of cysteine synthesis (25, 257, 389). Influences of Met-deficient diets on feed consumption, growth performance, immune response, mRNA translation efficiency, oxidative status and protein turnover have been observed in a variety of fish species (20, 103, 205, 260, 352, 398). The intestinal tract is a critical site for animal nutrient uptakes. Compared to mammals, considerably less information is available on the nutrient absorptive mechanisms in aquatic species. Initial studies on AA absorption in fish included goldfish *Carassius auratus* (255), white grunt *Haemulon plumieri* (364), rainbow trout *Salmo gairdneri* (182), killifish *Fundulus heteroclitus* (262), European yellow eel *Anguilla anguilla* (232), and sea bass *Dicentrarchus labrax* (14). Most of these studies demonstrated that the Na^+ electrochemical gradient is the driving force for the absorption of AAs.

AA absorption in the intestine is a complex process and an individual AA is typically transported by multiple transporters. AA transporter systems belong to solute carrier (SLC) gene superfamily and can be grouped into some categories such as neutral, basic and acidic systems. Being a neutral AA, Met transports have been described in both Na^+-dependent (system A, system ASC, system B^0, aka NBB, system IMINO and system y^+L) and Na^+-independent pathways (system L, system $b^{0,+}$-like, system y^+-like) (39, 202, 235, 269, 367). As mentioned earlier, current knowledge of how nutrients are absorbed in the fish intestine in comparison to mammals is very limited due to the diversity of the living environment and gut anatomy of aquatic species.

Here, we exploit the differences in the absorption kinetics of DL-Met and transport gene expression between diploid and triploid rainbow trout as tools to determine the mechanism of Met absorption in fish gut. It should be noted that the intention of this study was not to give mechanism to the controversial difference in growth rate between ploidy (250, 285, 289). Met absorption kinetics were successfully studied in the presence and absence of sodium at µM and mM DL-Met concentration gradients created by increasing sequential concentration of Met. Trout gut demonstrated Na^+-dependent, high-affinity kinetics at 0-150 µM DL-Met concentration and a Na^+-dependent, low-affinity kinetics at 0.2-20 mM DL-Met concentration. Genome and gene expression analysis indicated that ASCT2 (SLC1A5) and B^0AT1-like (SLC6A19-like) were possible candidates responsible for the apical Met absorption at µM and mM concertation gradients, respectively. Whereas basolateral transporter y^+LAT1 (SLC7A7) was associated with electrogenic recycling and LAT4-like (SLC43A2-like) was associated with Met exit.

3.3. Materials and methods

3.3.1. Genomic analysis to identify methionine transporter genes

All Met transporter candidates that were previously described in mammalian and aquatic species were first listed. The list included 18 transporter candidates: SNAT-1,2,4 (SLC38A-1,2,4), ASCT2 (SLC1A5), rBAT/$b^{0,+}$AT (SLC3A1/SLC7A9), IMINO (SLC6A20), 4F2hc/LAT1 (SLC3A2/SLC7A5), 4F2hc/LAT2 (SLC3A2/SLC7A8), LAT3 (SLC43A1), LAT4 (SLC43A2), 4F2hc/y^+LAT1 (SLC3A2/SLC7A7), 4F2hc/y^+LAT2 (SLC3A2/SLC7A6), $ATB^{0,+}$ (SLC6A14), B^0AT1 (SLC6A19), B^0AT2 (SLC6A15), CAT-1,2,3 (SLC7A-1,2,3). Zebrafish sequences were initially used as reference to identify sequences of candidate genes in trout. However, several listed genes were not available in zebrafish and the blast analysis (https://www.ncbi.nlm.nih.gov/) resulted in poor identification compared to similar process employed when using human

transporters sequences. Therefore, the nucleotides of 18 human transporters were used to blast against the rainbow trout genome to identify similar mRNA sequences in trout. The match between human and trout sequences was justified based on the e-values less than $10^{\wedge-15}$ which were accepted. The results were double checked in NCBI assembly software using gene name search. Subsequently, available trout mRNA sequences were retrieved from NCBI website (http://www.ncbi.nlm.nih.gov/) and aligned using CLUSTAL W and MEGA7 software (https://www.megasoftware.net/) to create a phylogenetic tree.

3.3.2. Fish source and husbandry

All fish were maintained in accordance with the guidelines of the Canadian Council on Animal Care (CCAC, 2005) (59). All animal protocols were approved by the Animal Care Committee at the University of Saskatchewan (AUP#: 20170056). Diploid and triploid rainbow trout (*Oncorhynchus mykiss*) were purchased from B&B Freshwater Fish Farm (Gunton, Manitoba, Canada) and Wild West Steelhead hatchery (Lucky Lake, Saskatchewan, Canada), respectively. Fish were housed in an indoor recirculating system which included 120L fiberglass tanks connected to a sump tank and a biofilter. Each tank was oxygenated using air stones to maintain the oxygen above 6 mg/L, and the temperature was kept at 11-12 ^{0}C throughout the experiments. Fish were fed twice daily (2-3% body weight/day) with commercial feed containing 45% crude protein and 16% lipid manufactured by EWOS Canada Limited (Surrey, British Columbia, Canada).

3.3.3. Tissue collection

Healthy fish at grow-out stage between 50-150 g were selected and transferred to a processing building for gut dissection. Fish were euthanized by blunt trauma. The intestine was collected immediately after dissection, opened and rinsed carefully with teleost buffer pH 7.7,

containing (in mM): 118 NaCl, 2.9 KCl, 2.0 $CaCl_2 \cdot 2H_2O$, 1.0 $MgSO_4 \cdot 7H_2O$, 0.1 $NaH_2PO_4 \cdot H_2O$, 2.5 Na_2HPO_4, 1.9 $NaHCO_3$, and 5.6 Glucose, which was adopted from the research of Small and co-authors (363). Feces and uneaten feed were removed from luminal content. Pyloric caeca (PC), midgut (MG) and hindgut (HG) regions were collected. Three segments were visually distinct from each other, which were described by Burnstock (52). Specifically, the pyloric ceca region was located directly behind the stomach. Midgut and hindgut were located about 5 cm and 13-15 cm from the stomach, respectively (376). Each figure N represents a biological replicate of an individual fish intestinal segment.

3.3.4. RT-qPCR analysis to quantify mRNA expression of Met-linked transporters

About 100 mg samples of PC, MG, and HG were obtained from the fish dissection and stored in RNA*later*® RNA Stabilization Solution (Fisher Scientific) at -80 ^{0}C for later use gene expression. Total RNA was extracted using Trizol (Thermo Fisher Scientific) according to the manufacturer's instruction. RNA quality and quantity were determined with Nano-Drop spectrophotometer (Fisher Scientific). cDNA synthesis via reverse transcription was performed using qScript cDNA Synthesis Kit (Quanta BioSciences) for 5 min at 25 ^{0}C, 30 min at 42 ^{0}C, and 5 min at 85 ^{0}C. To evaluate PCR efficiency, cDNA templates from biological samples were diluted to create dilution standard curves. Amplification efficiency of qPCR between 90-100% was considered acceptable. PCR products were purified with QIAquick kit (Quiagen), sequenced and BLAST searched before proceeding to RT-qPCR. RT-qPCR was performed using PerfeCTa® SYBR® Green SuperMix (Quanta BioSciences); initiated at 95 ^{0}C for 3 min, followed by 40 cycles of 95 ^{0}C for 10 s, 59 ^{0}C for 10 s and 72 ^{0}C for 30 s, using Bio-Rad T100 Thermal Cycler (Bio-Rad). Elongation factor 1 alpha (EFα1) was used as a reference to normalize mRNA expression of genes that were predicted to participate in Met transport. EFα1 has been extensively used as

housekeeping gene in different fish species (238, 278, 303, 391). Primer sequences along with Efα1 used for RT-qPCR were listed in Table 3.1.

Table 3.1. Rainbow trout (*Oncorhynchus mykiss*) primer sequences used for RT-qPCR.

SLC*	System (Gene name)	Location	Forward (5' – 3')	Reverse (5' – 3')	Gene Bank Accession #
SLC1A5	ASCT (ASCT2)	AM	AAA GAG TCG GTC ATG TAG AG	GAG AGA AGA CAC AAG GAG AG	XM021587427.1
SLC3A1	$b^{0,+}$ (rBAT)	AM	AGG CCG ATA CAG GTT TAT G	CCC AGT TCC AGT CAG ATT AG	XM021576370.1
SLC7A5	L (LAT1)	BM	TGG TCT GTT TGC CTA TGG	GTG AAG TAG GCC AGG TTA G	XM021568487.1
SLC43A1	L (LAT3)	BM	CTG TTG CCT GGA TAC CTA TT	TAT GCT AGA CCG TTG CTA TG	XM021583981.1
SLC43A2-like	L (LAT4-like)	BM	GAC GGA CGG AGA TTT GTT	GAG AGA GAG AGA GAG AGA GAG	XM021582086.1
SLC7A7	y^+L (y^+LAT1)	BM	GAG GAC TCA ACG CTT CTA TC	CAA CAC ACA GGT AGA CCA A	XM021614955.1
SLC6A19-like	B^0 (B^0AT1-like)	AM	GGT CCA TCC TGT TCT TCA T	TGA CAC CAG ACA GAC AAT AC	XM021562073.1
SLC6A15-like	B^0 (B^0AT2-like)	AM	TCT ACT TCT CCC AGT CCT T	GGA GTC AGA GAT GTT CAG AG	XM021604100.1
SLC6A14	$B^{0,+}$ ($ATB^{0,+}$)	AM	TGG AGT GAC TGT TTC TAC TG	CTG GGA TGC TGA TGA TGT	XM021610363.1
SLC7A3-like	y^+ (CAT3-like)	AM	GTT TAC TGG GCT CAA TGT TC	ATC AGG GCT GCT ACA ATA C	XM021561172.1
SLC3A2	4F2hc	/	GGA TCT GAC TCC CTA CTA TCT	CCC AAA GAG ACG GAA CTA C	XM021591192.1
Housekeeping	EFα1		AGC GAG CTC AAG AAG AAG	GAC CAA GAG GAG GGT ATT C	NM001124339.1

SLC*: Solute carrier
AM: Apical membrane
BM: Basolateral membrane

3.3.5. Flux transport and electrogenic studies in Ussing Chamber

EasyMount Ussing Chambers System model (Physiologic Instruments Inc., San Diego, CA) was used in this study. The Ussing chamber technique was adapted from descriptions in previous works (220, 376). In brief, three intestinal segments (PC, MG, and HG) were mounted as flat sheets on metal pins of the inserts with the exposure of a surface area of 0.3 cm^2. Another insert was put on the top like a sandwich and the unit was then placed into the middle of the chamber and secured with thumbwheel screws. Each side of the chamber reservoirs contained 5 mL fresh teleost saline buffer and oxygenated continuously with 1% CO_2 and 99% O_2 through needle valves. The buffer was maintained at a constant temperature (12 ^{0}C) throughout the experiment by a circulating water jacket connected with a heater.

3.3.5.1. ^{14}C radiolabeled DL-Met flux study

The teleost buffer was prepared freshly to initiate Na^+-dependent experiments. Meanwhile, sodium was iso-osmotically replaced with potassium to perform Na^+-independent experiments. Prior to adding radioactive isotopes, blank samples were taken to ensure that the chambers were not contaminated with isotope from previous use. 0.5 µCi of DL-[^{14}C]Met with the specific activity of 55 mCi $mmol^{-1}$ (American Radiolabel Chemicals) was added to the apical compartment as tracers. 0.5 µCi of [^{3}H]-Inulin with the specific activity of 9.25 MBq/0.5 mCi (PerkinElmer) was used to analyze and determine the viability of the tissues afterward along with resistances. Tissues were excluded if significant inulin flux or a drop in resistance of the tissues was noted. Tissues were allowed to equilibrate for 60 minutes. After equilibration time, unlabeled substrate DL-Met was added to the apical compartment, and mannitol was added to the basolateral compartment with the same concentration to maintain an equal osmolarity. Two sets of experiments were separately studied with two levels of substrate concentration gradient: 0 - 150 µM (21 increasing sequential

concentration) and 0.2 mM - 20 mM (19 increasing sequential concentration). Each level included Na^+-dependent and Na^+-independent experiments in both triploid and diploid trout. In cis-inhibition study, the effects of phenylalanine (20 mM) or leucine (20 mM) on DL-[^{14}C]Met flux were only studied in diploid fish at a concentration gradient of DL-Met 0.2-20 mM. In all cases, each data increment was at 10 min increment. 500 µL samples were taken from "cold side" mixed with 4 mL-UltimaGold cocktail solution (PerkinElmer) and counted using a Scintillation Counter (Beckman Coulter).

The unidirectional fluxes rates were calculated from the appearance of radiotracer on the "cold side" (aka receiver chamber or sink chamber) and specific activity in the "hot side" (aka donor chamber or source chamber) using adapted equation described by Schultz and Zalusky to determine J_{ms} (347). J_{ms} was then used to determine kinetic parameters (J_{max} and K_m).

$$J_{ms} = v_s(P_s2 - cP_s1)/(\Delta t * P_m * A)$$

J_{ms} = unidirectional substrate flux from mucosa to serosa in µmol/cm^2/ hr
v_s = volume of bathing solution perfusing the serosal surface in cm^3
P_s1 = Initial cpm/cm^3 in the serosal reservoir
P_s2 = cpm/cm^3 in the serosal reservoir after increment change
c = correction factor for dilution
A = area of tissue exposed
Δt = time interval between two samples in hour
P_m = specific activity of the radioactive isotopes in the mucosal solution in cpm/µmol

3.3.5.2. Electrophysiological recording

It is well documented that a large number of the transporters involved in Met transports are Na^+-dependent. Therefore, although Met is a neutral amino acid, its transport could be indirectly measured via changes in short-circuit current (I_{sc}) due to the movement of ions such as

Na^+ altering electrical membrane potential. The detailed protocol was followed as manufacturer instruction and described previously in the guide of Ussing chamber technique (72). In brief, to measure the changes in I_{sc}, the Ussing chamber system (Physiologic Instruments Inc., San Diego, CA) included two Ag/AgCl electrodes pairs: one voltage set and one current set measuring the short-circuit current across the fish tissue via agar bridges. The electrodes were attached to a voltage/current clamp (Physiologic Instruments Inc., San Diego, CA). Tissues were then clamped to 0.0 mV and the resulting short-circuit current measured by a computer in µA. The electrode configuration would result in a positive short-circuit current when a cation moves in the mucosal to serosal direction or an anion moving in the serosal to mucosal direction. The tissue was then pulsed with a constant 1 mV pulse to determine tissue resistance every 30s. These electrophysiological recordings were done concurrent to the flux sampling. The changes in currents were used to characterize the presence and function of electrogenic Met transporter, but not to quantify Met transport.

3.4. Kinetic and statistical analysis

To find out J_{max} (presented in µmol/cm^2/ hr), V_{max} (presented in µA/cm^2) and K_m (presented in µM or mM), changes in flux rate and short circuit current over all concentrations were computer fitted to nonlinear regression Michaelis-Menten equation denoted by equation (1) or (2) using GraphPad Prism version 5:

$$J = \{(J_{max} \times [S])/(K_m + [S])\} \quad (1)$$

$$V = \{(V_{max} \times [S])/(K_m + [S])\} \quad (2)$$

where J_{max} was the maximal flux rate and V_{max} was the maximal current at saturable substrate concentration, K_m was the substrate concentration that generated half J_{max} (or V_{max}), and [S] was

the substrate concentration. Results were presented as means ± SEM. The J_{max} and V_{max} values were compared between ploidy using student's *t*-test. Similarly, K_m values were compared between ploidy using student's *t*-test. J_{max}, V_{max} and K_m within intestinal segments of each ploidy were compared using one-way ANOVA, followed by Tukey HSD to determine differences among intestinal segments (PC, MG, and HG). Similar statistical analysis methods were used to analyze RT-qPCR data. All statistical tests were performed using SYSTAT version 13. A P-value less than 0.05 was accepted as a statistically significant difference.

3.5. Results

3.5.1. Genomic and gene expression analysis of trout transporters involved in Met transport

A genomic analysis for putative Met transporters resulted in 11 mRNA sequences of Met-linked transporters and 2 heavy subunits present in rainbow trout out of the 18 known transporters (39, 247). Although genes including y^+LAT2 (SLC7A6), CAT1 (SLC7A1), IMINO (SLC6A20), $b^{0,+}$AT (SLC7A9), and SNAT-1,2,4 (SLC38A-1,2,4) were previously reported to have Met transport function in mammalian and poultry species (39, 62, 228, 247, 276, 367, 437, 445), genomic analysis did not detect these genes. Figure 3.1 illustrates multiple transporters found, emphasizing complexity (both their diversity and similarity) of transporting methionine in the entire animal and gut specifically.

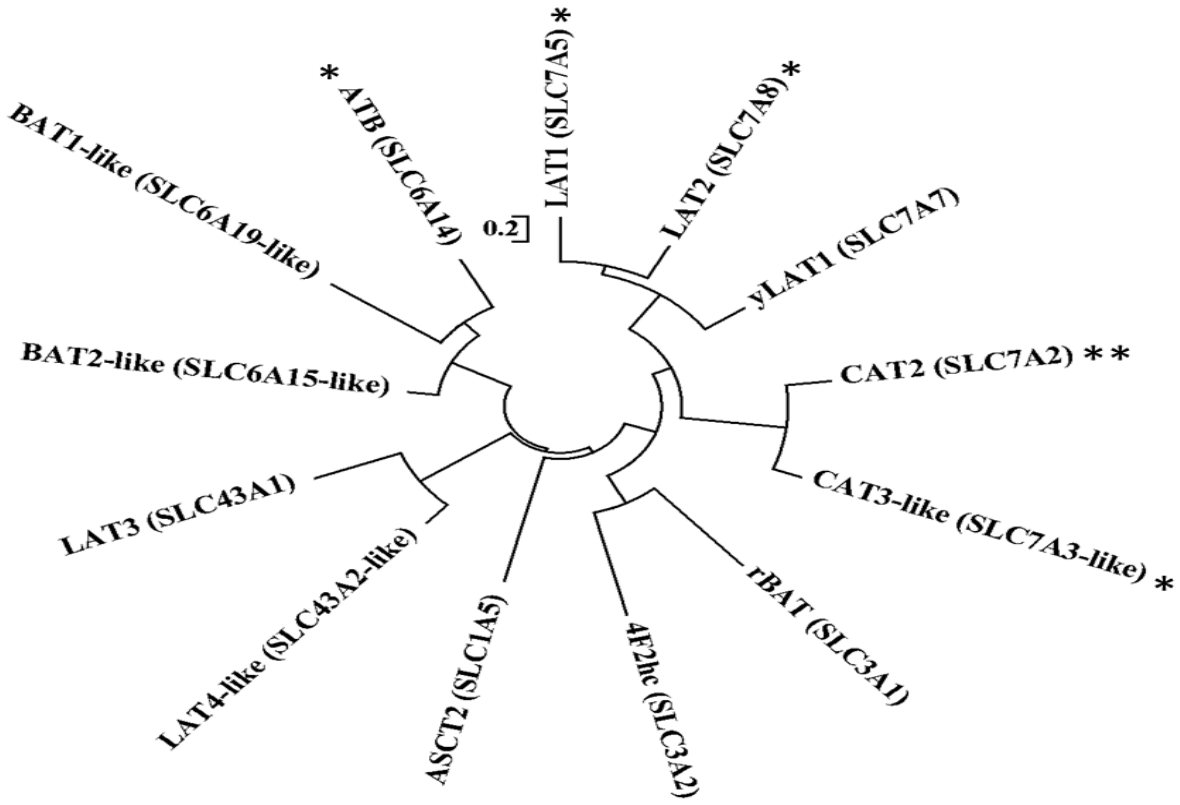

Figure 3.1. Phylogenetic tree of Methionine-linked transporters.

The analysis demonstrates the diversity of transporters that were capable of transporting Met found in the genome of rainbow trout (*Oncorhynchus mykiss*), emphasizing complexity (both their diversity and similarity) of transporting methionine in the entire animal and gut specifically. Transporters with (*) including CAT3-like, LAT1, LAT2 and $ATB^{0,+}$ might have minor role in Met transport due to low mRNA expression. Whereas, mRNA expression of CAT2 (**) was not detectable. Heavy chain 4F2hc typically associated with a number of light chain including LAT1, LAT2 and y^{+}LAT1, meanwhile heavy chain rBAT associated with $b^{0,+}$AT.

Among 11 genes and 2 heavy subunits found in the genome, RT-qPCR was performed in the three intestinal segments of 3N and 2N trout to identify which genes were present and potentially responsible for Met transport along the trout gut. Despite being present in the trout genome, RT-qPCR did not detect CAT2 (SLC7A2) in the intestine; while CAT3-like (SLC7A3-like), LAT1 (SLC7A5), LAT2 (SLC7A8) and $ATB^{0,+}$ (SCL6A14) had exceptionally low mRNA expression. More specifically the relative expression of these genes to EFα1 was less than 0.005, suggesting a minor or insignificant role of these transporters in gut methionine transport of rainbow trout. However, RT-qPCR analysis identified six candidate genes that might have direct contribution to Met transport and regulation in the intestine of rainbow trout including ASCT2 (SLC1A5), B^0AT1-like (SLC6A19-like), B^0AT2-like (SLC6A15-like), y^+LAT1 (SLC7A7), LAT3 (SLC43A1), and LAT4-like (SLC43A2-like) along with the heavy subunits rBAT (SLC3A1) and 4F2hc (SLC3A2) which were typically required for some transporters to be functional.

More specifically, RT-qPCR results showed that there was the mRNA expression of both high-affinity transporters (ASCT2, y^+LAT1, B^0AT2-like) and low-affinity transporters (B^0AT1-like, LAT3, LAT4-like). Details of the gene expression were presented along with kinetic analysis in the following sections. Due to the two transporter populations (high affinity and low affinity transports) we performed flux experiments in both micromolar (0-150 μM) and millimolar (0.2-20 mM) substrate concentration ranges to characterize the kinetics associated with these genes. Furthermore, these ranges were chosen due to relevance in aquaculture where plant-based diet could have exceptionally low methionine and supplementation could increase levels to mM concentration.

3.5.2. Transport of DL-Met at micromolar concentration

^{14}C radiolabeled Met flux

DL-[^{14}C]Met flux rate was performed in the presence or absence of Na^+ at a range of substrate concentration of 0-150 µM. In Na^+ buffer, the flux rate of DL-[^{14}C]Met in all three intestinal segments exhibited saturable kinetics with increasing concentration of DL-Met (Figure 3.2). Segmental comparison demonstrated that the flux rate (J_{max}) was signficantly higher in the PC and MG than in the HG. Table 3.2 showed that this phenomenon was observed in both types of ploidy ($P < 0.0001$). Moreover, ploidy comparison demonstrated that DL-[^{14}C]Met flux rate in the gut of 3N trout (0.003, 0.006 and 0.002 µmol/cm^2/hr in PC, MG and HG respectively) was statistically higher than that of 2N trout (0.0019, 0.0021, and 0.0006 µmol/cm^2/hr in PC, MG and HG respectively). The analysis of kinetic constants revealed that the high affinity for DL-[^{14}C]Met was identical (K_m values between 4-5 µM) in the entire intestinal tract regardless of type of ploidy or segment. On the contrary, the flux rate of DL-[^{14}C]Met was not a function of substrate concentration when the assays were carried out in Na^+-free buffer. Data from sodium free experiments could not be fitted to Michaelis-Menten kinetics nor linear regression (negative or poor R^2 values). These observations indicated that DL-Met transport at micromolar concentrations was strictly dependent on the existence of a Na^+-dependent, high-affinity transporter.

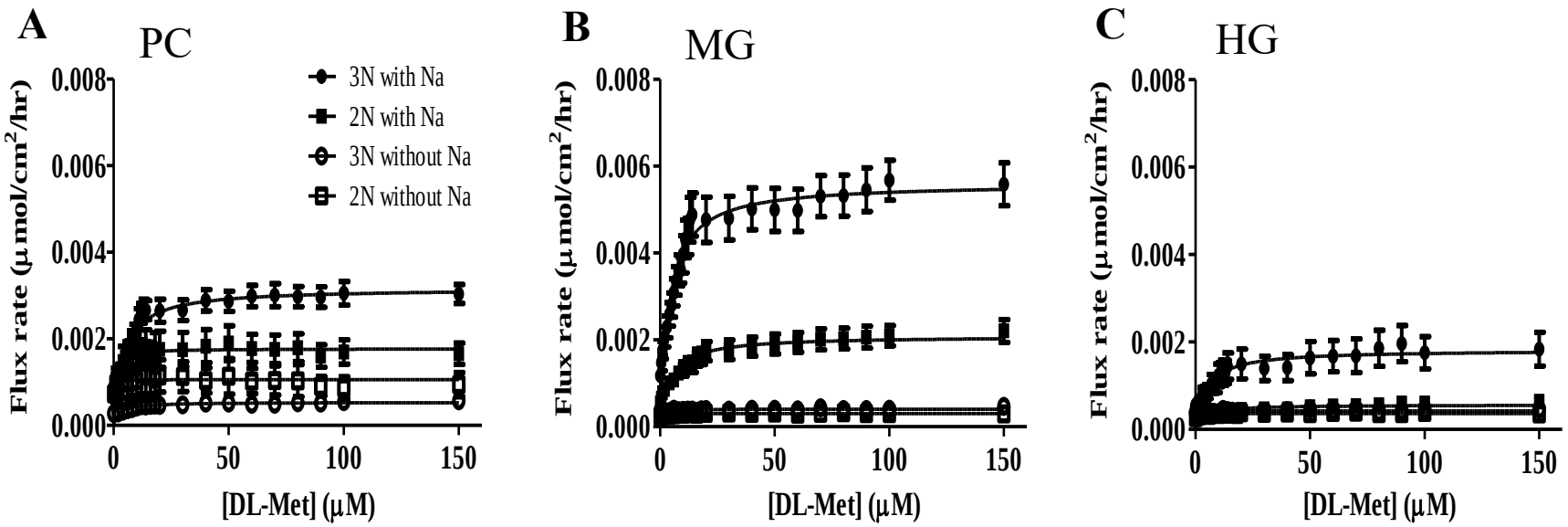

Figure 3.2. Transport of DL-Met at micromolar (µM) concentration.

Michaelis-Menten plots for the DL-[^{14}C]Met flux assays in the presence of Na^+ (N = 19-25) and absence of Na^+ (N=17-20) in (A) pyloric caeca (PC), (B) midgut (MG) and (C) hindgut (HG) of triploid (● 3N, ○ 3N) and diploid (■ 2N, □ 2N). Experiments were carried out with DL-Met gradient from 0-150 µM (21 increasing sequential concentration). Each data point was expressed as mean ± SEM.

Table 3.2. Transport of DL-Met at micromolar (µM) concentration.

	J_{max}(µmol/cm^2/hr)			K_m (µM)		
Intestinal segments	**Triploid**	**Diploid**	**J_{max} between triploid vs. diploid (P-value)**	**Triploid**	**Diploid**	**K_m between triploid vs. diploid (P-value)**
PC	0.003 ± 0.0003	0.0019 ± 0.0003	0.004*	5.48 ± 0.65	4.01 ± 0.86	0.324
MG	0.006 ± 0.0005	0.0021 ± 0.0003	<0.0001*	4.64 ± 0.41	4.71 ± 0.71	0.930
HG	0.002 ± 0.0004	0.0006 ± 0.00001	0.007*	3.93 ± 0.84	4.33 ± 0.95	0.753

J_{max} and K_m values generated by DL-[^{14}C]Met isotope flux along the GI tract of rainbow trout in the Na^+ buffer, substrate DL-Met gradient from 0-150 µM. Values were expressed as mean ± SEM (N=19-25). Asterisks represent significant difference in J_{max} between ploidies (Student's *t*-test, *p<0.05).

Gene expression of high-affinity transporters candidates affirmed high-affinity transport kinetics at micromolar concentrations

Among genes identified, ASCT2 (SLC1A5) and B^0AT2-like (SLC6A15-like) were Na^+-dependent, high-affinity transporters located in the apical membrane. There were statistically significant differences in gene expression between 2N and 3N trout. Figure 3.3A showed that mRNA expression of ASCT2 in PC (P=0.005) and MG (P=0.026) of triploid were significantly greater than that of diploid. This supports the greater transport rate in 3N fish at micromolar concentrations. A similar difference was observered with B^0AT2-like mRNA expression (Figure 3.3B, $P < 0.05$ in all three intestinal segments). However, the expression of B^0AT2-like transporter was less than ASCT2, particularly in diploid fish.

Additionally, y^+LAT1 (SLC7A7), a Na^+-dependent, high-affinity transpoter usually localized in the basolateral membrane was found to have expression throughout the intestine (Figure 3.4A). Data analysis revealed that mRNA expression of y^+LAT1 was significantly lower in HG than in PC and MG ($P = 0.019$ in triploid, $P = 0.037$ in diploid). There was no difference in the expression of 4F2hc, a heavy subunit of y^+LAT1 (Figure 3.4B). Finally, heavy chain rBAT (SLC3A1) of Na^+-independent, high-affinity apical transporter $b^{0,+}AT$ (SLC7A9) was found to have dominant expression along the trout gut, particularly in HG (data not shown). However, RT-qPCR could not be performed for the conducting light chain $b^{0,+}AT$ due to its absence in the genome. This was consistant with our flux studies which showed no transport of Met in Na^+-independent experiments, suggesting that rBAT/$b^{0,+}AT$ did not directly facilitate the Met uptakes. Thus, we assumed that Met transport at the concentration 0-150 µM was primarily mediated by ASCT2 and y^+LAT1.

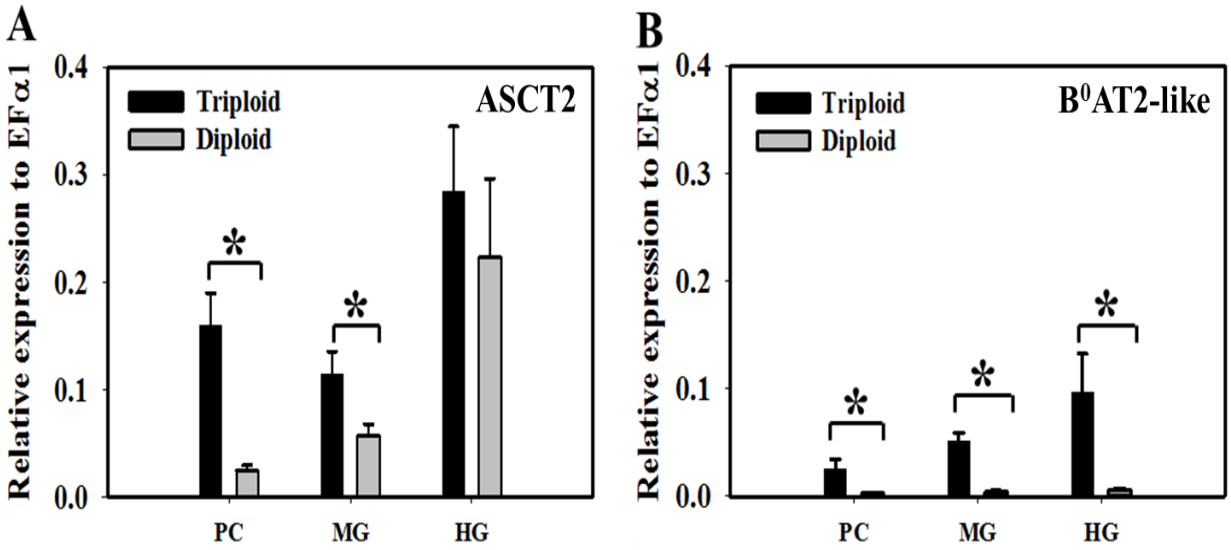

Figure 3.3. Expression of sodium dependent high-affinity (μM) apical transporters.

A) Relative mRNA expression of Na^+-dependent high-affinity apical transporter ASCT2 (SLC1A5). **B)** Relative mRNA expression of Na^+-dependent high-affinity apical transporter B^0AT2-like (SLC6A15-like) in pyloric caeca (PC), midgut (MG), and hindgut (HG) of triploid and diploid rainbow trout using RT-qPCR. Housekeeping gene EFα1 was used for normalization of mRNA abundance data. Values were expressed as means ± SEM (N=8-10). Asterisks represent significant differences between ploidy (Student's *t*-test, $p < 0.05$).

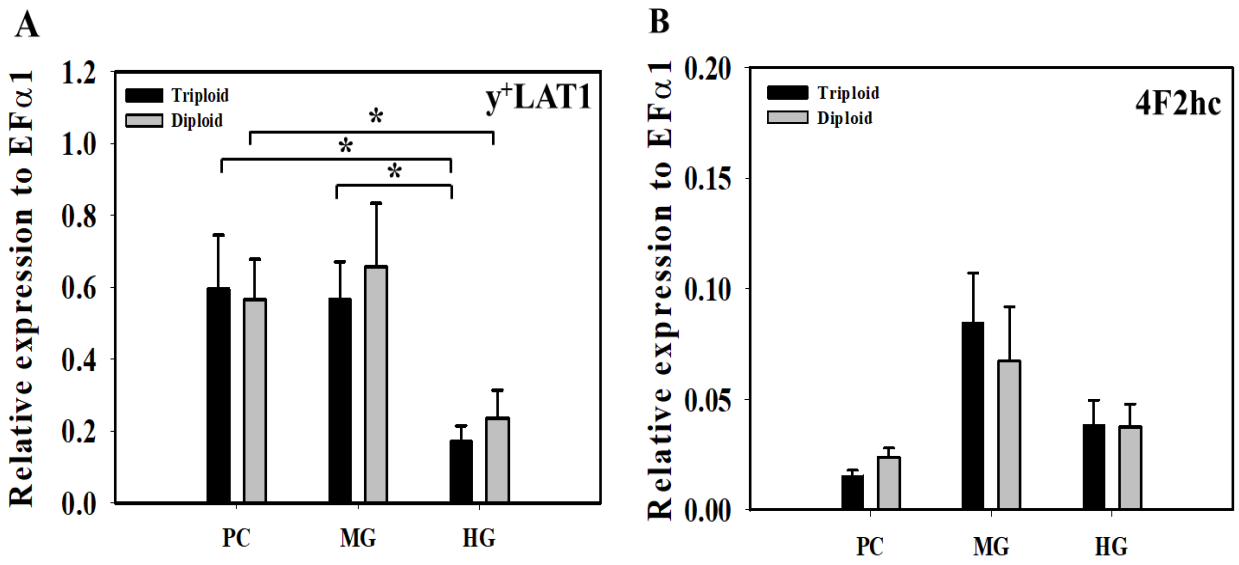

Figure 3.4. Expression of sodium dependent high-affinity (µM) basolateral transporter and its heavy subunit.

A) Relative mRNA expression of Na^+-dependent high-affinity basolateral transporter y^+LAT1 (SLC7A7). **B)** Relative mRNA expression of heavy subunit 4F2hc (SLC3A2) in pyloric caeca (PC), midgut (MG) and hindgut (HG) of triploid and diploid rainbow trout using RT-qPCR. Housekeeping gene EFα1 was used for normalization of mRNA abundance data. Values were expressed as means ± SEM (N=8-10). Asterisks represent significant differences among intestinal segments (one-way ANOVA, $p < 0.05$).

Electrophysiological recordings supported the presence of apical transporter ASCT2 and basolateral transporter y^+LAT1 functional expression

In the presence of sodium, DL-Met gradient induced an I_{sc} change in the intestine of rainbow trout. Increasing substrate concentration from 0-150 µM resulted in a negative I_{sc} in the PC and MG; and a positive I_{sc} in the HG (Figure 3.5). The changes in I_{sc} were found to display saturable kinetics resulting in a small K_m (micromolar ranges) regardless of segments (Table 3.3). Overall when comparing the effects of ploidy on the rate of short circuit current, V_{max} tended to be higher in 3N trout compared to V_{max} in 2N trout. P-values were 0.012 in PC (3.87 ± 1.10 µA/cm^2 in triploid versus. 1.12 ± 0.19 µA/cm^2 in diploid) and 0.054 in MG (4.24 ± 1.03 µA/cm^2 in triploid versus. 2.94 ± 0.70 µA/cm^2 in diploid), respectively. The larger negative I_{sc} was associated with higher expression of ASCT2 in triploid PC and MG (Figure 3.3A), likely resulting in higher basolateral Met available for y^+LAT1 recycling causing a larger negative V_{max} in triploid (Figure 3.5). However, the positive I_{sc} in the HG was associated with a decrease in y^+LAT1 (Figure 3.4A) and an increase in ASCT2 in both triploid and diploid (Figure 3.3A). The observation of electrophysiological recordings of DL-Met-induced currents and associated gene expression confirmed the possibility of Na^+-dependent, high-affinity transporter ASCT2 and y^+LAT1 facilitated DL-Met uptake at the range of substrate concentration less than 150 µM.

Table 3.3. Electrogenic V_{max} and K_m values generated by DL-Met in Na^+ buffer at micromolar (µM) concentration.

	V_{max} (µA/cm^2)			K_m (µM)		
Intestinal segments	**Triploid**	**Diploid**	**V_{max} between triploid vs. diploid (P-value)**	**Triploid**	**Diploid**	**K_m between triploid vs. diploid (P-value)**
PC	3.87 ± 1.10	1.12 ± 0.19	0.012*	15.5 ± 4.01	14.6 ± 3.31	0.572
MG	4.24 ± 1.30	2.94 ± 0.70	0.054	6.3 ± 1.72	6.2 ± 1.18	0.259
HG	1.94 ± 0.26	1.81 ± 0.34	0.504	13.5 ± 3.47	6.4 ± 1.11	0.052

Values were expressed as mean ± SEM (N=13-18). Asterisks represent significant differences in V_{max} between ploidies (Student's *t*-test, *$p < 0.05$).

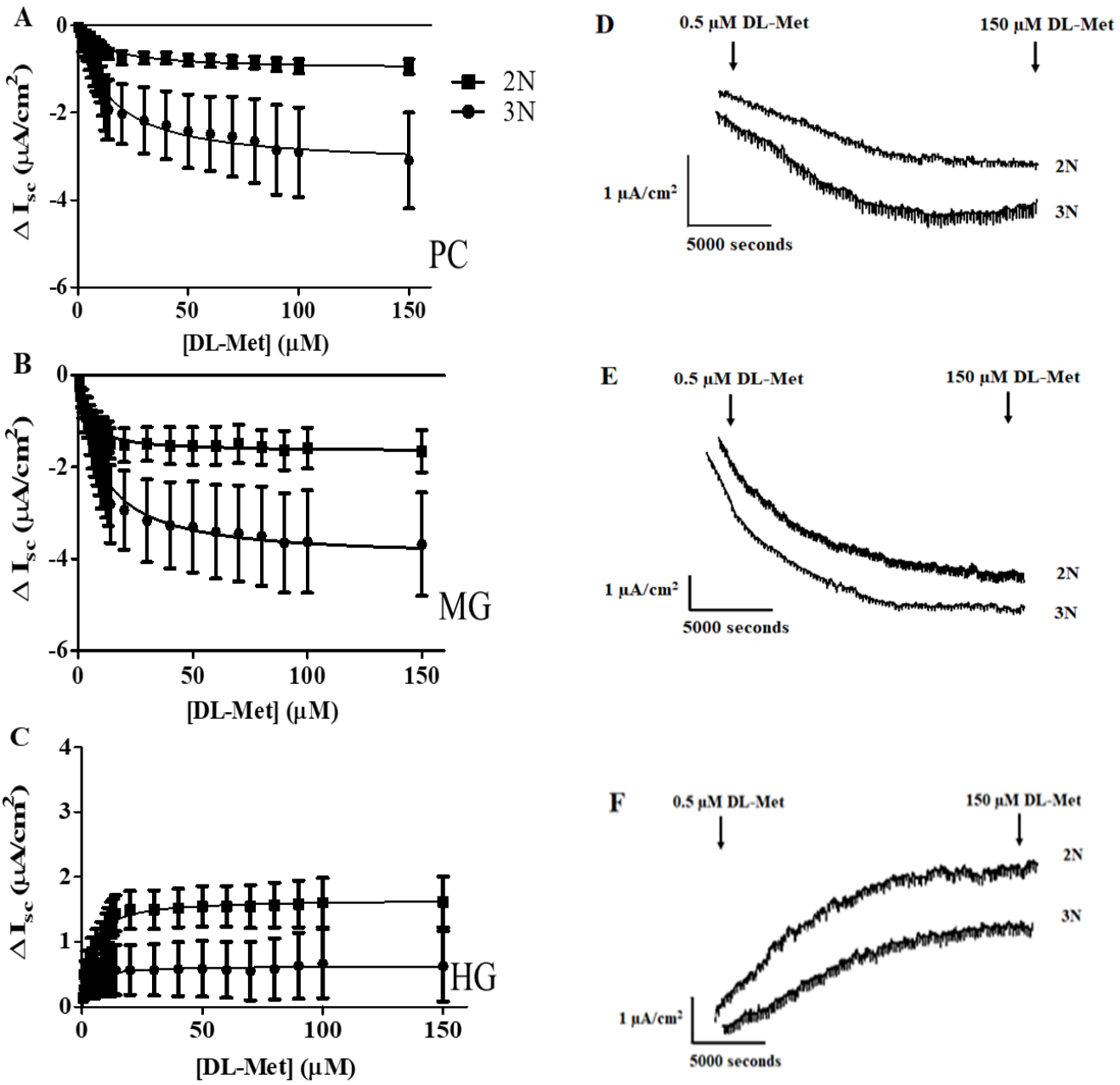

Figure 3.5. Electrogenic short-circuit current (I_{sc}) induced by DL-Met.

Increasing concentrations of DL-Met in Na^+ media induced changes in I_{sc} **(A)** in pyloric caeca (PC), **(B)** midgut (MG), and **(C)** hindgut (HG) of triploid (● 3N) and diploid (■ 2N) with segmental representative traces (D, E, and F) presented on the right side. The DL Met-induced current was plotted as a function of the extracellular substrate concentrations using Michaelis-Menten equation. Experiments were carried out with DL-Met gradient from 0-150 µM (21 increasing sequential concentration). Each data point was expressed as mean ± SEM (N=13-18).

3.5.3. Transport of DL-Met at millimolar concentration

^{14}C radiolabeled Met flux results

DL-[^{14}C]Met flux rate was performed in the presence or absence of Na^+ at a higher substrate DL-Met concentration gradient 0.2-20 mM. In Na^+-conditions, the result demonstrated that the flux rate of DL-[^{14}C]Met at mM concentration fitted Michaelis Menten kinetics, revealing another transporter that mediated Met transport at mM substrate concentration. The kinetic analysis demonstrated low-affinity kinetics (mM ranges) (Table 3.4). J_{max} in PC and MG of 3N trout were 0.0009 ± 0.0001 and 0.0013 ± 0.0001 µmol/cm^2/hr respectively. These were significantly lower than 0.0014 ± 0.0002 and 0.002 ± 0.0002 µmol/cm^2/hr in PC and MG, respectively of 2N trout (Figure 3.6). These differences could be accounted for by the higher mRNA expression of B^0AT1-like in diploid, the significant of which was discussed below. Additionally, data could not be fitted to Michaelis-Menten equation (negative R^2) in Na^+-independent assays and reduced flux to almost zero. This indicated that DL-Met was strictly regulated by Na^+-dependent transporter even at mM DL-Met concentrations.

Table 3.4. Transport of DL-Met at millimolar (mM) concentration.

	J_{max} (µmol/cm^2/hr)			K_m (mM)		
Intestinal segments	**Triploid**	**Diploid**	**J_{max} between triploid vs. diploid (P-value)**	**Triploid**	**Diploid**	**K_m between triploid vs. diploid (P-value)**
PC	0.0009 ± 0.0001	0.0014 ± 0.0002	0.035*	0.65 ± 0.12	0.73 ± 0.10	0.659
MG	0.0013 ± 0.0001	0.002 ± 0.0002	<0.0001*	1.00 ± 0.09	0.98 ± 0.13	0.897
HG	0.0006 ± 0.0001	0.0006 ± 0.00001	0.696	0.55 ± 0.09	0.67 ± 0.14	0.623

J_{max} and K_m values generated by DL-[^{14}C]Met flux assays along the GI tract of rainbow trout in the Na^+ buffer, substrate DL-Met gradient from 0.2-20 mM. Values were expressed as mean ± SEM (N=21-27). Asterisks represent significant difference in J_{max} between ploidies (Student's *t*-test, *p<0.05).

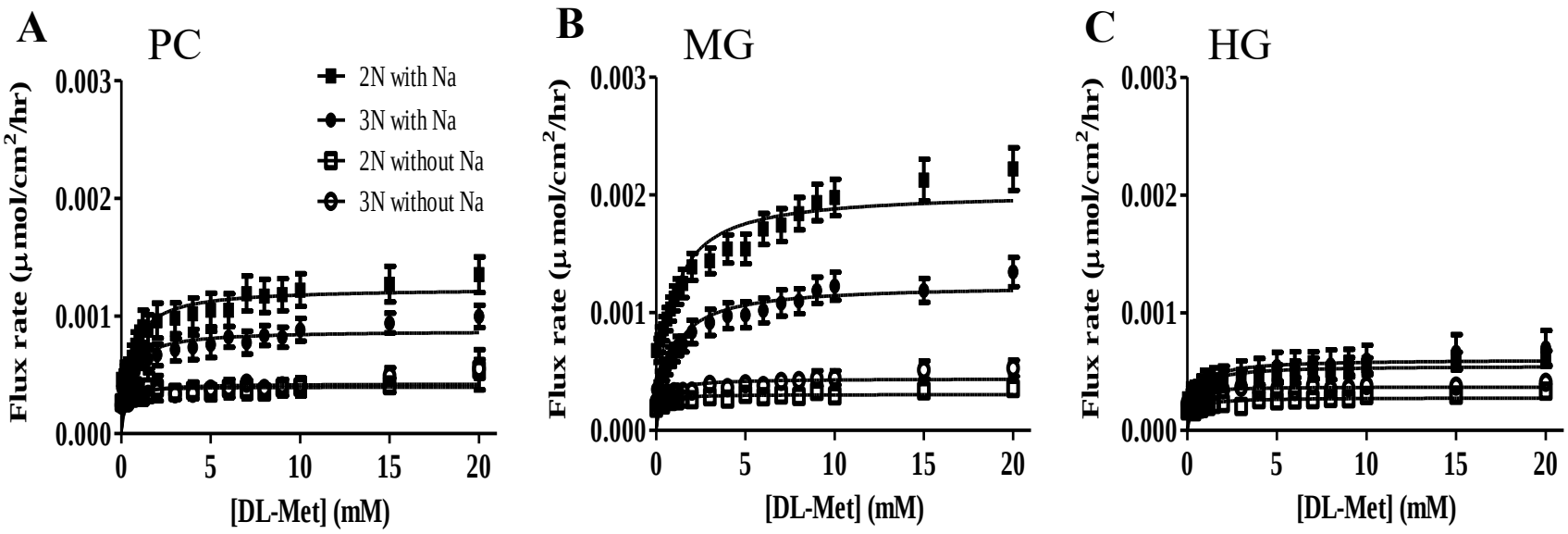

Figure 3.6. Transport of DL-Met at millimolar (mM) concentration.

Michaelis-Menten plots for the DL-[^{14}C]Met flux assays in the presence of Na^+ (N = 21-27) and absence of Na^+ (N = 14-20) in **(A)** pyloric caeca (PC), **(B)** midgut (MG) and **(C)** hindgut (HG) of triploid (● 3N, ○ 3N) and diploid (■ 2N, □ 2N). Experiments were carried out with DL-Met gradient from 0.2-20 mM (19 increasing sequential concentration). Each data point was expressed as mean ± SEM.

Gene expression of low-affinity transporters candidates affirmed low-affinity kinetics

B^0AT1-like (SLC6A19-like) is a Na^+-dependent, low-affinity apical transporter that was found to be expressed throughout the trout gut. Its mRNA expression was significantly higher in diploid than in triploid (Figure 3.7, P=0.009 and P=0.01 in MG and HG respectively, Student's *t*-test) associating with the observed Met flux across the mucosa at mM concentration. Whereas, the low-affinity sodium independent transporter mRNA expession of LAT3 with its undetermined location was low and there was no significant difference between triploid and diploid, exception for PC (Figure 3.8A). On the other hand, LAT4-like (SLC43A2-like) is a Na^+-independent, low-affinity transporter which typically is located in basolateral membrane. Its mRNA expression tended to be higher in 2N compared to 3N fish (Figure 3.8B), again supporting greater flux across the serosa. That being said LAT3 contribution was likely minor compared to B^0AT1-like due to the lack of Met transport in sodium-independent experiments along with the low expression of LAT3 mRNA. Thus, B^0AT1-like was likely to be the major contributer to apical transporter mediating Met flux across the intestine at mM concentration. Whereas, transporting Met from enterocytes to the basolateral side was most likely controlled by LAT4-like.

Cis-inhibition study

In diploid trout experiment, common neutral AA substrates of B^0AT1 transporter including phenylalanine and leucine were added to apical bathing buffer with a concentration of 20 mM each. The results demonstrated that both phenylalanine and leucine significantly reduced DL-[^{14}C]Met flux in PC and MG (Figure 3.9) which ranged between 0.0007-0.0009 μmol/cm^2/hr. Although K_m values of radiolabeled DL-Met tended to increase in the dominant presence of phenylalanine and leucine, there were no significant differences (P>0.05). In HG, no inhibitory effects on flux rate and affinity were observed (Table 3.5).

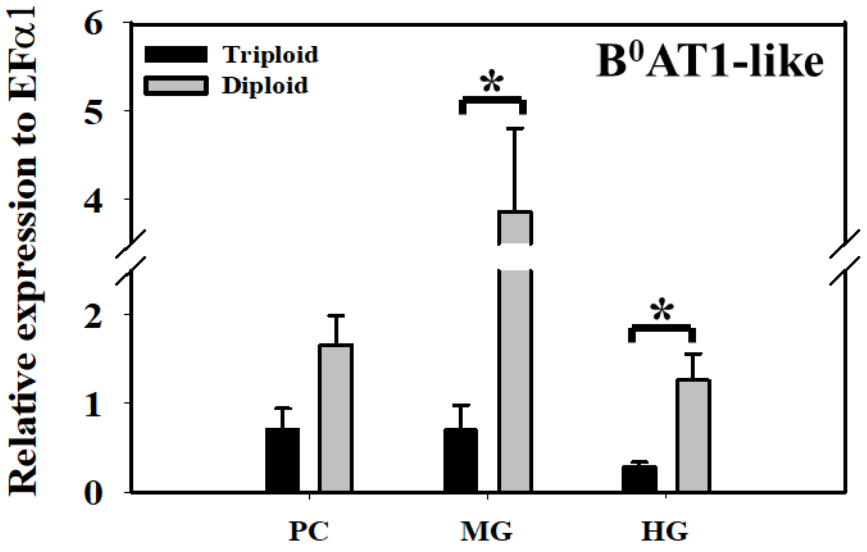

Figure 3.7. Expression of sodium dependent low-affinity (mM) apical transporter.

Relative mRNA expression of Na^+-dependent low-affinity apical transporter B^0AT1-like (SLC6A19-like) in pyloric caeca, midgut and hindgut of triploid and diploid rainbow trout using RT-qPCR. Housekeeping gene EFα1 was used for normalization of mRNA abundance data. Values were expressed as means ± SEM (N=8-10). Asterisks represent significant differences between ploidy (Student's *t*-test, $p < 0.05$).

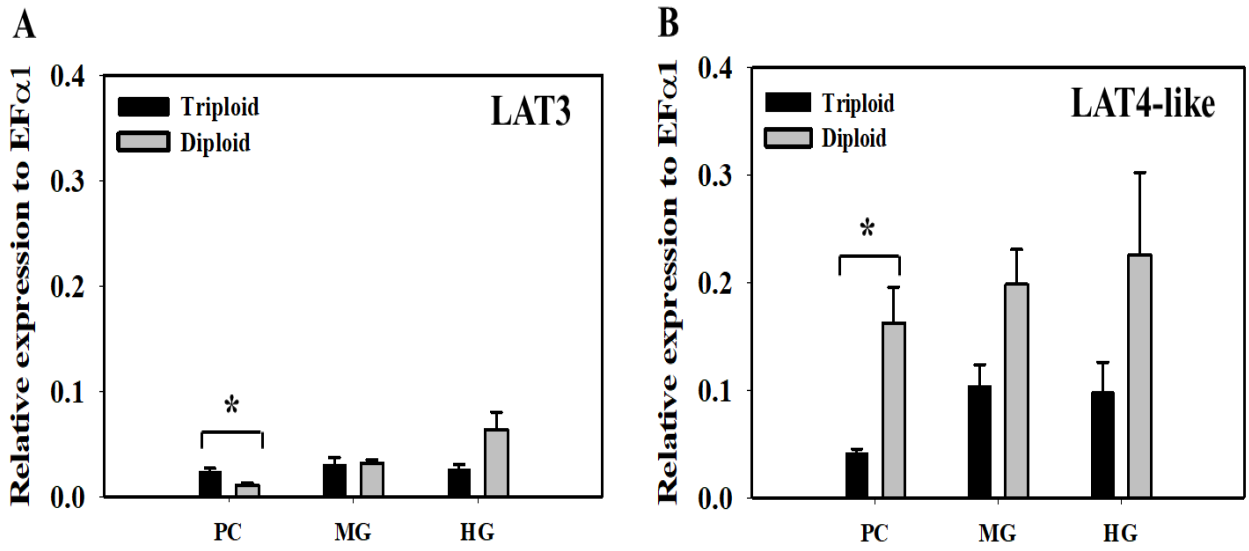

Figure 3.8. Expression of sodium independent low-affinity (mM) transporters.

A) Relative mRNA expression of Na^+-independent low affinity apical transporter LAT3 (SLC43A1). **B)** Relative mRNA expression of Na^+-independent low-affinity basolateral transporter LAT4-like (SLC43A2-like), in pyloric caeca, midgut and hindgut of triploid and diploid rainbow trout using RT-qPCR. Housekeeping gene EFα1 was used for normalization of mRNA abundance data. Values were expressed as means ± SEM (N=8-10). Asterisks represent significant differences between ploidies (Student's *t*-test, $p < 0.05$)

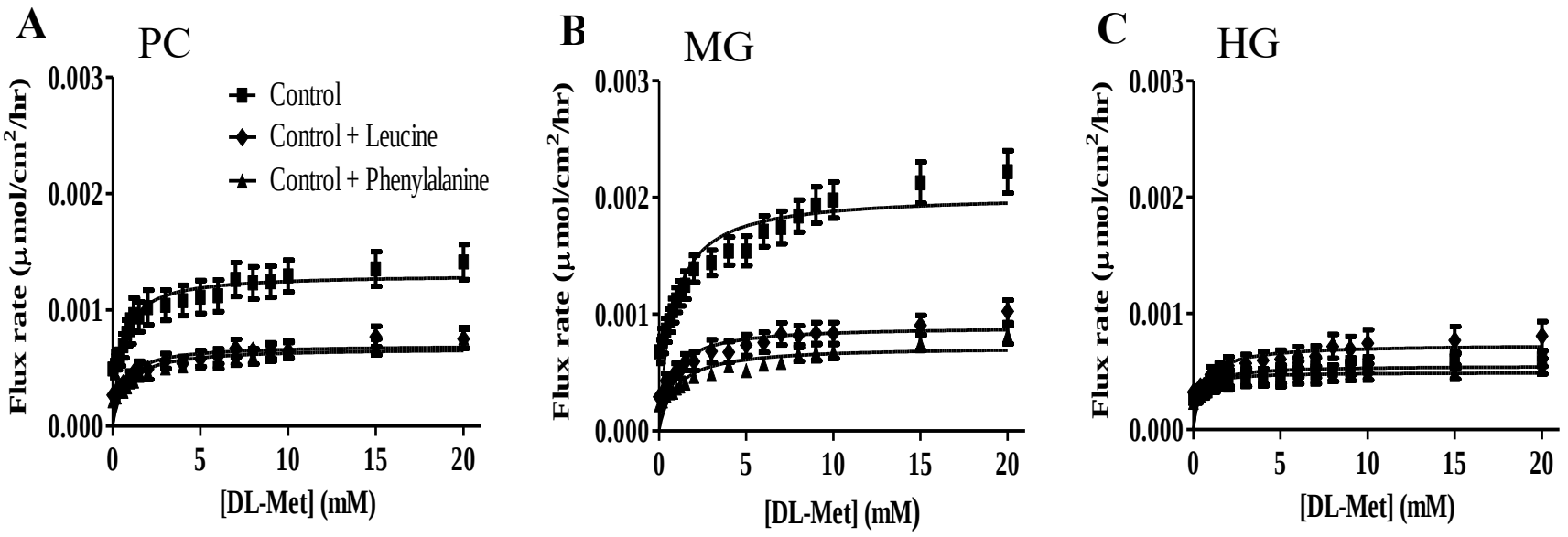

Figure 3.9. Effects of cis inhibition on transport of DL-Met at millimolar (mM) concentration.

Michaelis-Menten plots for the DL-[^{14}C]Met flux control assays (■), or in the presence of 20 mM phenylalanine (▲) or leucine (●) on apical buffer in (A) pyloric caeca (PC), (B) midgut (MG), and (C) hindgut (HG). Experiments were performed in diploid trout with DL-Met gradient from 0.2-20 mM (19 increasing sequential concentration). Values were means ± SEM (N=21-27 control, N=9-11 phenylalanine or leucine).

Table 3.5. Effects of cis inhibition on transport of DL-Met at millimolar (mM) concentration.

	J_{max} (µmol/cm^2/hr)				K_m (mM)			
Intestinal segments	**Control**	**+ Phe**	**+ Leu**	**P-value**	**Control**	**+ Phe**	**+ Leu**	**P-value**
PC	0.0014 (± 0.0002)	0.0007 (± 0.00001)	0.0007 (± 0.00001)	0.002*	0.73 (± 0.10)	1.21 (± 0.23)	0.92 (± 0.21)	0.244
MG	0.002 (± 0.0002)	0.0008 (± 0.00001)	0.0009 (± 0.00001)	<0.001*	0.98 (± 0.13)	1.28 (± 0.24)	0.93 (± 0.14)	0.560
HG	0.0006 (± 0.00001)	0.0005 (± 0.00001)	0.0008 (± 0.00014)	0.349	0.67 (± 0.14)	0.34 (± 0.07)	0.87 (± 0.24)	0.264

J_{max} and K_m values generated by DL-[14C]Met flux assays in the presence or absence of phenylalanine and leucine along the GI tract of diploid trout, substrate DL-Met gradient from 0.2-20 mM. Values were expressed as mean ± SEM (N=21-27 control, N=9-11 phenylalanine or leucine). Asterisks represent significant difference in J_{max} among treatments (one-way ANOVA *$p<0.05$).

Electrophysiological recordings at mM concentration

Attempts to characterize electrogenics at mM concentration were inconclusive (data not shown), with electrophysiological changes not fitting kinetic models. This was possibly due to the competing or opposing electrical signals generated by the apical and basolateral sodium dependent transporters that were more closely paired at mM concentration.

3.6. Discussion

Despite its important roles, there is a scarcity of research investigating the mechanisms of Met absorption in the fish intestine. This study was conducted to differentiate transport routes and transporters participating in Met transport in the trout gut. Here, we postulate that ASCT2 and y^+LAT1 are responsible for Met uptake at µM concentration into the enterocyte from the apical and basolateral locations, respectively. There are five lines of evidence to support our assumption: (1) lack of Na^+-independent kinetics, (2) low expression of Na^+-dependent B^0AT2-like gene, (3) Na^+-dependent, high-affinity (K_m, µM ranges) Met radiotracer flux, (4) association of ASCT2 and y^+LAT1 mRNA expression with high-affinity kinetics, and (5) negative electrogenic currents in PC and MG, positive electrogenic currents in HG induced by Met. B^0AT1-like, however, is responsible for absorption at mM concentration based on the gene expression and Na^+-dependent, low-affinity kinetics (K_m, mM ranges) and cis inhibition. Finally, it would appear that major route of exit for Met from the basolateral side of the epithelium is through LAT4.

3.6.1. ASCT2 and y^+LAT1 associate with DL-Met transport at concentration gradient 0-150 µM

Absences of Na^+-independent transport kinetics support ASCT2 and y^+LAT1 function

At the concentration gradient 0-150 µM, DL-Met transport strictly depends on the presence of Na^+. Removal of Na^+ from the buffer abolished all kinetics properties of DL-[^{14}C]Met flux. This is consistent with the absence of $b^{0,+}$AT, the Na^+-independent high-affinity transporter, in the genome, despite the presence of mRNA expression for rBAT- the heavy non conducting subunit of $b^{0,+}$AT. Although there was no saturable kinetics observed in our flux study in Na^+-free buffer, we cannot rule out the possibility that rBAT/$b^{0,+}$AT might act as an exchanger exporting Met back into the lumen once Met has accumulated inside the enterocytes. This assumption is supported in several studies suggesting that rBAT/$b^{0,+}$AT typically behaves as an obligatory antiporter facilitating the influx of cationic AAs at the expense of neutral AAs efflux (54, 65, 306, 395). However, the role of rBAT in this study is not fully interpreted as there is no genomic presence of $b^{0,+}$AT to create primers for expression analysis. The expression of rBAT without $b^{0,+}$AT is odd, suggesting rBAT interaction with other transporters in fish species. Nonetheless, no Na^+-independent mucosal to serosal flux is observed at µM concentration ruling out a significant contribution of rBAT/$b^{0,+}$AT. Therefore, absences of Na^+-independent transport kinetics and gene expression support ASCT2 and y^+LAT1 function in Met transport.

Low expression of Na^+-dependent B^0AT2-like gene supports ASCT2 and y^+LAT1 function

The question arising is that which Na^+-dependent, high-affinity transporter is responsible for Met-uptake at the concentration gradient 0-150 µM. RT-qPCR results revealed three important gene candidates B^0AT2-like, ASCT2, and y^+LAT1 which could explain the high-affinity sodium-dependent flux. However, B^0AT2-like mRNA expression was relatively insignificant (Figure 3.3B), particularly in the diploid fish compared to ASCT2 and y^+LAT1. Hence, it may not directly contribute to the kinetics observed in diploid and only minor contribution in triploid. This leaves

ASCT2 and y^+LAT1 as the best-fit Na^+-dependent, high-affinity candidates for transporting Met at the concentration of 0-150 µM.

Na^+-dependent, high-affinity (K_m, µM ranges) Met radiotracer flux support ASCT2 function

Observations in the current study predict that DL-Met transport is mediated by the Na^+-dependent, high-affinity transporter ASCT2. In Na^+ conditions, measurements of flux rate versus substrate concentration displayed typical Michaelis-Menten curves with high affinity (K_m between 4-5 µM). These values are lower than K_m values generated by ASCT2 in other research such as 240 µM in pregnant mice tissues (413), and 288 µM in mouse testis (402). The differences in the affinity determinations of the current research with previous studies could be due to two reasons. Firstly, different research techniques are carried out. In our study, tissues were used, and the experiments were performed at a cold physiological temperature of trout (12 ^{0}C); while vesicles, cell lines, or transporter-expressed *Xenopus oocyte* were carried out at room temperature or warmer. Secondly, kinetic properties of a transporter could differ from one species to another to some extent. For example, the K_m for D-Glucose transported by GLUT1 (SLC2A1) varies greatly within species and taxonomic lines; namely 2.5-75 mM in human (51, 84, 143, 151, 431), 14-26 mM in rat (277, 327), or 9.3 mM in rainbow trout (387).

Gene expression supports ASCT2

In the flux studies, K_m values are similar along the intestine while J_{max} in PC, MG, and HG of 3N is statistically higher than 2N trout. A similar K_m implies that Met transport is likely mediated by the same type of transporter along the entire intestine. Meanwhile the difference in J_{max} suggests different density of transporter expression. This correlates well with RT-qPCR results (Figure 3.3A) where higher ASCT2 mRNA expression in the 3N fish is observed, compared to that of 2N fish (P=0.005 and 0.026 in PC and MG, respectively).

Negative currents in PC and MG, and positive currents in HG induced by DL-Met support ASCT2 and y^+LAT1 functional contribution

The functional contribution of ASCT2 and y^+LAT1 was further affirmed by electrophysiological recording associated with the expression of these two transporters. In Na^+-containing buffer, robust negative I_{sc} in PC and MG and positive I_{sc} in HG in both 2N and 3N were found when increasing the concentration of DL-Met.

To give clarity, in our Ussing chambers a negative current would occur if an anion is moving in the mucosal to serosal direction or a cation is moving in the serosal to mucosal direction. On the other hand, a positive current would occur if a cation is moving in mucosal to serosal direction or an anion moving from the serosal to mucosal direction. With this above in mind, it appears that the negative current in PC and MG is due to Met transport through basolateral y^+LAT1 with sodium. It is widely reported that y^+LAT1 is an AA exchanger that mediates influx of basic/cationic AAs within the enterocytes into the blood and re-influx of neutral AAs from the blood back into the enterocytes (41, 307). It transports basic AAs without the requirement of Na^+, whereas it is dependent on Na^+ when transporting neutral AAs (123, 189, 396). This process of neutral AA absorption is thought to be generally electroneutral exchanging the available intracellular basic AAs for Na^+ and the neutral AAs. However, in our Ussing chamber assay we did not supply cationic AAs. Thus, this created a very limited intracellular pool of cationic AA to exchange with Met and Na^+. This would result in an electrogenic signal from y^+LAT1 as Met, a neutral AA can stimulate the efflux of neutral AA through y^+LAT1, while also driving Na^+ uptake (189). Thus, the negative currents observed here are probably due to Na^+ and accumulated fluxed Met entering from the basolateral side of the enterocytes via y^+LAT1. This electrical contribution from y^+LAT1 may also explain why interpretable electrophysiological data was unattainable at

mM concentration, where B^0AT1-like electrical signal (apical entry of sodium) would be masked by y^+LAT1 electrical signal (basolateral sodium entry in the absence of cationic AAs).

On the other hand, the positive currents in the HG could be due to the dominate expression of ASCT2 on the apical membrane and a decrease in y^+LAT1. Although ASCT2 is generally reviewed as a transporter transporting alanine, serine, cystine, glutamine, and asparagine at high affinity (313, 350), it also accepts methionine, leucine, and glycine with lower affinity (312, 402, 413). Studies on the functional characteristics of ASCT2 confirms that the transporter is an obligatory antiporter (exchanger) which utilizes Na^+-electrochemical gradient to equilibrate cytoplasmic glutamine and neutral AAs pools, but the exact stoichiometry of the transport is still unknown (312). The matter of net electrical ion flux generated by ASCT2 is a subject of controversy (33, 340, 402). The positive current in the HG is possibly not due to sodium transport by ASCT2. However, ASCT2 has also been characterized to have channel like anion conductance (37). Thus, if ASCT2 anion conductance is activated by AA transport, the resting membrane potential of the epithelial cell would likely drive chloride out of the cell into the lumen creating a positive current. More specifically, the reduction of basolateral y^+LAT1 would reduce sodium entry on the basolateral membrane (a serosal to mucosal movement) contributing less negative current to the overall tissue and the increase of apical ASCT2 would result in more chloride movement out the cell to the mucosal surface creating a positive current.

Additionally, the higher V_{max} in the 3N was associated with higher expression of ASCT2 in the PC and MG. The higher ASCT2 likely accounts for the larger mucosal to serosal flux, which then results in higher basolateral methionine concentration available for y^+LAT1 reabsorption causing a larger negative V_{max} in triploid (Figure 3.3A). In short, the dominant functional y^+LAT1 expression would produce a negative current when bringing sodium and methionine into the cell

on the basolateral side of the epithelium. This is further supported by gene expression and the positive currents in the HG, where expression of ASCT2 is much higher than the expression y^+LAT1.

The low expression of the sodium dependent transporter B^0AT2-like, and poor association with changes in I_{sc} suggests a very minor contribution in 3N and almost none in 2N. Therefore, B^0AT2-like is unlikely to account for the robust changes in I_{sc} observed between segment and ploidy. Hence, ASCT2 and y^+LAT1 are the most likely major contributors to mediating DL-Met electrogenic currents at the concentration range of 0-150 μM.

3.6.2. B^0AT1-like transporter associates with DL-Met transport at concentration gradient 0.2-20 mM

At the concentration gradient 0.2-20 mM, DL-Met transport was also dependent on Na^+ as the driving force for absorption. Repeatedly, the flux of DL-[^{14}C]Met was absent when sodium was removed from the buffer. Flux measurement without Na^+ could not be mathematically modeled using both either linear or non-linear regression. This reinforces the role of sodium in regulating AAs absorption of teleost species (14, 182, 226, 232, 255, 262, 364, 417).

Supporting this sodium dependent flux at mM concentrations was the strong expression of B^0AT1-like transporter gene. B^0AT1, is a Na^+-dependent apical transporter, typically has a low affinity (K_m in mM ranges) likely eliminating its contribution to the flux at μM concentration (39, 200). Therefore, the B^0AT1-like transporter is the sole candidate gene that could participate in Met absorption at high substrate concentration. This is supported by the gene expression which is higher in diploid compared to triploid (Figure 3.7), resulting in greater J_{max} in diploid. The transporter belongs to system B^0. The system has been previously identified in brush border membrane preparations (268, 322), a bovine renal epithelial cell line (93), and Caco-2 cells (368).

These works have demonstrated that system B^0 accepts all neutral AAs, obviously with varying affinity levels. Mouse B^0AT1 transporter studied in the *X.* oocyte expression system using two electrode voltage-clamp techniques and tracers shows that K_m values for neutral AAs ranged between 1-10 mM (29). Preston and coworkers (322) found that the L-Met maximal influx and affinity in rabbit ileum were 2.2 μmol/cm^2/hr and 1.6 mM, respectively over a concentration range of 0.1-16 mM. This is relatively compatible with our study in terms of results. The K_m calculated in the present study for high concentration 0.2-20 mM were between 0.6-1.0 mM in both triploid and diploid trout (Table 3.4). The maximal flux in our study is lower, which could be due to differences in species, the isomeric form of substrate, or the involvement of other Met transporters. The contribution of B^0AT1 in DL-Met transport is further supported by cis inhibition study in which flux rates are reduced but affinities are unchanged. This indicates that phenylalanine and leucine are non-competitive substrates that could compete with Met for the same transporter. It is important to note that high concentration of phenylalanine and leucine are used in the inhibition study to demonstrate the presence of B^0AT1 (or LAT4) and its broad substrate specificity for neutral AAs. This is not necessary to imply the inhibitory effects of these AAs on Met absorption by fish in practical feed formulation.

Lower J_{max} at mM concentration

Noticeably, the J_{max} observed in the mM concentration gradient is lower than the J_{max} in the μM concentration gradient. A comprehensive explanation for this phenomenon requires understandings about transport modes and expression of genes involved. Met exit from the enterocytes across the basolateral membrane is most likely mediated by LAT4-like transporter, based on expression levels (Figure 3.8B), the absence of other known basolateral transporters in the genome and LAT4's previously defined basolateral function in mammalian species. The

preferential substrates of LAT4 included branched-chain AAs, phenylalanine, and methionine (27). Transport via LAT4 expressed in *X. laevis oocytes* is Na^+-independent with low affinity: K_m for L-phenylalanine was between 4-6 mM (27, 148). The role of LAT4 is further validated with a knockout model in which mice lacking LAT4 protein suffer growth defects and early postnatal lethality, presumably due to malnutrition with low Met and branched-AAs in plasma (148).

However, the expression of the LAT4-like transporter is substantially less than that of B^0AT1-like transporter potentially resulting in DL-Met accumulation in the enterocytes. If this is occurring, accumulative cytosol Met must be exported back into the lumen. This may explain why the maximal flux rate is smaller in HG than in PC and MG, due to high expression of ASCT2. This notion is supported by the observation that several AAs can be bidirectionally transported by ASCT2 (33, 85). For example, human ASCT2 expressed in *Pichia pastoris* shows that extracellular side displays high affinity (micromolar range K_m), while intracellular side shows low affinity (millimolar range K_m) when analyzing the kinetics of [^{3}H]glutamine (312). Thus, in our study when methionine reaches mM concentration, ASCT2's low internal affinity could then transport methionine back to the lumen decreasing J_{max}. However, based on our current understanding of ASCT2 stoichiometry it likely only recycles at the higher concentration. Thus, this suggests an alternative channel with an internally low K_m allowing back flux. A possible candidate would be $b^{0,+}$AT as we have found high expression of associated rBAT (data not shown). However, we are unable to find $b^{0,+}$AT in the trout genome, suggesting a yet to be identified channel interacts with rBAT. This is not surprising as rBAT has been suggested to associate with an unidentified subunit in the kidney (114). For instance, renal apical membrane transporter AGT1 (SLC7A13) has been identified as the second partner of rBAT involving in cystine reabsorption (274), but it has not been proven to transport Met.

3.7. Conclusion

Amino acid transporters have been intensively studied in the intestine of mammalian species. Here we present the very first description of the kinetic properties of Met epithelial transport and associated transporter gene expression in fish intestine. Similar to mammals, sodium is physiologically important for many nutrient transport functions in fish. In this study, we have clearly demonstrated that it is the driving force governing Met absorption in trout intestine through the Na^+-dependent transporters. The mucosal to serosal flux of DL-Met at µM concentration gradient seems to be primarily governed by the apical ASCT2 transporter. This is supported by gene expression, Na^+-dependence, and a high affinity kinetics (K_m in µM ranges) that are relatively similar to basic functional properties of ASCT2 that have been described by others in literature (37, 135, 340). Meanwhile y^+LAT1 may play a role in the basolateral reabsorption of methionine. This is supported by electrogenics and gene expression of y^+LAT1. At mM concentration, evidence including Na^+-dependence, low affinity kinetics (K_m in mM ranges), cis inhibition and association of gene expression suggest that transport at these concentrations is primarily mediated by apical B^0AT1-like transporter. Genomic and gene expression analysis along with lower J_{max} in the mM concentration suggest the sole contribution of basolateral exit of methionine through a LAT4-like transporter. This first description begins to define the overall mechanism of methionine transport in trout intestine which is summarized in Figure 3.10.

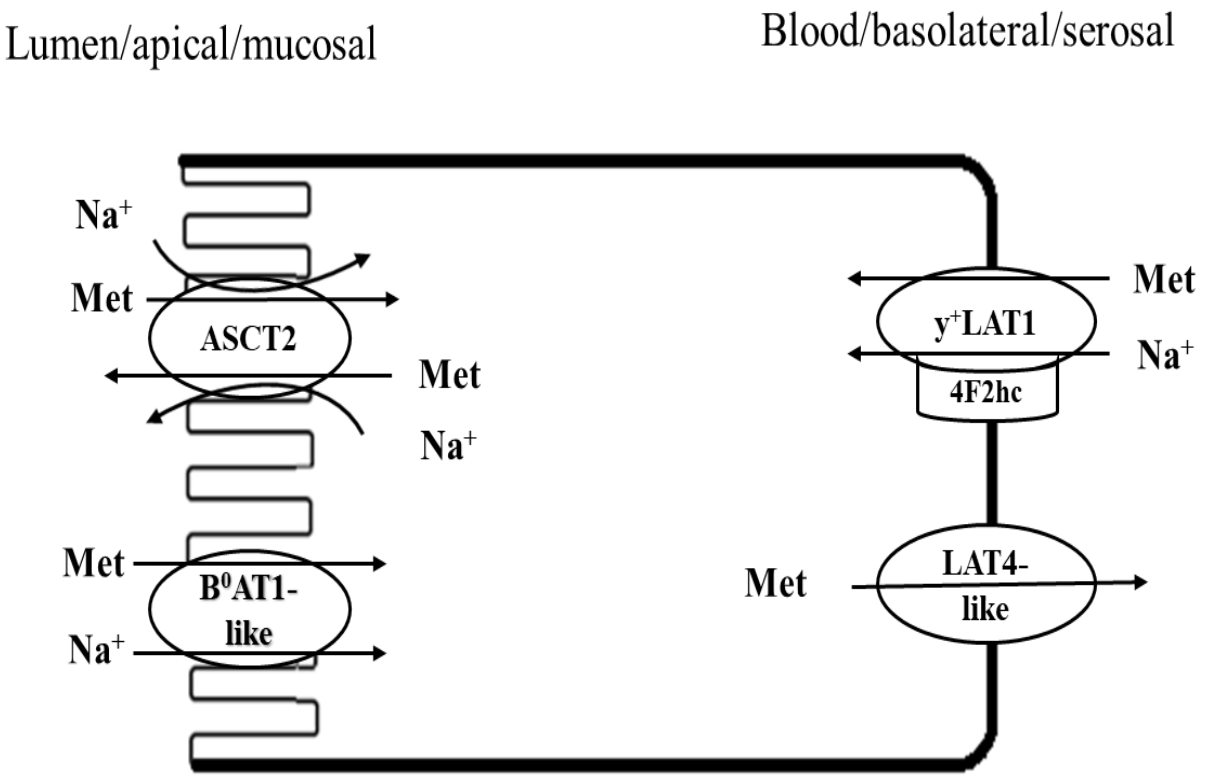

Figure 3.10. Schematic model of Methionine transport in the intestine of rainbow trout.

At µM concentration, Met uptakes across the mucosal membrane of epithelial cells were facilitated by the Na^+-dependent high-affinity apical transporter ASCT2 (SLC1A5). At mM concentration, Met was taken up into the epithelium via the Na^+-dependent low-affinity apical transporter B^0AT1-like (SLC6A19-like). Whereas, the basolateral transporter LAT4-like (SLC43A2) appeared to be the sole gate controlling Met exit from enterocytes into the blood stream. Presence of 4F2hc/y^+LAT1 (SLC3A2/SLC7A7) on the serosal side allowed some Met to be recycled back into enterocytes, and eventually exported back into the lumen via intracellular low affinity ASCT2 and/or unidentified subunit associates with rBAT.

Transition

The following chapter focuses on addressing the 2nd objective and the 2nd hypothesis. Besides DL-Met, DL-MHA is also used to supplement methionine in deficient diets. It is predicted that DL-MHA is transported by the monocarboxylate carrier mechanism, which is proton-dependent. In mammals, monocarboxylates are mainly produced in the large intestine by bacterial fermentation. Since fermentation is minimal in carnivorous fish, we predict that rainbow trout intestine may be capable of transporting MHA along the intestinal tract. This chapter and some data of chapter 5 have been published in Comparative Biochemistry and Physiology. The chapter has been reformatted from the original manuscript to fit the structure of the thesis.

Objective: Characterize proton-dependent DL-MHA transport in the intestinal tract of rainbow trout using Ussing chamber and gene expression analysis.

Hypothesis: DL-MHA transport is proton-dependent, and there are segmental differences in DL-MHA transport along the intestinal tract of rainbow trout.

Manuscript: To, V.P.T.H.[1], Subramaniam, M.[1], Masagounder, K.[2], Loewen, M.E [1]. Characterization of the segmental transport mechanisms of DL-methionine hydroxy analogue along the intestinal tract of rainbow trout with an additional comparison to DL-methionine. Comp Biochem and Physiol Part A: Molecular and Integrative Physiology (2020): 110776.

[1]Veterinary Biomedical Science, University of Saskatchewan, Saskatoon, SK, Canada
[2]Evonik Nutrition and Care GmbH Rodenbacher Chaussee 4D-63457 Hanau, Germany

Contribution: VT designed and performed experiments, analyzed data and interpreted data, prepared manuscript and revised manuscript. MS helped to design experiments. KM revised manuscript. ML received funding, designed experiments, interpreted data and revised manuscript.

CHAPTER IV
DL-MHA TRANSPORT IN THE INTESTINAL TRACT OF RAINBOW TROUT

4.1. Abstract

The aim of this study was to identify the unknown transport mechanism of the extensively used monocarboxylate methionine feed supplement DL-methionine hydroxyl analogue (DL-MHA) in rainbow trout. Here characterization of DL-MHA transport was performed in segmental regions of trout intestine: pyloric caeca (PC), midgut (MG), and hindgut (HG). These anatomic locations were placed in Ussing chambers and the Na^+- and H^+-dependence of DL-[^{14}C]MHA flux were kinetically studied. Gene expression of monocarboxylate (MCTs) and sodium monocarboxylate transporters (SMCTs) were assessed to determine any association between transporter expression and function. Results demonstrated that DL-MHA transport from 0.2 - 20 mM concentration was Na^+-dependent and obeyed Michaelis-Menten kinetics. J_{max} and K_m were 0.0007-0.0009 ± 0.00001 µmol/cm^2/hr and ~1 mM, respectively in PC and MG in apical/basal pH of 7.7/7.7. Changes in apical/basal pH (6.0/6.0, 6.0/7.7, and 7.7/8.7) had insignificant effects on kinetics in PC and MG. In contrast, HG flux kinetics were only obtained in pH 7.7/8.7 or in the presence of lactate with medium affinity. Finally, incremental increases from 0-150 µM demonstrated the potential presence of another Na^+-dependent high-affinity transporter (K_m in micromolar ranges) in PC and MG. Conclusively, two distinct carrier-mediated DL-MHA transport mechanisms along the trout gut were found: 1) in PC and MG: apical transport of DL-MHA was regulated by Na^+-requiring systems that possibly contained low- and high-affinity transporters, and basolateral transport was primarily achieved through H^+-independent transporter; 2) in HG: uptake was apically mediated by a Na^+-dependent medium-affinity transporter, and basolateral exit was largely controlled by an H^+-dependent transporter.

4.2. Introduction

Classified as an essential amino acid (EAA), methionine (Met) and its metabolic precursors participate in numerous biochemical processes such as protein synthesis, immune defence, and physiological homeostasis. One of the most important metabolites of Met cycle is S-adenosylmethionine (SAM), which donates methyl group for a wide range of receptors such as nucleic acids, phospholipids, and protein; subsequently used for over 100 methylation reactions (248). Due to its importance, dietary Met in plant-based aquaculture feed is commonly supplemented with DL-methionine (DL-Met) or liquid methionine hydroxy analogue free acid DL-2-hydroxy-4-(methylthio)butanoic acid (DL-HMTBA-FA, or DL-MHA in short), or DL-MHA calcium salt. MHA molecular structure is chemically unlike Met, in which the amine group (NH_2) is replaced by the hydroxyl group (OH). Therefore, MHA is a monocarboxylate rather than a true AA, which has a different transport pathway compared to Met. A large number of studies have compared the difference in bioefficacy of the two products. Several studies in poultry (99, 172, 209, 300, 390) and pigs (113, 194, 288, 448) have demonstrated that bioefficacy of DL-MHA is significantly lower than DL-Met. Similarly, studies in fish have shown lower bioefficacy of DL-MHA relative to DL-Met (192, 331). Recently, Powell et al. (319) demonstrated in rainbow trout that calcium salt of DL-MHA was only 60-73% biologically available relative to DL-Met depending on performance parameters. Studies in poultry and swine have demonstrated the possible physiological reasons behind for differences observed in biological efficacy using radiolabelled methionine sources (95, 104, 231, 234). However, such understanding is mostly lacking in fish. Information about how DL-MHA transports would greatly aid in our understanding of the differences in bioefficacy between the two. Additionally, it would begin to give insight into monocarboxylate transport in the trout gut, which has not been characterized.

As a monocarboxylate, DL-MHA is thought to be transported by either two families: SLC16 family comprises of proton-linked monocarboxylate transporters (MCTs), and SLC5 family comprises of sodium-linked monocarboxylate transporters (SMCTs). Maenz and Engelle-Schaan (230) originally describes the dependence of H^+ in MHA transport in chick intestinal brush border membrane vesicles (BBMV). Likewise, DL-MHA transport in Caco-2 cells is H^+-dependent and demonstrates similar characteristics with MCT1 (245). MCT-1,2,3,4 are known as proton-coupled transporters of monocarboxylate compounds such as pyruvate, lactate, and ketone bodies (155–157). Whereas MCT9 and possibly other members are thought to be proton-independent (379). Furthermore, the transport of DL-MHA is demonstrated to be Na^+-independent in chick intestinal BBMV and X*enopus* oocytes injected with poly(A)$^+$ RNA isolated from broiler intestinal mucosa (32, 298); while partial Na^+-dependence of MHA uptake is reported in everted sacs of the chicken small intestine by Martín-Venegas and co-workers (244). Differences in techniques and experimental species may have resulted in the absence or presence of the observed sodium dependence. Thus, monocarboxylate or MHA transport across the trout gut may be sodium- or proton-dependent or independent.

Previous studies have demonstrated that MCTs and SMCTs play a major role in transporting short-chain fatty acids (SCFAs-products of dietary fiber fermentation by colonical bacteria) (130, 198, 266) and there are segmental differences in SCFAs transport observed in mammalian intestine (353, 419). Therefore, here we characterize the segmental differences of DL-MHA transport kinetics in trout intestine in Ussing chambers, along with identifying the association of candidate MCT/SMCT genes involved in the DL-MHA transport. The DL-[^{14}C]MHA flux was kinetically characterized in Na^+- and H^+-dependent conditions. The results of radiolabeled substrate flux kinetics and association between gene expression and physiological

transport suggested that DL-MHA transport across the PC and MG was different from HG. Specifically, the apical influx in the PC and MG was mediated by low- and high-affinity Na^+-dependent transporters, and basolateral efflux was H^+-independent. Whereas, it appeared that apical influx into the HG cells was governed by a Na^+-dependent medium-affinity transporter with basolateral exit controlled by an H^+-dependent transporter.

4.3. Materials and methods

4.3.1. Fish source and husbandry

The animals used in this research were maintained in accordance with the guidelines of the Canadian Council on Animal Care (59). All animal procedures were approved by the Animal Care Committee at the University of Saskatchewan (AUP#: 20170056). Rainbow trout (*Oncorhynchus mykiss*) were purchased from BandB Freshwater Fish Farm (Gunton, Manitoba, Canada). Fish were kept in an indoor recirculating system. Water quality was monitored and maintained at desirable conditions for optimal health. Oxygen was maintained at above 6 mg/L with air stones, and the temperature was kept at 11-12 ^{0}C with a chiller throughout the trials. Floating commercial feed containing 45% crude protein and 16% lipid manufactured by EWOS Canada Limited (Surrey, British Columbia, Canada) was offered twice per day at the daily ration of 2-3% fish body weight.

4.3.2. Intestinal tissue collection

Healthy rainbow trout about 100 - 350 g each were transferred from the housing tank to the lab for gut collection. Fish was euthanized by blunt force trauma to head. After dissection, luminal contents such as feces and uneaten feed were removed. The collected intestine segments (PC, MG, and HG) were rinsed with physiological teleost buffer containing the following

composition (in mM):118 NaCl, 2.9 KCl, 2.0 $CaCl_2 \cdot 2H_2O$, 1.0 $MgSO_4 \cdot 7H_2O$, 0.1 $NaH_2PO_4 \cdot H_2O$, 2.5 Na_2HPO_4, 1.9 $NaHCO_3$, and 5.6 Glucose, at pH 7.7 adjusted with 2-(*N*-morpholino) ethanesulfonic acid (MES) or trisaminomethane (Tris) base (363, 393). Each replicate N represented an individual fish. Three segmental regions were distinctly different from each other. The PC region was defined as the region directly behind the stomach with finger-like pouches, followed by MG region, and finally the HG region that was thicker and darker compared to the MG (52).

4.3.3. RT-qPCR analysis to quantify mRNA expression of MHA-linked transporters

During fish dissection, intestinal fish segments (about 100 mg PC, MG, and HG samples) were collected and cold-stored in RNA*later*® RNA Stabilization Solution (Fisher Scientific) at −80 ^{0}C for later analysis of gene expression. PC, MG, and HG samples were homogenized using Trizol (Thermo Scientific). Total RNA was extracted following the manufacturer's protocol. The purity assessment and RNA quantification concentration were determined using Nano-Drop spectrophotometer (Thermo Scientific). cDNA was synthesized using qScript cDNA Synthesis Kit (Quanta BioSciences) according to the manufacturer's instruction. The reactions were run as follows: incubation at 25 ^{0}C for 5 min, then at 42 ^{0}C for 30 min, and finally at 85 ^{0}C for 5 min in the PXE 0.2 Thermal Cycler (Thermo Scientific). All RT-qPCR assays were performed using Bio-Rad T100 Thermal Cycler (Bio-Rad). The total PCR reaction volume was 12.5 µl containing a mixture of 6.25 µL SYBR® Green SuperMix (Quanta BioSciences), 0.5 µL mix of forward and reverse primers, 2.5 µL cDNA template and 3.25 µL free-RNA water. The cycling condition was activated at 95 ^{0}C for 3 min for denaturation, followed by 40 cycles of 95 ^{0}C for 10 s, 59 ^{0}C for 10 s, and 72 ^{0}C for 30 s. Standard curves for each gene were generated to determine PCR primer efficiencies using a serial dilution of cDNA. Data were normalized to expression levels

of housekeeping gene α-elongation factor 1 (EFα1). Primer sequences designed for RT-qPCR were presented in Table 4.1.

Table 4.1. Rainbow trout (*Oncorhynchus mykiss*) primer sequences used for RT-qPCR.

SLC*	System (Gene name)	Forward (5' – 3')	Reverse (5' – 3')	Gene Bank Accession #
SLC16A1-like	MCT1-like	GAA GAA GGC GGA GTC TAA TC	TAG CGT AGT TGG AGA GGA A	XM_021567179.1
SLC16A7-like	MCT2-like	GTG GAC CTA TCA GCA GTA TT	GTC CAA ACC CTC CAA TGA	XM_021609615.1
SLC16A3	MCT4	TGT TCG TGG TGA GCT ATG	GCT GAA CAG GTA AAC AAC TC	XM_021576234.1
SLC16A5-like	MCT6-like	GGC AAA TCT GAA CCC ATA AA	GTA GGT CCG TGT AGA AGA TG	XM_021576090.1
SLC16A2-like	MCT8-like	GAG AGA GAC GAT TGG CAT TA	GCC AGC TCT ATA TGG TAC AC	XM_021583413.1
SLC16A9-like	MCT9-like	GTT GTT GGG TGG TTC TTT G	GTC GAT GTC AGC CTT CTT	XM_021580615.1
SLC16A13	MCT13	GTA GGC TAT GCG TGA GTA AG	GCC TCG AGC TAG TTG AAT AA	XM_021615.062.1
SLC5A8-like	SMCT1-like	GGC ATC AGA ACC TGA GAT AA	CAG TTG ACA GAG TGC ATT TAG	XM_021569991.1
SLC5A12-like	SMCT2-like	GGG TCA ACC AGT CAA CTA TAC	GGC GTA GAA AGC GTA CAT AA	XM_021578511.1
House keeping	EFα1	AGC GAG CTC AAG AAG AAG	GAC CAA GAG GAG GGT ATT C	NM_001124339.1

SLC* Solute carrier

4.3.4. ^{14}C radiolabeled DL-MHA flux studies

The collected intestinal segments were mounted as flat sheets between two sliders. The exposure of a tissue surface area was 0.3 cm^2. The sliders were then inserted in between two halves of chambers and kept tight by thumbwheel-driven screws. 5 mL of fresh teleost buffer was filled each side of the chamber compartment and was constantly gassed with 1% CO_2 and 99% O_2. The temperature was maintained around 12 ^{0}C through the experiment by a circulating water bath.

In all cases, the transport of liquid DL-[^{14}C]MHA free acid was carried out according to the procedure briefly described as follows. After a blank sample, 0.5 µCi of DL-[^{14}C]MHA (specific activity 55 mCi/mmol produced by Moravek Inc.) was added to the apical compartment to measure isotopic flux from the mucosal bath to the serosal bath (J_{ms}). 0.5 µCi of [^{3}H]-Inulin (specific activity 9.25 MBq/0.5 mCi produced by PerkinElmer) was also added to the apical compartment for later analysis of tissue viability. Exclusions from data analysis were made for tissues with considerable inulin flux, or tissue resistance decreased over the course of the experiment. After 60 min equilibration, increasing consecutive concentrations of unlabelled DL-MHA were added to the apical compartment, and mannitol was added to the basolateral compartment for balanced osmolality. Two levels of substrate were independently examined: 0.2 - 20 mM (19 consecutively increasing concentration) and 0 - 150 µM (21 consecutively increasing concentration). Na^+-dependent manners were evaluated in both concentration levels, but pH dependence and cis-inhibition were only evaluated in mM concentration ranges. A flux period was performed by sampling from the basolateral compartment at 10 min after each data increment. 500 µL radioactive sample withdrawn from the basolateral side was mixed with 4 mL-liquid scintillation cocktail (PerkinElmer) and subsequently counted using the Scintillation Counter (Beckman Coulter).

Sodium dependent/independent studies. Transport rate measurement of DL-[^{14}C]MHA was performed in the presence or absence of Na^+ at apical/basal pH of 7.7/7.7. In Na^+-free condition, NaCl, $NaH_2PO_4 \cdot H_2O$, Na_2HPO_4, and $NaHCO_3$ in bathing buffer were substituted with an equimolar concentration of KCl, $KH_2PO_4 \cdot H_2O$, K_2HPO_4, and $KHCO_3$, respectively.

Proton dependent studies. Assays were performed using physiological Na^+-containing buffer with variable apical/basal pH of 6.0/6.0, 6.0/7.7, and 7.7/8.7. pH was adjusted with MES (acidic) or Tris (basic). In all cases, DL-[^{14}C]MHA flux was measured in the range of unlabeled DL-MHA concentration 0.2-20 mM.

Cis inhibition studies: Effects of sodium lactate (20 mM) or sodium acetate (20 mM) on DL-[^{14}C]MHA flux were studied in buffer pH 7.7/7.7, the concentration gradient of DL-MHA 0.2-20 mM.

4.4. Kinetic and statistical analysis

The calculation of unidirectional isotopic fluxes rate was described as follows (347).

$$J_{ms} = v_s(P_s2 - cP_s1)/(\Delta t * P_m * A)$$

J_{ms} = unidirectional DL-[^{14}C]MHA flux from mucosa to serosa in µmol/cm^2/hr
v_s = volume of buffer solution perfusing the serosal surface in cm^3
P_s1 = Initial cpm/cm^3 in the serosal reservoir
P_s2 = cpm/cm^3 in the serosal reservoir after increment change
A = area of tissue exposed = 0.3 cm^2
Δt = time interval between two samples in hour
P_m = specific activity of the radioactive isotopes in the mucosal solution in cpm/µmol

The radioisotopic flux rates of carrier-mediated transport were then fitted to classical nonlinear regression Michaelis-Menten equations using GraphPad Prism to determine maximal

flux rate (J_{max}) and kinetic constant (K_m). The formula of Michaelis-Menten equation was: $J = \{(J_{max} \times [S])/(K_m + [S])\}$, where J_{max} the maximal transport rate, S substrate concentration, K_m half-saturation constant.

J_{max} and K_m data were presented as means ± SEM. Data were analyzed using one-way ANOVA to determine whether J_{max}/K_m values for each intestinal segment was significantly different. Student's *t*-test was used to compare between two groups. Gene expression data were analyzed with similar methods using SYSTAT software. In all cases, a P-value < 0.05 was considered statistically significant for the difference between mean values.

4.5. Results

4.5.1 ^{14}C radiolabeled DL-MHA flux at millimolar concentration 0.2-20 mM

Sodium dependent/independent studies: DL-[^{14}C]MHA flux kinetics were characterized in Na^+ and Na^+-free conditions at a substrate concentration of 0.2-20 mM. In the presence of Na^+ buffer pH 7.7/7.7, DL-[^{14}C]MHA flux displayed a saturable Michaelis-Menten mechanism with similar kinetic parameters in the first two segments (Figure 4.1). The K_m values were 1.10 ± 0.23 mM and 0.97 ± 0.14 mM in PC and MG, respectively; and J_{max} values were 0.0007 ± 0.00001 μmol/cm^2/hr and 0.0009 ± 0.00001 μmol/cm^2/hr in the PC and MG, respectively. On the other hand, the flux rate was dramatically reduced in the HG and void of characterizable transport kinetics. Likewise, no concentration-dependent transport kinetics were detected when Na^+ ions were removed from the buffer 7.7/7.7 (Figure 4.1). Together this suggested the participation of a Na^+-dependent carrier-mediated mechanism in DL-MHA transport in PC and MG.

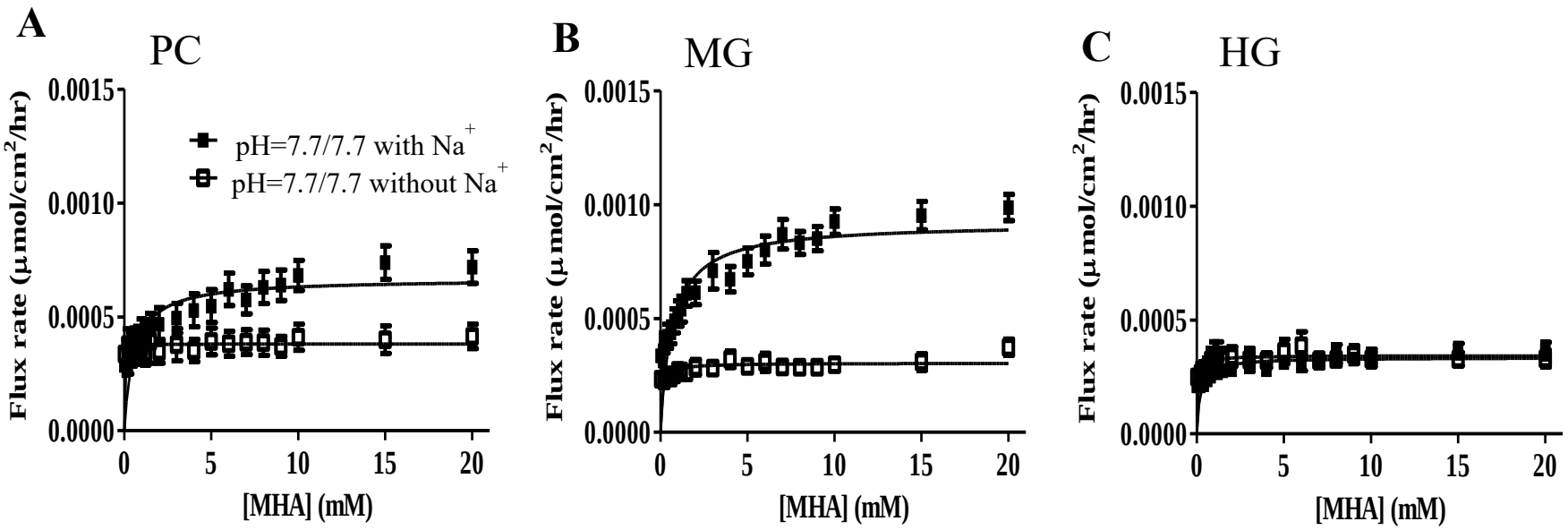

Figure 4.1. Effects of sodium on DL-MHA transport at millimolar (mM) concentration.

Michaelis-Menten plots for the DL-[^{14}C]MHA flux assays in the presence of Na^+ (N=16-18) (■) and absence of Na^+ (N=11-12) (□) with apical pH/basal pH of 7.7/7.7 in (A) pyloric caeca (PC), (B) midgut (MG), and (C) hindgut (HG). Experiments were performed with DL-MHA gradient from 0.2-20 mM (19 increasing sequential concentration). Values were means ± SEM.

Proton dependent studies: With the same sodium concentration, the proton-dependent transport was evaluated at variable apical/basal pH including 6.0/6.0, 6.0/7.7, and 7.7/8.7 (Figure 4.2). Reducing the pH to 6.0/6.0 or 6.0/7.7 did not result in significant changes in transport rates and affinity values between PC and MG, suggesting a similar apical transport mechanism in these two segments. At pH 6.0/6.0, the J_{max} in PC and MG were 0.0007 ± 0.00001 and 0.0008 ± 0.00001 µmol/cm^2/hr, respectively; K_m values in PC and MG were 0.56 ± 0.12 and 0.80 ± 0.13 mM, respectively. Similarly, a strong proton gradient across the apical membrane under pH conditions of 6.0/7.7 produced little effect. J_{max} in PC and MG were 0.0006 ± 0.00001 and 0.0007 ± 0.00001 µmol/cm^2/hr, respectively; K_m values in PC and MG were 0.77 ± 0.15 and 0.66 ± 0.17 mM, respectively. These small changes in affinity and flux rates were not statistically significant (Table 4.2). Correspondingly, the poor flux in the HG remained unaffected in both pH conditions. Together this suggested the limited apical proton dependence of apical MHA transport throughout the intestine. Likewise, increasing pH on the basolateral side to pH 7.7/8.7, creating a proton gradient across the basolateral membrane in the PC and MG produced insignificant differences in J_{max} and K_m in comparison with pH 7.7/7.7. This suggested a proton independent mechanism of MHA exit in the PC and MG. However, in the HG this pH 7.7/8.7 gradient markedly increased J_{max} flux and obeyed the Michaelis-Menten equation with J_{max} and K_m of 0.0006 ± 0.00001 µmol/cm^2/hr and 0.39 ± 0.10 mM, respectively (Figure 4.2 and Table 4.2). Under the same pH conditions, the removal of sodium eliminated the response (data not shown). These observations proposed that DL-MHA transport involved low-affinity Na^+-dependent apical transporters and H^+-independent basolateral transporters in PC and MG, while it appeared that there was the participation of an H^+-coupled MHA basolateral transporter in HG.

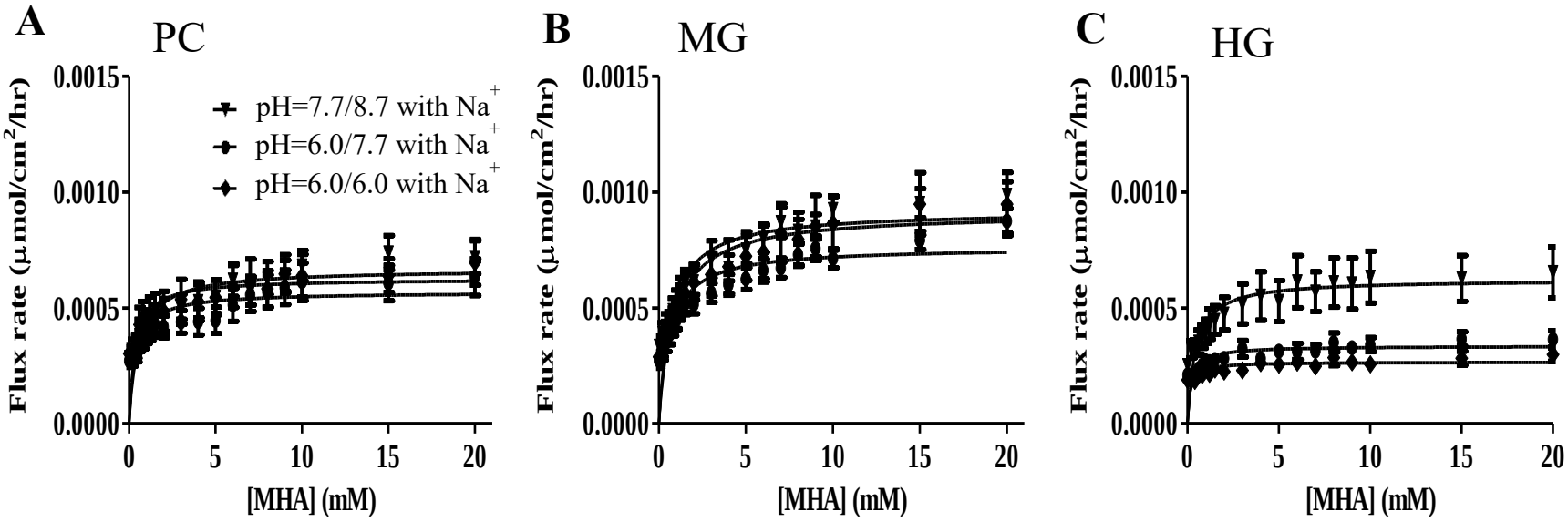

Figure 4.2. Effects of proton on DL-MHA transport at millimolar (mM) concentration.

Effects of proton on DL-MHA transport at millimolar (mM) concentration. Michaelis-Menten plots for the DL-[^{14}C]MHA flux assays in the presence of Na^+ with apical/basal pH of 7.7/8.7 (▼), 6.0/7.7 (●), and 6.0/6.0 (◆) in (A) pyloric caeca (PC), (B) midgut (MG), and (C) hindgut (HG). Experiments were performed with DL-MHA gradient from 0.2-20 mM (19 increasing sequential concentration). Values were means ± SEM (N=10-16).

Cis-inhibition studies: Common substrates of MCTs including sodium lactate/sodium acetate (20 mM) were added to apical bathing buffer pH 7.7/7.7. The results demonstrated that sodium lactate had insignificant inhibitory effects on J_{max} of DL-[^{14}C]MHA flux in PC and MG. Remarkably, HG flux obeyed Michaelis-Menten kinetics with J_{max} and K_m of 0.0007 ± 0.00013 µmol/cm^2/hr and 0.36 ± 0.08 mM, respectively (Figure 4.3 and Table 4.2). On the other hand, the flux rate in MG was significantly reduced in the presence of sodium acetate: J_{max} of 0.0006 ± 0.00001 µmol/cm^2/hr compared to 0.0009 ± 0.00001 µmol/cm^2/hr in acetate-free containing buffer (Student's *t*-test, P=0.02). Nonetheless, regardless of dissimilarities of how lactate and acetate affected on flux rate, K_m values tended to decrease in both cases (Table 4.2). A decrease in K_m indicated an increased affinity, which would be consistent with the inhibition of a low-affinity transporter and a shift to the dependence of the transport on a high-affinity transporter.

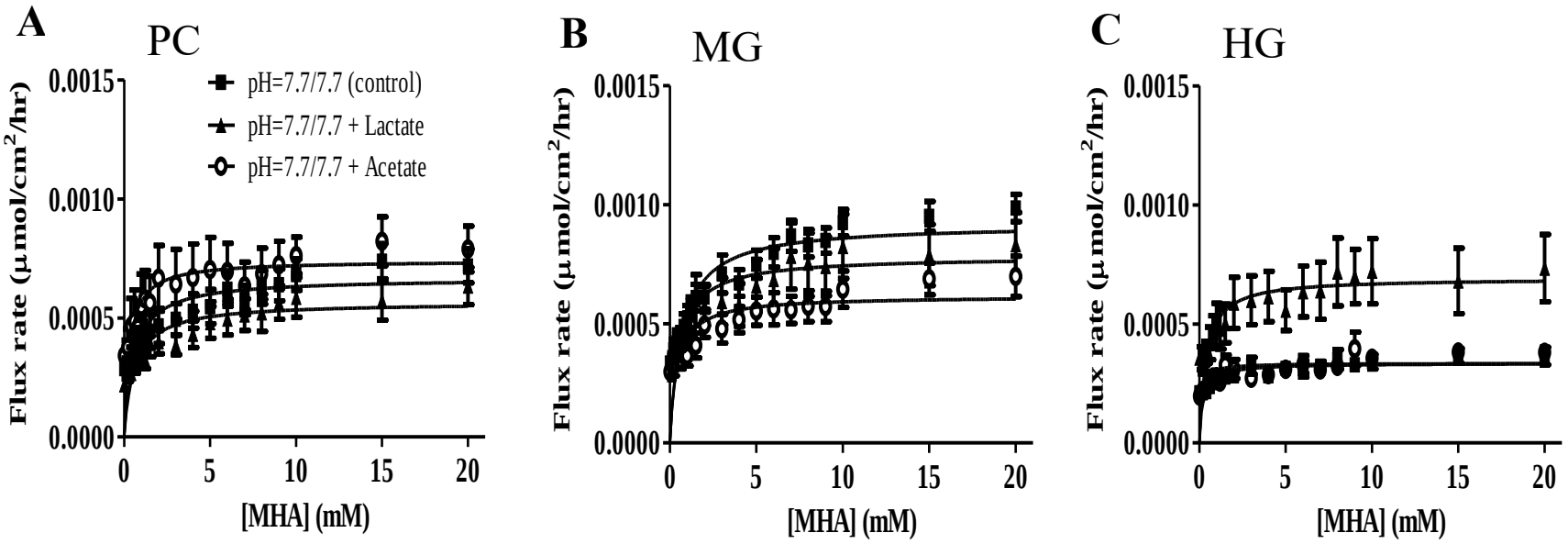

Figure 4.3. Effects of cis inhibition on DL-MHA transport at millimolar (mM) concentration.

Effects of cis inhibition on transport of DL-MHA at millimolar (mM) concentration. Michaelis-Menten plots for the DL-[^{14}C]MHA flux control assays (■), or in the presence of 20 mM sodium lactate (▲) or sodium acetate (O) on apical buffer in (A) pyloric caeca (PC), (B) midgut (MG), and (C) hindgut (HG). Experiments were performed with DL-MHA gradient from 0.2-20 mM (19 increasing sequential concentration). Values were means ± SEM (N=10-18).

Table 4.2. Transport of DL-MHA at millimolar (mM) concentration.

		J_{max} (µmol/cm^2/hr)			K_m (mM)		
	Apical pH/basal pH	**PC**	**MG**	**HG**	**PC**	**MG**	**HG**
Na$^+$ dependent assays	7.7/7.7 with Na^+	0.0007 ± 0.00001 (control)	0.0009 ± 0.00001 (control)	ND (control)	1.10 ± 0.23 (control)	0.97 ± 0.14 (control)	ND (control)
	7.7/7.7 without Na^+	ND	ND	ND	ND	ND	ND
H$^+$ dependent assays	6.0/6.0 with Na^+	0.0007 ± 0.00001	0.0008 ± 0.00001	ND	0.56 ± 0.12	0.80 ± 0.13	ND
	6.0/7.7 with Na^+	0.0006 ± 0.00001	0.0007 ± 0.00001	ND	0.77 ± 0.15	0.66 ± 0.17	ND
	7.7/8.7 with Na^+	0.0006 ± 0.00001	0.0009 ± 0.00001	0.0006 ± 0.00012	0.50 ± 0.10	0.89 ± 0.18	0.39 ± 0.10
Cis inhibition	7.7/7.7 + lactate	0.0006 ± 0.00001	0.0008 ± 0.00014	0.0007 ± 0.00013	0.59 ± 0.11	0.55 ± 0.11*	0.36 ± 0.08
	7.7/7.7 + acetate	0.0008 ± 0.0001	0.0006 ± 0.00001*	ND	0.80 ± 0.16	0.52 ± 0.11*	ND

J_{max} and K_m values generated by DL-[^{14}C]MHA flux assays along rainbow trout intestine, unlabeled substrate DL-MHA gradient 0.2-20 mM (19 increasing consequential concentration). Values were expressed as means ± SEM (N=10-18 in Na^+, N=11-12 in Na^+ free). Asterisks represent significant differences in J_{max} or K_m from the control 7.7/7.7 (Student's *t*-test, $p < 0.05$). J_{max} and K_m values derived from Na^+-free experiments and HG in Na^+-containing buffer were not obtainable and shown as non detectable (ND).

4.5.2. ^{14}C radiolabeled DL-MHA flux at micromolar concentration 0-150 µM

To identify a potential existence of a high-affinity transporter, DL-[^{14}C]MHA flux was performed in the presence or absence of Na^+ pH 7.7/7.7 at the substrate concentration 0-150 µM (Figure 4.4). In the presence of Na^+, DL-[^{14}C]MHA mucosal to serosal flux exhibited a saturable process that could be described by the Michaelis-Menten equation. Although J_{max} was significantly lower in PC (0.0008 ± 0.00001 µmol/cm^2/hr) than in MG (0.001 ± 0.00001 µmol/cm^2/hr), no significant differences in affinity was detected between the two segments (Table 4.3), suggesting similar transporter involvement. In Na^+-free conditions at pH 7.7/7.7, there was no flux. The HG again displayed poor MHA transport. In both Na^+ and Na^+-free conditions at pH 7.7/7.7, there was little or no substrate-dependent flux in HG. The DL-[^{14}C]MHA flux was not significantly impacted in any of the segments (Figure 4.4) by lowering the pH to 6.0/6.0 apical/basal conditions in Na^+-containing buffer. No significant differences in flux rates and kinetics constant values ($P>0.05$) were detected between pH 6.0/6.0 and 7.7/7.7 (Table 4.3). Together these results indicated the presence of a MHA Na^+-dependent high-affinity transporter in trout PC and MG, which could explain the decrease in K_m with cis-inhibition described earlier in the 0.2- 20 mM concentrations.

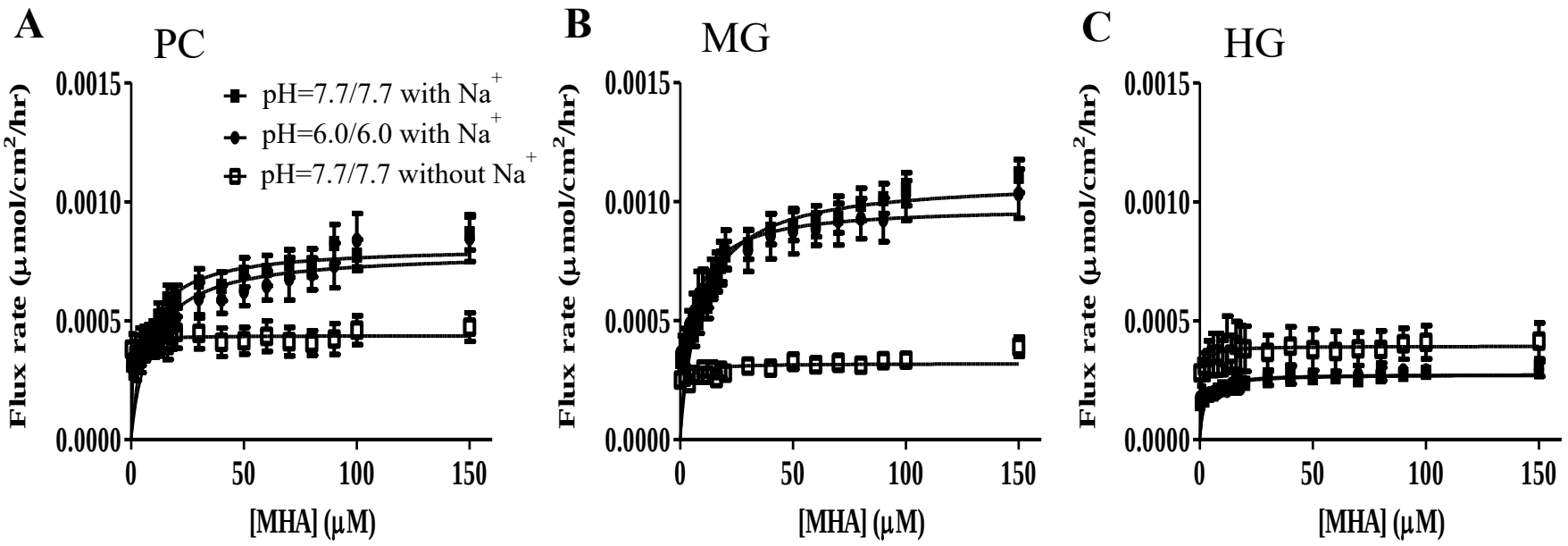

Figure 4.4. Transport of DL-MHA at micromolar (µM) concentration.

Michaelis-Menten plots for the DL-[^{14}C]MHA flux assays in the presence of Na^+ (N=13-19) with apical/basal pH of 7.7/7.7 (■) and 6.0/6.0 (●) and absence of Na^+ (N=10-12) with apical/basal pH of 7.7/7.7 (□) in (A) pyloric caeca (PC), (B) midgut (MG), and (C) hindgut (HG). Experiments were carried out with DL-MHA gradient from 0-150 µM (21 increasing sequential concentration). Values were means ± SEM.

Table 4.3. Transport of DL-MHA at micromolar (µM) concentration.

	J_{max} (µmol/cm^2/hr)				K_m (µM)			
Apical pH/basal pH	**PC**	**MG**	**HG**	**P-value**	**PC**	**MG**	**HG**	**P-value**
7.7/7.7 with Na^+	0.0008 (± 0.00001)	0.001 (± 0.00001)	ND	0.006*	8.76 (± 1.26)	10.65 (± 1.10)	ND	0.264
7.7/7.7 without Na^+	ND	ND	ND	-	ND	ND	ND	-
6.0/6.0 with Na^+	0.0008 (± 0.00001)	0.001 (± 0.00001)	ND	0.041*	10.1 (± 1.59)	6.97 (± 0.94)	ND	0.199

J_{max} and K_m values generated by DL-[^{14}C]MHA flux assays along rainbow trout intestine in the Na^+ and Na^+ free buffer, unlabeled substrate DL-MHA gradient 0-150 µM (21 increasing sequential concentration). Values were expressed as mean ± SEM (N=13-19 in Na^+, N=10-12 in Na^+ free). Asterisks represent significant differences in J_{max} or K_m between PC and MG (Student's *t*-test, $P < 0.05$). J_{max} and K_m values derived from Na^+-free experiments and HG in Na^+-containing buffer were not obtainable and shown as non detectable (ND).

4.5.3. Gene expression of monocarboxylate transporters (MCTs) and sodium monocarboxylate transporters (SMCTs)

Here we determine if there is an association between the members of the two major class of monocarboxylates transporters and the transport of MHA seen in this study. RT-qPCR was performed for all genes of MCT family (SLC16A) and SMCT family (SLC5A) found in the trout genome. Among 14 members, RT-qPCR was not performed for MCT3 (SLC16A8), MCT11 (SLC16A11), and MCT14 (SLC16A14) due to no genomic presence of these genes in rainbow trout. RT-qPCR was not detectable for genes including MCT5-like (SLC16A4-like), MCT7-like (SLC16A6-like), TAT1-like (SLC16A10-like), and MCT12-like (SLC16A12). On the other hand, genes including MCT2-like (SLC16A7-like), MCT4 (SLCA16A3), MCT6-like (SLC16A5-like), MCT8-like (SLC16A2-like), and SMCT2-like (SLC5A12-like) were negligibly expressed in trout gut (Table 4.4).

There seemed to be an association of four candidate genes that could potentially contribute to MHA transport. They included SMCT1-like (SLC5A8-like), MCT1-like (SLC16A1-like), MCT9-like (SLC16A9-like), and MCT13 (SLC16A13). Specifically, relative mRNA expression of sodium-dependent SMCT1-like gene and the putative proton-independent MCT9-like gene were significantly higher in PC and MG in comparison with HG (Figure 4.5A and Figure 4.6B). An opposite trend was detected for the proton dependent MCT1-like and MCT13 in which there was significantly greater expression found HG segment (Figure 4.5B and Figure 4.6A).

Table 4.4. RT-qPCR results of genes with low relative mRNA expression in intestine.

Gene	PC	MG	HG
MCT2-like	0.001 ± 0.0002	0.001 ± 0.00001	0.002 ± 0.0005
MCT4	0.004 ± 0.0008	0.009 ± 0.0022	0.022 ± 0.0071
MCT6-like	0.002 ± 0.0002	0.002 ± 0.00001	0.017 ± 0.0025
MCT8-like	0.006 ± 0.0031	0.002 ± 0.0002	0.006 ± 0.0009
SMCT2-like	0.004 ± 0.0014	0.020 ± 0.0054	0.003 ± 0.0008

House keeping gene α-elongation factor 1 (EFα1) was used to normalize expression data. Values were expressed as means ± SEM (N=8-10).

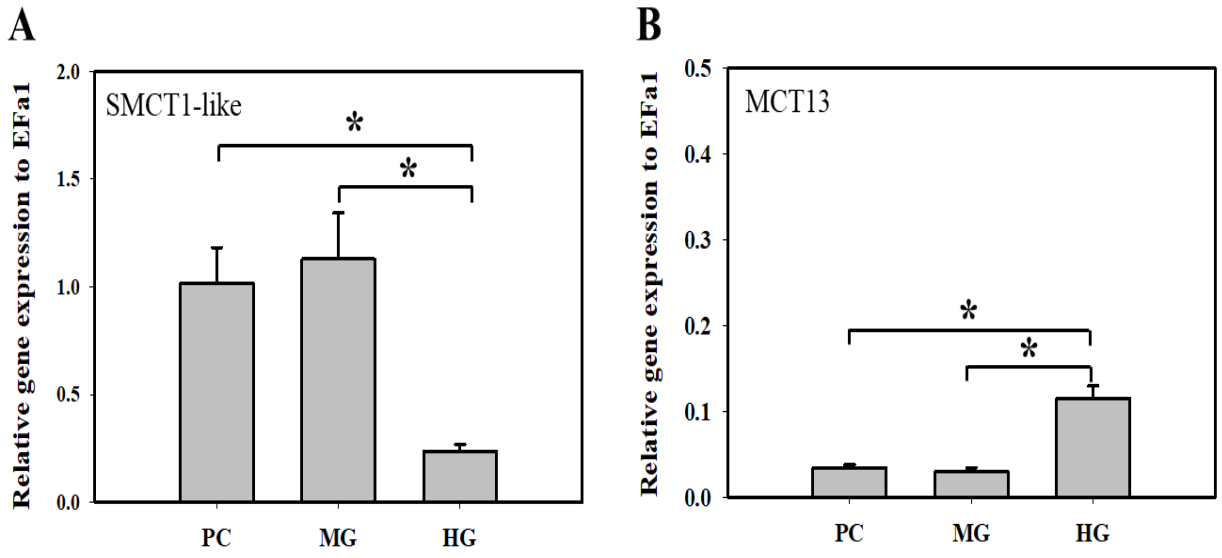

Figure 4.5. Gene expression of SMCT1-like (SLC5A8-like) and MCT13 (SLC16A13)

A) Relative mRNA expression of SMCT1-like (SLC5A8-like), and **B)** Relative mRNA expression of MCT13 (SLC16A13) in pyloric caeca, midgut and hindgut of rainbow trout using RT-qPCR. House keeping gene α-elongation factor 1 (EFα1) was used to normalize expression data. Values were expressed as means ± SEM (N=8-10). Significant differences among segments were indicated with asterisks (one-way ANOVA, $p < 0.05$).

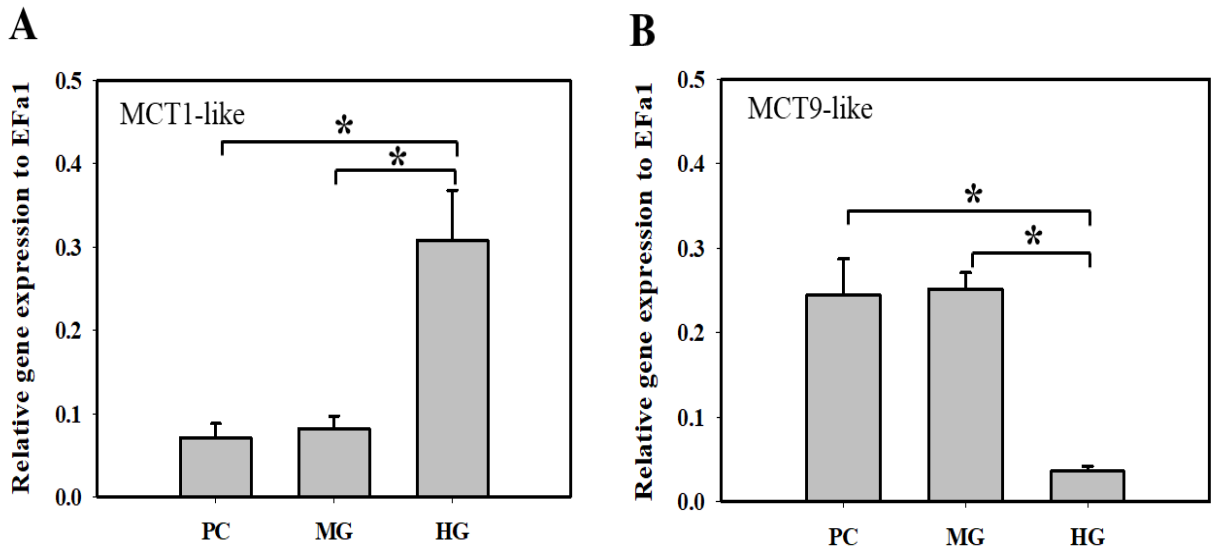

Figure 4.6. Gene expression of MCT1-like (SLC16A1-like) and MCT9 (SLC16A9-like)

A) Relative mRNA expression of MCT1-like (SLC16A1-like), **B)** Relative mRNA expression of MCT9-like (SLC16A9-like) in pyloric caeca, midgut and hindgut of rainbow trout using RT-qPCR. House keeping gene α-elongation factor 1 (EFα1) was used to normalize expression data. Values were expressed as means ± SEM (N=8-10). Significant differences among segments were indicated with asterisks (one way ANOVA, $p < 0.05$).

4.6. Discussion

Since Met is one of the first limiting EAAs in animal diets, dietary inclusion of Met sources such as DL-Met or DL-MHA has been commonly practiced for optimal growth and health of farm-raised animals, particularly in aquaculture (283). Understanding the mechanism of how these Met sources transported is an important step to better understand their biological efficacy and to approach a cost-effective feed formulation. Reports suggest that MHA gut transport is proton-dependent, but dependence on sodium is inconsistently observed, which is likely due to difference in techniques, tissue and cells used (32, 230, 244, 245, 298). As a monocarboxylate, the intestinal transport pathway of DL-MHA is expected to be similar to SCFAs. Although SCFAs are mainly produced in the colon by bacterial fermentation of dietary fibre, they could be still absorbed in the small intestine (366). This is also true in several fish species (365, 392). Additionally, segmental differences and membrane specific locations of transporters could be also attributed to the dependence of sodium and proton in intestinal MHA transport. Unidirectional flux J_{ms} of SCFAs (acetate, butyrate, and propionate) is found to be higher in the distal colon than in caecum of guinea-pig, and absorption appears to be H^+-independent when reducing luminal pH (326, 419). Therefore, segmental differences in DL-MHA transport are studied using an isotopically-labelled DL-MHA to determine its transport kinetics throughout the length of the fish intestine. Our results indicate that perhaps there are two distinct DL-MHA transport mechanisms existing in different segments of trout gut: 1) in PC and MG regions: apical influx and basolateral efflux of DL-MHA are likely facilitated by Na^+-dependent and H^+-independent carrier-mediated transporters, respectively; 2) in HG region: it seems that apically localized Na^+-dependent medium-affinity transporter supports DL-MHA influx while H^+-dependent transporter mediates basolateral exit. Additionally, the interaction between DL-MHA and lactate/acetate predicts that apically DL-MHA

transport probably involves more than one transporter with different affinity ranges in PC and MG; and a not yet identified transport pathway in HG favouring MHA recycling resulting in lower flux rate in HG.

4.6.1. DL-MHA transport in PC and MG

Apical influx and basolateral efflux were mediated by Na^+-dependent and H^+-independent mechanism, respectively

Presence of apical Na^+-dependent and absence of H^+-dependent transport evidence in PC and MG

Firstly, results demonstrated that DL-MHA transport at concentration 0.2-20 mM greatly relied on the presence of a Na^+-dependent low-affinity transporter (K_m in mM ranges) at the physiological pH of 7.7/7.7 (Figure 4.1). Replacement of the sodium resulted in a complete lack of DL-MHA flux across the trout intestine. This was in agreement with the role of sodium in nutrient absorption previously observed in trout gut (182, 376, 393), although this observation was unlike previous reports of MHA transport in chicken (32, 298) or acetate transport in tilapia (392). This difference could be due to technique and species used, as care must be taken when comparing between teleost species as well animal categories (mammals, fish and avian).

However, the possibility still existed for the contribution of proton dependence to MHA transport along with sodium-dependent transport. With similar sodium conditions, excess provision of proton in pH 6.0/6.0 resulted in insignificant differences in maximal flux rates and kinetic constants (Figure 4.2 and Table 4.2). It was possible to argue that the apical/basal pH of 7.7/7.7 and 6.0/6.0 did not provide reasonable proton gradients for initiating the full functions of MCTs. Therefore, pH 6.0/7.7 and 7.7/8.7 were designed to explore potential location-specific

regulation of proton-coupled transporters further. The results demonstrated that the increasing H^+ gradient across the lumen-facing apical membrane by lowering pH in the apical reservoir with buffers pH 6.0/7.7 did not alter kinetic affinities and transport rates (Table 4.2). Similarly, increasing H^+ gradient across the basolateral membrane by increasing pH on the basolateral reservoir in buffer pH 7.7/8.7 also resulted in insignificant differences in J_{max} and K_m in PC and MG. These results associated with low expression of monocarboxylate H^+-dependent transporter MCT1-like in PC and MG (Figure 4.6A). These observations indicated that the H^+-coupled mechanism was unlikely involved in mediating DL-MHA transport in the first two intestinal segments PC and MG, which left only H^+-independent and Na^+-coupled mechanism of DL-MHA absorption.

Kinetic constants and gene expression support apical Na^+-dependent and H^+-independent transport mechanism in PC and MG

As noted above, the apical influx of DL-MHA was unlikely regulated by H^+-gradient dependent transporters but relied on the presence of Na^+-requiring system instead. MCTs (14 members) and SMCTs (2 members) were known transporters mediating the transports of monocarboxylate compounds. The former belongs to the SLC16A family, while the latter belonged to the SLC5A family. Although substrate specificity was found to be similar, MCTs and SMCTs mediated substrate transport by different chemical driving forces: MCTs relied on H^+-electrochemical gradient, whereas SMCTs relied on Na^+-gradient (16, 139, 152, 186, 264, 265, 371). It was generally agreed that SMCTs were apically localized in the membrane of the intestine and kidney tubules with absorptive functions (140, 142, 184, 388, 435).

In the absence of published transport kinetics of DL-MHA via cloned SMCTs in a functional heterologous expression systems makes comparisons difficult. However, this is the first

study that demonstrates an association between transport kinetics of DL-MHA and the MCTs/SMCTs transporters. In our study, the kinetic constants (K_m) calculated for DL-MHA transport were ranging between 0.5-1.1 mM and 7-10 μM in PC and MG at high concentration (0.2-20 mM) and low concentration (0-150 μM), respectively. These K_m values could correspond with a low-affinity SMCT2 and a high-affinity transporter SMCT1, respectively (130, 153). In the current study, SMCT2 mRNA was poorly expressed in trout gut (Table 4.4), and the expression pattern was not thoroughly related to flux rates observed, while segmental mRNA expression of SMCT1-like (Figure 4.5A) highly correlated to segmental differences in flux rate in high concentration. However, the affinity difference of these two transporters in trout has not been investigated, and affinity constant values generated by a transporter could differ from substrate to substrate. For instance, K_m ranges of monocarboxylate compounds were relatively large for human SMCT1 transport in *X. laevis* oocytes: 72-81 μM for butyrate, 159 - 235 μM for L-lactate, 1.6 mM for γ-hydroxybutyrate, 2.5 mM for acetate, 6.5 mM for 5-aminosalicylate (76, 130, 246, 264). Or there might be species differences in transport functions. For example, Ohkubo et al. (287) found that K_m for nicotinate transported by SMCT1-like and SMCT2-like in rat intestine were 8.62 μM and 1.18-2.36 mM, respectively; while it was 390 μM in human SMCT1 (299) and 23.7 mM in zebrafish SMCT2 (315). Taken together, it seemed inappropriate to distinctively conclude whether SMCT1 or SMCT2 was responsible for DL-MHA transport at high or low concentration. However, experimental observation and gene expression analysis in this study clearly demonstrated the participation of apical Na^+-dependent transporters in DL-MHA influx.

The remaining question is the mechanism of DL-MHA export from the basolateral side. Since the flux rate remained unchanged throughout different pH-dependent experiments, the delivery of DL-MHA from intracellular cells to bloodstream was possibly mediated by an H^+-

independent process. MCT9-like was a feasible candidate responsible for this. Although its functions and substrate specificity has not been fully discovered, experimental evidence has indicated that MCT9 found on the basolateral side of epithelium, acted as H^+-independent carnitine efflux when expressed in *X.* oocytes (379). Moreover, gene expression of MCT9-like in the current study was also well associated with H^+-independent flux rates in PC and MG (Figure 4.6B).

Cis-inhibition in millimolar concentration and transport kinetics in micromolar concentration revealed multiple Na^+-dependent transporters in PC and MG for DL-MHA

Cis-inhibition studies demonstrated that lactate had minor inhibitory effects on DL-MHA flux in PC and MG, while acetate significantly reduced the transport rate of DL-MHA in MG. Despite the differences in inhibitory degree, both lactate and acetate tended to shift affinity constants towards higher affinity (lower K_m values). This could be simply explained by kinetic characteristics in which uncompetitive inhibition reduced both K_m and J_{max} (286). However, an alternative explanation was that there existed two transporters with different affinity ranges. At high DL-MHA concentrations (0.2-20 mM), the role of high-affinity transporter would probably be negligible compared to low-affinity transporter. In the presence of cis-inhibition, the low-affinity transporter could be inhibited, giving a chance for the high-affinity transporter to be exposed. Therefore, DL-MHA flux at 0-150 µM concentration was carried out to illustrate the concept. The results clearly demonstrated that there was the potential existence of Na^+-dependent high-affinity transport mechanism at low concentration in PC and MG (Figure 4.4 and Table 4.3). It was unclear which high-affinity transporter was responsible for DL-MHA transport at micromolar concentration. As discussed earlier, SMCT2-like would seem to be not a candidate because known literature suggests that SMCT2 was a low-affinity transporter (130, 140, 153, 371).

Nevertheless, we could not eliminate the possibility that the affinity of SMCT2 in trout is higher than that in mammals, and/or there is the existence of a not yet-identified high-affinity transporter.

These experimental observations concluded that apical DL-MHA influx in PC and MG was mediated by Na^+-dependent low- and high-affinity transporters, meanwhile efflux from basolateral side likely involved in the participation of H^+-independent transporter. The schematic model of DL-MHA transport in PC and MG was presented in Figure 4.7.

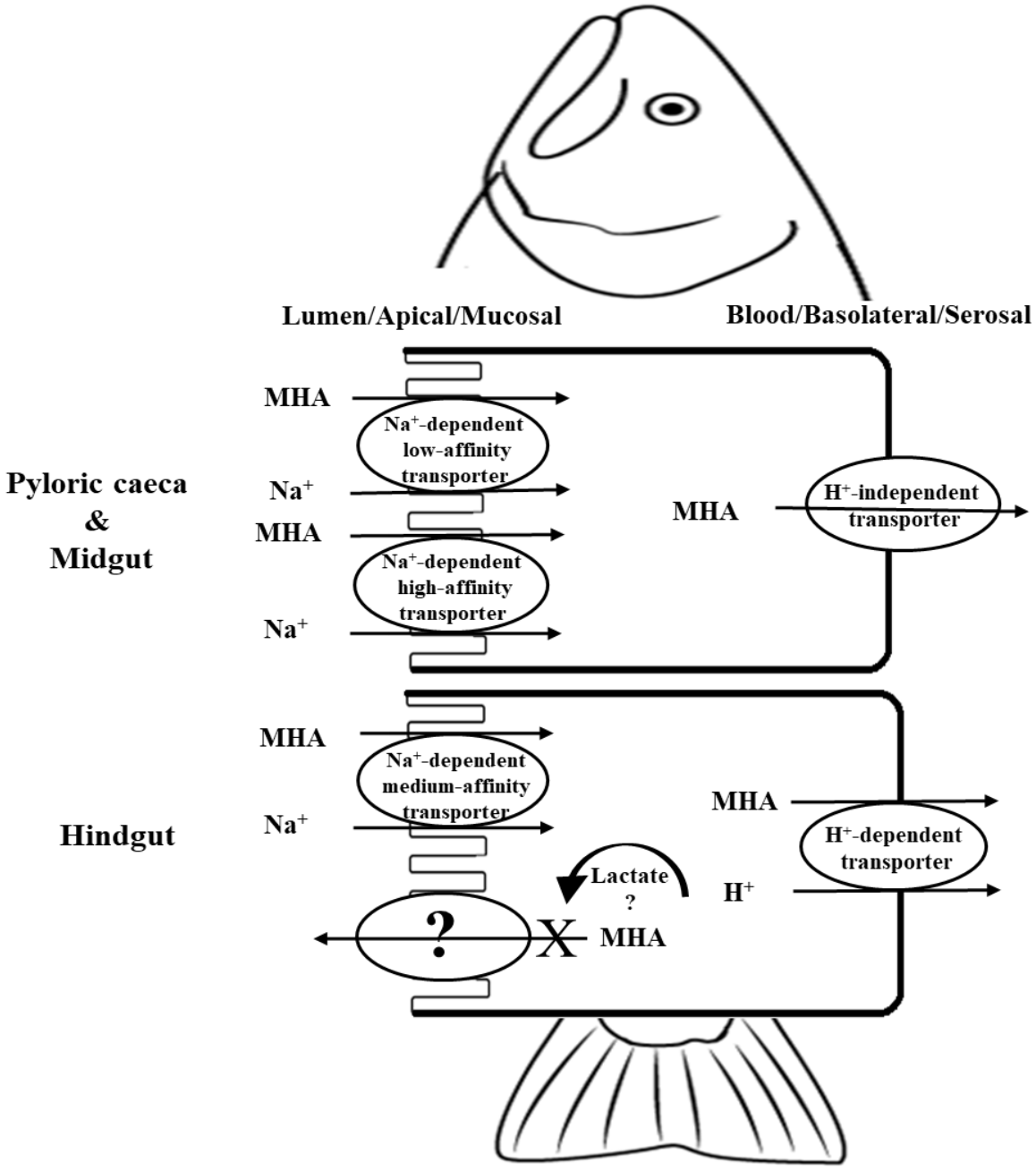

Figure 4.7. Simplified illustration of DL-MHA transport in the GI tract of rainbow trout.

DL-MHA transports differed in the first two segments compared to the last segments. In PC and MG, apical uptake was likely mediated by Na^+-dependent low- and high- transporters (predictively SMCT1-like and SMCT2-like) and basolateral delivery was primarily controlled by H^+-independent process (predictively MCT9-like). In HG, apical absorption was perhaps responsible by a Na^+-dependent medium-affinity transporter, but basolateral efflux was mainly dependent on H^+-coupled MHA transporter (possibly MCT1-like). There might be an unidentified back flux transporter (MCT13?) that could be inhibited by lactate.

4.6.2. DL-MHA transport in HG

Apical influx and basolateral efflux were facilitated by Na^+-dependent and H^+-dependent mechanism, respectively

pH-dependent experiments and gene expression revealed basolateral H^+-dependent efflux in HG

Unlike PC and MG, HG appeared to perform DL-MHA transport functions differently. Segmental differences in transport kinetics were likely due to dynamic changes in expression and location-specific regulation of Na^+, H^+-dependent and Na^+, H^+-independent transport systems along the intestinal tract. Firstly, hindgut DL-[^{14}C]MHA flux was unsuccessfully achieved with typical physiological Na^+-buffer. Suggested above, the Na^+-dependent transporter SMCT1 was most likely responsible for apical DL-MHA uptake in PC and MG at 0.2-20 mM. Thus, the absence of transport kinetics in the HG of DL-[14C]MHA could be partly explained by the low expression of SMCT1 (Figure 4.5A). Secondly, pH-dependent studies elucidated the association of flux kinetics with side-specific H^+-dependent regulation. DL-MHA transport from the lumen into epithelial cells seemed to be proton-independent since the flux rates remained unchanged when decreasing pH (increase H^+ concentration) on the apical side in pH 6.0/7.7 buffer. In contrast, a substantial increase in J_{max} was seen when lower H^+ concentration imposed on the basolateral side in pH 7.7/8.7 assays. The hindgut K_m-derived value was 0.39 ± 0.10 mM, which was higher than PC and MG K_m values. Additionally, Na^+-free experiment in pH 7.7/8.7 (data not shown) demonstrated no kinetics in HG. Together, it appeared that apical uptake of DL-MHA still relied on Na^+-dependent transporter, but basolateral exit could be facilitated by H^+-dependent transporter. RT-qPCR result demonstrated that H^+-dependent transporter MCT1-like was dominantly expressed in the HG (Figure 4.6A). The dominant expression of MCT1-like in the HG

was not surprising, given the transport kinetics in this study and its observed role in the mammal colon transporting SCFAs produced by bacteria via dietary fibre fermentation (138, 198, 359, 418).

Whether MCT1 is located on the apical and/or basolateral membrane is still controversial. Several studies have reported that MCT1 was mainly expressed in the apical membrane (55, 63, 273, 308), while some found exclusive expression of MCT1 on the basolateral surface of epithelial cells (131, 132, 184), whereas additional studies found it on both apical and basolateral surfaces (243, 384). Findings in the current study in trout gut suggested that H^+-dependent transporter, probably MCT1-like, played an essential role in the basolateral exit of DL-MHA from HG epithelium. In agreement with this suggestion, lactate transport across the basolateral membrane was found to be H^+-dependent using rat BBMV (292) and MCT1 mRNA injected into *Xenopus laevis* oocytes (291). This finding required an additional basolateral pH-regulating mechanism to compensate for H^+-taken out from the epithelial cells such as Na^+/H^+ exchanger NHE1 (58). This was in contrast to MCT1 mediated apical DL-MHA uptake in Caco-2 cell (243, 245).

Cis-inhibition and gene expression revealed the possible existence of an apical back-flux mechanism in HG

Noticeably, Michaelis-Menten affinity constant calculated in pH 7.7/8.7 was smaller in HG (0.39 ± 0.10 mM) than in PC and MG (0.50 ± 0.10 and 0.89 ± 0.18 mM, respectively), revealing a different transporter involved in HG with higher affinity. Thus, there is likely the involvement of a Na^+-dependent medium-affinity transporter in trout HG. Likewise, a kinetic flux in the HG was obtainable in the presence of lactate. This observation could be due to competition of DL-MHA and lactate through another orphan not yet-identified back-flux transporter, which might push intracellularly trapped DL-MHA cross the basolateral membrane increasing overall transport rate. mRNA expression of MCT13 tended to be elevated in HG (Figure 4.5B), which might

associate with exporting DL-MHA back to the lumen, causing low/non-detectable flux in HG. However, MCT13 is still an orphan transporter with unknown functions. The mechanism underlying this sophisticated observation requires further investigation in the future.

Experimental evidence here supported the conclusion that the apical DL-MHA influx in HG was likely controlled by a Na^+-dependent medium-affinity transporter, while basolateral efflux was largely governed by an H^+-dependent transport mechanism. Illustration of DL-MHA transport in HG was simplified in Figure 4.7.

4.7. Conclusion

This is the first study characterizing DL-MHA kinetic flux using radio-isotopic labelled substrate to gain knowledge of the transport mechanism in the fish intestine at a molecular level. The current study demonstrated the reliance of DL-MHA transport on sodium and protons with the association of the SMCTs and MCTs genes. Two distinct segmental kinetics reveals different transport mechanisms along trout intestine: 1) in PC and MG: DL-MHA apical uptakes are primarily governed by Na^+-dependent low- and high-affinity transporters and basolateral exit relies on H^+-independent transporter, 2) in HG: apical uptake seems to be controlled by Na^+-dependent medium-affinity transporter and basolateral exit is mainly mediated by an H^+-dependent process.

Transition

The following chapter focuses on addressing the 3rd objective and the 3rd hypothesis. There has been an ongoing debate about the effectiveness of DL-Met versus. DL-MHA supplementation in animal feeds. Understanding the transport rates of these synthetic methionine products in the intestine could contribute to explain observed differences in bioefficacy. Part of this chapter is combined with chapter 4 for one manuscript, as indicated previously. The chapter has been reformatted from the original manuscript to fit the structure of the thesis.

Objective: Compare the transport kinetics between DL-Met and DL-MHA by reanalyzing data obtained from the mentioned objectives.

Hypothesis: DL-Met is transported with higher affinity and rate than DL-MHA in rainbow trout intestine.

CHAPTER V

A COMPARISION OF DL-MET VERSUS DL-MHA TRANSPORT IN THE INTESTINAL TRACT OF RAINBOW TROUT

5.1. Abstract

Dietary methionine (Met) supplementation is an important aspect in animal nutrition since Met is an indispensable amino acid (AA). Numerous studies have been conducted to compare the effectiveness of DL-Met and DL-MHA which are the primary forms of synthetic Met. The knowledge of the transport mechanism involved in these products in the intestine is essential to elucidate the continuing arguments centred on the relative bioefficacy of DL-Met and DL-MHA. The aim of this study is to compare the intestinal transport of DL-Met and DL-MHA based on the pre-established understanding of the transport mechanism of these Met substrates in rainbow trout (*Oncorhynchus mykiss*). Flux rates of radiolabeled DL-Met and DL-MHA were extracted from data pools in previous chapters. The comparison was made at low concentrations (2, 10, 50, 100, and 150 µM) and high concentrations (1, 5, 10. 15, and 20 mM) in trout intestine, including PC, MG and HG. Overall, Michaelis-Menten analysis illustrated a significantly higher maximal flux rate (J_{max}) and affinity (K_m) for DL-[^{14}C]Met compared to DL-[^{14}C]MHA. Specifically, at µM concentrations, results showed that DL-[^{14}C]MHA flux rates were considerably lower than DL-[14C]Met, with intestinal flux rates of radiolabeled DL-MHA about 25.4-49.4% in PC, 39.3-48.4% in MG, and 47.2-70.1% in HG of DL-Met. Likewise, intestinal flux rates of radiolabeled DL-MHA were only about 61.9-66.0% in PC and 42.2-50.4% in MG compared to DL-Met at high concentrations. Conclusively, DL-Met transport was higher than DL-MHA in the intestinal tract of rainbow trout.

5.2. Introduction

Since Met is one of the first limiting essential AAs in plant-based diets, synthetic Met is often supplemented to fortify nutritional balance in diets of monogastric animals. There are two primary forms of commercially synthetic Met: DL-Methionine (DL-Met, ≥ 99 % purity) and DL-2-hydroxy-4-(methylthio) butanoic acid (DL-HMTBA or DL-MHA, 88% active substances and 12% water). DL-Met is a pure powder product with a 50:50 mixture of D- and L-isomers, while 88% active substances of liquid DL-MHA contains approximately 65% monomeric form and the remaining 23% are dimers and oligomers (28, 356). The effects of dietary DL-Met and DL-MHA supplementation on growth performance, feed conversion, protein synthesis, etc. have been widely evaluated to compare bioefficacy or bioavailability which indicates the effectiveness and cost-effective purchase of these Met sources. Several studies have revealed similar effectiveness of the two products (122, 136, 218, 334, 410). However, the relative bioefficacy of DL-MHA has often found to be lower than DL-Met across different species, including poultry (83, 171, 209, 337, 405), swine (194, 288, 358) and aquatic species (191, 192, 317, 319, 331). This conclusion is confirmed by a meta-analysis estimating that the relative bioefficacy of DL-MHA is ≤ 81% compared to DL-Met on an equal molar basis depending on performance parameters (339). DL-Met and DL-MHA are chemically unlike and are transported by different mechanisms in the GI tract, possibly explaining the different bioefficacies.

As a neutral amino acid, DL-Met transport could be achieved via multiple carrier-mediated Na^+-dependent systems (A, ASC, B^0, $B^{0,+}$, IMINO, and y^+L) and Na^+-independent systems ($b^{0,+}$, y^+-like, and L) (39, 367, 393, 445). Each of these systems could be composed of one or several transporters. In chapter III, DL-Met transport was kinetically studied in Ussing chambers. It appears that ASCT1, B^0AT1, y^+LAT1, and LAT4 are the major transporters that participate in DL-

Met transport. Whereas DL-MHA is a monocarboxylate since it contains a hydroxyl group (OH) instead of an amine group (NH2), which is believed to be transported by monocarboxylate transporters (MCTs) or sodium monocarboxylate transporters (SMCTs). Previous studies have shown that DL-MHA absorption is Na^+-independent (32) and H^+-dependent (230, 298) with similar transport kinetics of MCT1 (245). In chapter IV, an association between the segment-specific location of MCT/SMCT and DL-MHA flux was observed. Based on these findings, the transport rates of these Met sources are compared by reanalyzed DL-[^{14}C]Met and DL-[^{14}C]MHA flux data. The result demonstrated that there were significant differences in transport capacity and affinity between Met sources. At low concentration (µM), DL-[^{14}C]Met was transported with higher affinity and greater flux rates compared to DL-[^{14}C]MHA. At high concentration (mM), DL-[^{14}C]Met and DL-[^{14}C]MHA were transported with similar affinity, but higher flux rates were found for the former. Overall, DL-Met had higher transport capacity than DL-MHA in the intestine of rainbow trout.

5.3. Materials and methods

DL-Met and DL-MHA data were derived from previous chapters. All fish were held and maintained under identical conditions, as described in previous chapters. Both DL-[^{14}C]Met and DL-[^{14}C]MHA flux were studied in Na^+-containing buffer with apical/basal pH of 7.7/7 at 12 ^{0}C. Unidirectional radioisotopes mucosal-serosal flux was assessed in all three intestinal segments at the micromolar concentration (2, 10, 50, 100, and 150 µM) and millimolar concentration of unlabelled substrates (1, 5, 10, 15, and 20 mM). Fish used for the comparative experiments were obtained from the same hatchery and were at a similar growth stage with the mean size of 138.3 ± 9.3g for DL-Met and 156 ± 9.1g for DL-MHA.

5.4. Statistical analysis

Flux rates were obtained from flux experiments: four increments (2, 10, 50, 100 and 150 µM) from low concentration gradient, and five increments (1, 5, 10, 15, and 20 mM) from high concentration gradient. The radioisotopic flux rates of carrier-mediated transport were fitted to classical nonlinear regression Michaelis-Menten equations using GraphPad Prism to determine maximal flux rate (J_{max}) and kinetic constant (K_m). The formula of Michaelis-Menten equation was: $J = \{(J_{max} \times [S])/(K_m + [S])\}$, where J_{max} the maximal transport rate, S substrate concentration, K_m half-saturation constant. J_{max} and K_m data were presented as means ± standard error of the mean (SEM). The radioisotopic flux rates, maximal flux rate, and affinity of DL-Met and DL-MHA were compared using Student's *t*-test. Each intestinal segment (PC, MG, and HG) were analyzed independently. Significance was set at $P < 0.05$.

5.5. Results

Flux rates were compared for DL-Met and DL-MHA under experimental apical/basolateral pH 7.7/7.7 in Na^+-conditions. The comparison was made in both µM and mM concentration since Met content in plant-based diets is relatively low, and supplementation could increase the Met content to a high concentration. Results demonstrated that the transport of both Met sources primarily occurred in PC and MG regardless of concentration. There were significant differences in transport rates between DL-Met and DL-MHA. At µM concentration DL-[^{14}C]MHA flux rates were significantly lower than DL-Met in all concentrations of 2, 10, 50, 100, and 150 µM (Figure 5.1). Specifically, the flux rates of DL-[^{14}C]MHA were approximately 25.4-49.4% in PC, 39.3-48.4% in MG, and 47.2-70.1% in HG of DL-[^{14}C]Met flux. Radiolabeled substrates transport exhibited saturable Michaelis-Menten kinetics with significant differences found in both maximal flux rate and affinity (Table 5.1). J_{max} for DL-[^{14}C]Met were 0.002 ± 0.0004 µmol/cm^2/hr in PC

and 0.002 ± 0.0003 in MG, which were statistically greater than J_{max} for DL-[^{14}C]MHA of 0.001 ± 0.00001 µmol/cm^2/hr and 0.011 ± 0.00001 µmol/cm^2/hr in PC and MG, respectively. K_m values for DL-[^{14}C]Met were 4.25 ± 0.99 µM in PC and 4.68 ± 0.67 µM in MG, which were significantly lower than K_m for DL-[^{14}C]MHA with 7.66 ± 1.19 µM and 9.58 ± 1.23 µM in PC and MG, respectively. These data suggested that DL-Met was transported with a higher rate and higher affinity compared to DL-MHA along the intestinal tract of rainbow trout at low concentration.

Similar patterns were also observed when comparing these two products at high concentrations 1, 5, 10, 15, and 20 mM. Results demonstrated that radiolabeled DL-MHA flux rates were only about 61.9-66.0% and 42.2-50.4% relative to radiolabeled DL-Met flux rates in PC and MG, respectively (Figure 5.2). In HG, no statistical difference was found at high concentrations. Transports of both substrates obeyed Michaelis–Menten saturation kinetic behaviour with similar affinity but different maximal velocity. J_{max} for DL-[^{14}C]Met were 0.0014 ± 0.0001 µmol/cm^2/hr in PC and 0.0021 ± 0.0002 µmol/cm^2/hr in MG, which were significantly greater than J_{max} of DL-[^{14}C]MHA with 0.0008 ± 0.00001 and 0.0011 ± 0.00001 µmol/cm^2/hr in PC and MG, respectively. The flux rates were lowest in HG with no detectable kinetics of DL-MHA (Table 5.2). These results indicated that DL-Met transport in trout intestine was more efficient than DL-MHA.

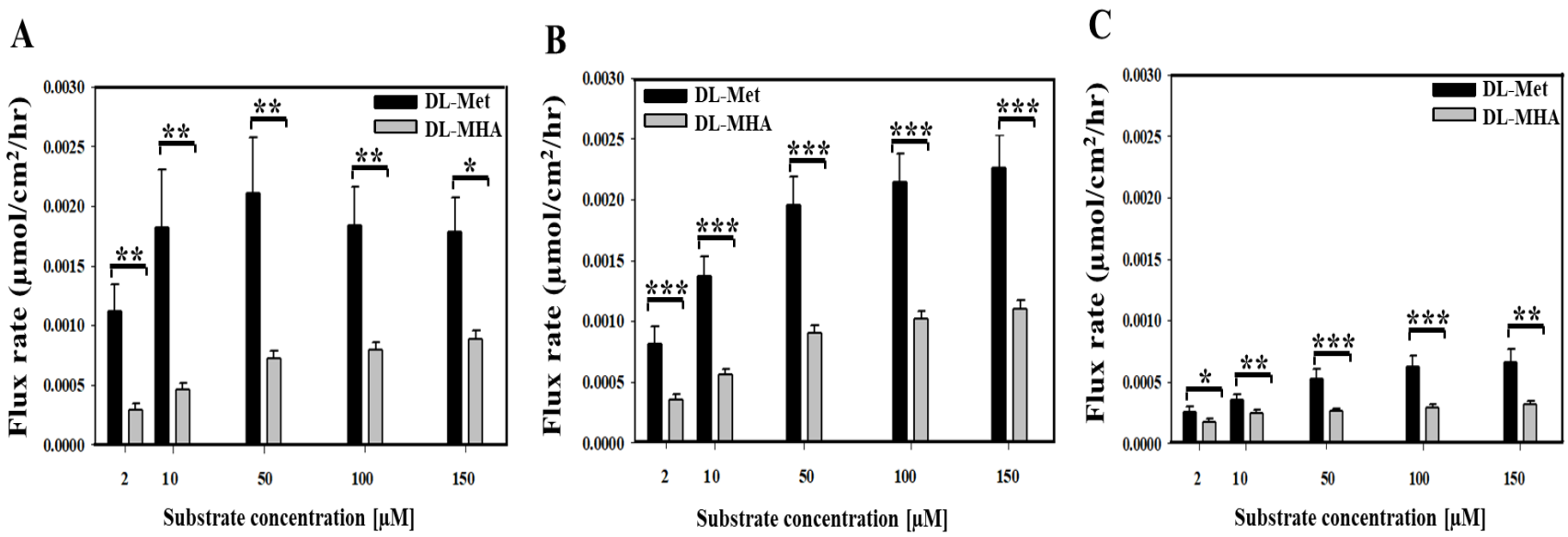

Figure 5.1. Flux rates DL-[^{14}C]Met and DL-[^{14}C]MHA at micromolar concentration

Flux rates of DL-[^{14}C]Met and DL-[^{14}C]MHA were performed in Na^{+}-containing buffer with apical/basal pH of 7.7/7.7 in (A) pyloric caeca (PC), (B) midgut (MG), and (C) hindgut (HG). Met substrate concentration was in micromolar concentration. Values were means ± SEM (N=19-22). Asterisks represent significant difference in flux rates between Met sources (Student's *t*-test P*< 0.05. P**<0.01, P***<0.001).

Table 5.1. Michaelis-Menten parameters of DL-[^{14}C]Met and DL-[^{14}C]MHA at micromolar concentration.

	J_{max}(µmol/cm^2/hr)			K_m(µM)		
Intestinal segments	**DL-Met**	**DL-MHA**	**P-value**	**DL-Met**	**DL-MHA**	**P-value**
PC	0.002 ± 0.0004	0.001 ± 0.00001	0.006*	4.25 ± 0.99	7.66 ± 1.19	0.030*
MG	0.002 ± 0.0003	0.011 ± 0.00001	<0.001*	4.68 ± 0.67	9.58 ± 1.23	0.002*
HG	0.0006 ± 0.0001	ND	-	6.24 ± 1.17	ND	-

J_{max} and K_m values DL-[^{14}C]Met and DL-[^{14}C]MHA along the intestinal tract of rainbow trout in the Na^+-containing buffer with apical/basal pH of 7.7/7.7. Substrate DL-Met and DL-MHA gradient were from 2-150 µM. Values were expressed as mean SEM (N=19-22). Asterisks represent significant difference in J_{max} between substrates (Student's *t*-test, *P < 0.05). J_{max} and K_m values derived DL-MHA flux were not obtainable in HG and shown as non-detectable (ND).

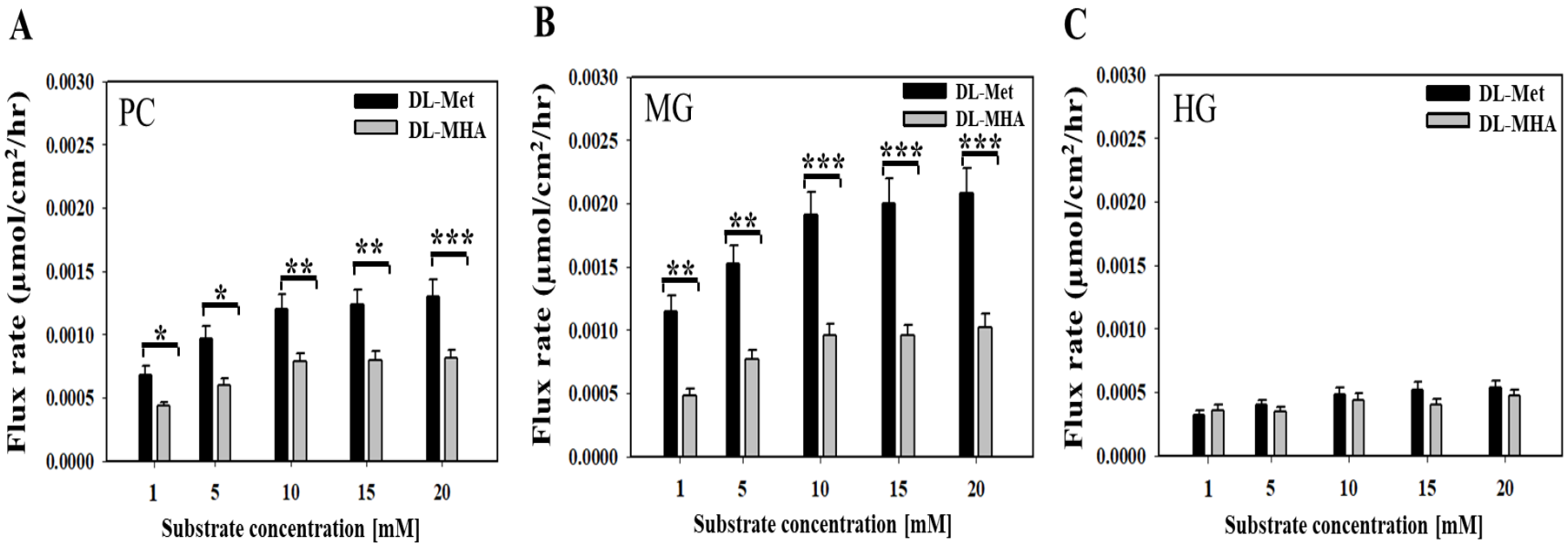

Figure 5.2. Flux rates DL-[^{14}C]Met and DL-[^{14}C]MHA at millimolar concentration

Flux rates of DL-[^{14}C]Met and DL-[^{14}C]MHA were performed in Na^+-containing buffer with apical/basal pH of 7.7/7.7 in (A) pyloric caeca (PC), (B) midgut (MG), and (C) hindgut (HG). Met substrate concentration was in millimolar concentration. Values were means ± SEM (N=17-22). Asterisks represent significant difference in flux rates between Met sources (Student's *t*-test P*< 0.05. P**<0.01, P***<0.001).

Table 5.2. Michaelis-Menten parameters of DL-[^{14}C]Met and DL-[^{14}C]MHA at millimolar concentration.

	J_{max}(µmol/cm^2/hr)			K_m(mM)		
Intestinal segments	**DL-Met**	**DL-MHA**	**P-value**	**DL-Met**	**DL-MHA**	**P-value**
PC	0.0014 ± 0.0001	0.0008 ± 0.00001	0.003*	1.33 ± 0.24	1.12 ± 0.15	0.466
MG	0.0021 ± 0.0002	0.0011 ± 0.00001	<0.001*	1.10 ± 0.12	1.44 ± 0.11	0.056
HG	0.0005 ± 0.00001	ND	-	0.96 ± 0.27	ND	-

J_{max} and K_m values DL-[^{14}C]Met and DL-[^{14}C]MHA along the intestinal tract of rainbow trout in the Na^+-containing buffer with apical/basal pH of 7.7/7.7. Substrate DL-Met and DL-MHA gradient were from 1-20 mM. Values were expressed as mean SEM (N=17-22). Asterisks represent significant difference in J_{max} between substrates (Student's *t*-test, *P < 0.05). J_{max} and K_m values derived DL-MHA flux were not obtainable in HG and shown as non detectable (ND).

5.6. Discussion and conclusion

Supplementation of synthetic AAs in plant-based diets is a strategy to produce cost-effective diets. Dietary Met supplementation is typically achieved with DL-Met or DL-MHA. Although several *in vivo* studies have been conducted, controversy about relative bioefficacy between DL-Met and DL-MHA still remains. Research in poultry and swine suggests that bioefficacy of DL-MHA is lower than DL-Met, ranging from 57-69% on product-product (wt/wt) basis in poultry (83, 236, 300, 405) and) and 64-71% in swine (194, 288, 358). Similar conclusions are also made in different fish species (191, 192, 317, 319, 331), although a few studies indicated similar performance (122, 136). Differences in bioefficacy could depend on the efficiency in gut absorption and the degree of microbial metabolism of the substrate. Determination of how much and how fast Met is intestinally transported is an initial critical step in evaluating bioefficacy. In the current study, radiolabeled DL-MHA flux rates were appreciably less than DL-Met flux. At low concentrations, DL-MHA flux rates were only 25.4-49.4% in PC, 39.3-48.4% in MG, and 47.2-70.1% in HG compared to DL-Met. Lower K_m values indicated that DL-Met was transported with higher affinity (Table 5.1). Similarly, at high concentrations, DL-MHA flux rates were only 61.9-66.0% in PC and 42.2-50.4% in MG (Figure 5.2). These findings contradicted an *in vitro* study using everted intestinal slices in chicken. Richards et al. (328) found that the uptake rates of DL-Met were only higher than that of DL-MHA at 2 mM, but significantly lower uptake rates over the concentration 5-50 mM. Overall results in the current study showed that DL-Met was transported faster than DL-MHA. A study in broilers found that only 4.4% of the administered DL-[^{14}C]Met was recovered in the excrement as opposed to 17% DL-[^{14}C]MHA calcium salt (217). This indicated that the intestinal absorption of DL-MHA was not as complete as DL-Met. Faster intestinal absorption rate would reduce the potential conversion of substrate into non-

absorbable products and/or metabolism by gut microorganisms. It was reported that the absorption of L-[^{3}H]-Met per gram intestinal tissue was higher in germ-free than in conventional and monoassociated chicks (439). Several other studies in chicken revealed that the initial dietary radioactivity of DL-MHA in feed found in distal segments of the small intestine were 10-21% compared to 2.5-4.5% of DL-Met, which was likely attributed to microbial activity (95, 104, 231). Likewise, Malik et al. (234) reported that residual activities of conventional pigs fed DL-MHA supplemented diets (34%, 15% and 13%) were higher than pigs fed DL-Met supplemented diets (16%, 8% and 7.8%) at 25%, 75% and 95% along the small intestine length. This was associated with a higher population of aerobe (5.42 CFU/g) and lactobacilli (6.22 CFU/g) in digesta for the pigs fed DL-MHA compared to aerobe count (4.9 CFU/g) and lactobacilli (5.63 CFU/g) in the DL-Met group (234). Thus, it appears that DL-MHA is more readily used by microbial bacteria than DL-Met, either as preferential substrate or less being transported by intestine, leaving it to be used by bacteria. In rainbow trout, it is not surprising that DL-Met is transported more efficiently than DL-MHA because proteins (AAs) are the major dietary components as opposed to monocarboxylate compounds in carnivorous fish. The comparison data here concluded that DL-Met transport across the intestinal tract of rainbow trout was higher than DL-MHA. This could be the possible reason why the bioefficacy of DL-Met is found to be higher in rainbow trout (317, 319) and other fish species (191, 332). Given the fact that Met is an EAA in fish diets, the findings in this study is possibly informative for formulating cost-effective diets.

CHAPTER VI

GENERAL DISCUSSION

6.1. Implication

The increasing use of plant-based protein in feeds is necessary for a profitable and sustainable aquaculture industry. Dietary methionine (Met) is indispensable for the normal growth and development of animals. The current practical approach to correct Met deficiency in a plant-based diet is to supplement it with synthetic Met, such as DL-Met and its analogue liquid DL-MHA. There has been an ongoing discussion regarding these Met sources' bioefficacy because both could be converted to biologically active L-Met. Knowledge of the intestinal transport mechanism involved would be important to explain the controversial debate concerning relative biological efficacy and economic implication of DL-Met and DL-MHA.

In chapter III, the transport of radiolabeled DL-Met across intestinal epithelium was investigated in PC, MG and HG of triploid and diploid rainbow trout at low (µM) and high concentration (mM) gradient of the substrate. At low concentration, both flux and electrogenic studies revealed that DL-Met transport was dependent on sodium and displayed a saturable mechanism with high affinity (K_m in micromolar ranges). Greater flux was higher in triploid than in diploid, which associates with the higher expression of sodium-dependent apical high-affinity transporter ASCT2. At high concentration, DL-[^{14}C]Met flux was also found to be strictly dependent on sodium and was transported with low affinity (K_m in millimolar ranges). Association between ploidy differences in flux rates and gene expression along with cis inhibition using phenylalanine and leucine supported that apical Na^+-dependent low-affinity transporter B^0AT1-like mediated the uptake of DL-Met. Whereas, the expression of basolateral transporters y^+LAT1 and LAT4 likely had implications in recycling Met and mediating efflux to the blood circulation,

respectively. Overall, the kinetic properties of Met epithelial transport, and gene expression showed that sodium was important for the transport of DL-Met and the transport mechanism in fish appeared to be simpler than mammalian and avian species. Additionally, the transporters responsible for Met transport identified in the current study appeared to have similar affinity, but lower transport rates than transporters in mammalian species (322). This might be a result of the substantially lower temperatures used in the trout 12 ^{0}C versus 37 ^{0}C in mammals or the technique used. The comparison of transport kinetic characteristics of Met is difficult between studies. For instance, transport/flux rates could be presented as the amount of substance across membrane per unit of surface area (Ussing chamber), per unit of weight (BBMV and everted sac), or per cell (cell culture model). Therefore, caution needs to be taken when concluding the transport kinetics among animal categories when different techniques are used. However, this thesis does not aim to establish the true total *in vivo* flux rate in fish gut, but to describe the transport mechanism of Met in association with exploring the responsible transporters.

In chapter IV, the characterization of DL-MHA transport across trout intestine was studied in diploid trout. Although Martin-Venegas et al. (245) suggested that DL-MHA uptake was mediated by proton-dependent transporter MCT1, there was evidence showing that DL-MHA transport was partially dependent on sodium (244). That was why the radioisotope flux of DL-MHA was studied in both sodium and proton conditions. The result demonstrated that there were different transport mechanisms along the intestinal tract of rainbow trout. Specifically, the apical influx of DL-MHA was dependent on sodium throughout the intestine. However, basolateral efflux occurred in PC and MG tended to be proton-independent, but proton-dependent in HG. Regional distribution of MCT1 was primarily expressed in the colon of omnivorous mammals, corresponding to the segmental distribution of SCFAs production (101, 134). This was

interestingly similar to rainbow trout in which MCT1 expression was significantly higher in the HG. However, unlike omnivorous mammals where SCFAs/monocarboxylate transport mainly occurred in the colon/large intestine, there appeared segmental inversion in which these compounds were primarily transported in the proximal intestine (PC) and mid intestine (MG) in trout. This was probably due to the significant expression and function of the apical sodium-dependent transporters SMCTs in these segments. It was questionable why rainbow trout could transport monocarboxylate or why they had monocarboxylate transpoters in the intestine as they were carnivorous fish and would likely not produce significant amounts of SCFAs. However, SCFAs had been found with high concentration during the summer in largemouth bass (365), suggesting the capability of fermentation in carnivorous fish with the production and use of SCFAs, with the hypothesis that temperature is the primary limit factor. It was understandable that rainbow trout were a cold water fish and would likely not produce many SCFAs. Thus, alternatively the presence and function of intestinal monocarboxylate transporters could be for the uptake of micronutrients, such as nicotinate (141, 299). This might partially explain the segmental inversion of monocarboxylate transport observed in trout compared to mammalian species. Additionally, the low mRNA expression of apical SMCT1 and high mRNA expression of the putative basolateral located MCT1 in trout hindgut associated with substantially lower flux that would also match with the physiology of carnivores which relied less on bacterial fermentation products.

In chapter V, the comparison of DL-Met and DL-MHA transport in trout intestine was performed by reanalyzing data obtained from previous chapters. Noticeably, fish of similar growth phase were sourced from the same hatchery, and the experimental conditions were identically kept to make the comparisons of two data set valid. Overall results showed that radiolabeled DL-Met

flux rates were significantly higher than radiolabeled DL-MHA in all segments regardless of low (μM) and high substrate concentration (mM). Furthermore, DL-Met was transported with higher affinity compared to DL-MHA at low concentration, suggesting that the binding affinity of AA transporter for Met was more efficient than the binding affinity of MCT/SMCT transporter for DL-MHA. Unquestionably, both Met sources could be converted into L-Met for biological activities and metabolism. However, the conversion primarily happens in the liver and kidney (409, 445) after GI tract uptakes. The higher transport rate and affinity observed in trout intestine possibly contributed to explaining the higher relative bioefficacy of DL-Met over DL-MHA and better economic efficiency of the former.

Together, studies in this thesis provided new insight into the epithelial transport mechanism of different Met sources in the fish intestine. DL-Met and DL-MHA in fish followed different transport routes as previously reviewed in mammals and avian (409, 444, 445), which were mediated by amino acid transporters and sodium monocarboxylate/monocarboxylate transporters, respectively. These physiological understandings gave important explanations about the higher transport capacity of DL-Met compared to DL-MHA, supporting dietary designs in nutrition to improve fish growth and performance.

6.2. Limitation

The techniques and experiments used in this thesis had a couple of limitations and challenges. Firstly, mRNA levels did not always correlate with protein expression. However, currently there were no available fish antibodies for these transporters to be assessed by Western blot. Similarly, the lack of fish antibodies made it impossible to determine the tissue distribution of a transporter of interest, particularly localization of apical and basolateral transporters using immunohistochemistry technique. Thirdly, there was scarce information about DL-MHA

transport, and kinetic characterization of this substrate had not been studied in any protein expression system. This limited only mRNA expression of MCTs and SMCTs family as the potential candidates to be investigated. Finally, the use of specific inhibitors would have been advantageous to confirm the role of the associated transporters involved. However, mammalian inhibitors generally did not work in trout. This could be due to the lower temperature at which the experiments were run. Previous work demonstrated glucose transport inhibitors worked in tilapia at 26 ^{0}C but not in trout at 12 ^{0}C (376). This was not too surprising as the temperature was known to affect a drug's ability to inhibit its target (121). Unfortunately, elevating the temperature of the trout tissue resulted in the death of the tissue. These limitations and challenges generated new questions that should be addressed in future research.

6.3. Future research

The transporters for DL-Met and DL-MHA in trout intestine are proposed here based on their functions in mammalian tissues matching with the observed kinetics of this study. In addition, some transporters have not been or minimally characterized. Thus, to confirm the association of known transporters with the observed transport kinetics, the fish clones of the expressing transporters that are capable of transporting these Met substrates is necessary. For example, molecular cloning and functional expression of trout/salmon ASCT2, B^{0}AT1, MCTs and SMCTs in *X*. Oocytes would greatly increase our knowledge of these transporters in fish, and also further confirm our work. The transport of AAs and monocarboxylic compounds could be investigated with other types of fish species to allow a broader conclusion between carnivorous and herbivorous fish. Moreover, diet composition would likely modify the gene/protein expression of transporters, especially with lumen-facing apical transporters. Therefore, before there are available fish antibodies to examine protein expression and immunohistochemical analysis, diet (or culture

medium) manipulation could be an alternative method to study electrophysiological intestinal epithelial properties and gene expression of transporters using *ex vivo* tissue-based approach (or *in vitro* cell-based method). For instance, if high/low protein diets could modify the expression of amino acid transporters, and if there is association between the gene expression and intestinal flux rates, this would further support the identified transporters responsible for AA transport.

REFERENCES

1. **Albers A**, **Bröer A**, **Wagner CA**, **Setiawan I**, **Lang PA**, **Kranz EU**, **Lang F**, **Bröer S**. Na+ transport by the neural glutamine transporter ATA1. *Pflugers Arch Eur J Physiol* 443: 92–101, 2001.

2. **Alberts B**, **Johnson A**, **Lewis J**, **Raff M**, **Roberts K**, **Walter P**. Carrier proteins and active membrane transport. In: *Molecular Biology of the Cell. 4th edition. Garland Science*. 2002.

3. **Almansa E**, **Sanchez J**, **Cozzi S**, **Casariego M**, **Cejas J**, **Díaz M**. Segmental heterogeneity in the biochemical properties of the Na+-K+-ATPase along the intestine of the gilthead seabream (Sparus aurata L.). *J Comp Physiol - B Biochem Syst Environ Physiol* 171: 557–567, 2001.

4. **Angelo S**, **Devés R**. Amino acid transport system y+L of human erythrocytes: Specificity and cation dependence of the translocation step. *J Membr Biol* 141: 183–192, 1994.

5. **Arriza JL**, **Kavanaugh MP**, **Fairman WA**, **Wu YN**, **Murdoch GH**, **North RA**, **Amara SG**. Cloning and expression of a human neutral amino acid transporter with structural similarity to the glutamate transporter gene family. *J Biol Chem* 268: 15329–15332, 1993.

6. **Babu E**, **Kanai Y**, **Chairoungdua A**, **Kim DK**, **Iribe Y**, **Tangtrongsup S**, **Jutabha P**, **Li Y**, **Ahmed N**, **Sakamoto S**, **Anzai N**, **Nagamori S**, **Endou H**. Identification of a Novel System L Amino Acid Transporter Structurally Distinct from Heterodimeric Amino Acid Transporters. *J Biol Chem* 278: 43838–43845, 2003.

7. **Bae JY**, **Ok IH**, **Lee S**, **Hung SSO**, **Min TS**, **Bai SC**. Re-evaluation of dietary methionine requirement by plasma methionine and ammonia concentrations in surgically modified rainbow trout, Oncorhynchus mykiss. *Asian-Australasian J Anim Sci* 24: 974–981, 2011.

8. **Baeverfjord G**, **Krogdahl Å**. Development and regression of soybean meal induced enteritis in Atlantic salmon, Salmo salar L., distal intestine: A comparison with the intestines of fasted fish. *J Fish Dis* 19: 375–387, 1996.

9. **Baik HW**, **Russell RM**. Vitamin B12 deficiency in the elderly. *Annu Rev Nutr* 19: 357–77, 1999.

10. **Baker DH**. Utilization of isomers and analogs of amino acids and other sulfur-containing compounds. *Prog Food Nutr Sci* 10: 133–178, 1986.

11. **Baker DH**. Comparative species utilization and toxicity of sulfur amino acids. *J Nutr* 136: 1670S-1675S, 2006.

12. **Baker SK**, **Mccullagh KJA**, **Bonen A**. Training intensity-dependent and tissue-specific increases in lactate uptake and MCT-1 in heart and muscle. *J Appl Physiol* 84: 987–994, 1998.

13. **Balimane P V.**, **Chong S**, **Morrison RA**. Current methodologies used for evaluation of intestinal permeability and absorption. *J Pharmacol Toxicol Methods* 44: 301–312, 2000.

14. **Balocco C**, **Boge C**, **Roche H**. Neutral amino acid transport by marine fish intestine: role of the side chain. *J Comp Physiol* 61: 340–347, 1993.

15. **Baltz JM**, **Corbett HE**, **Richard S**. Measuring transport and accumulation of radiolabeled

substrates in oocytes and embryos. In: *Homer H. (eds) Mammalian Oocyte Regulation. Humana Press, Totowa, NJ*. 2013, p. 163–178.

16. **Barac-Nieto M**, **Murer H**, **Kinne R**. Lactate-sodium cotransport in rat renal brush border membranes. *Am J Physiol Physiol* 239: F496-506, 1980.

17. **Barbarat B**, **Podevin RA**. Stoichiometry of the renal sodium-L-lactate cotransporter. *J Biol Chem* 263: 12190–12193, 1988.

18. **Barker G**, **Ellory J**. The identification of neutral amino acid transport systems. *Exp Physiol* 75: 3–26, 1990.

19. **Barthe L**, **Woodley J**, **Houin G**. Gastrointestinal absorption of drugs: methods and studies. *Fundam Clin Pharmacol* 13: 154–168, 1999.

20. **Belghit I**, **Skiba-Cassy S**, **Geurden I**, **Dias K**, **Surget A**, **Kaushik S**, **Panserat S**, **Seiliez I**. Dietary methionine availability affects the main factors involved in muscle protein turnover in rainbow trout (Oncorhynchus mykiss). *Br J Nutr* 112: 493–503, 2014.

21. **Benfey TJ**, **Bosa PG**, **Richardson NL**, **Donaldson EM**. Effectiveness of a commercial-scale pressure shocking device for producing triploid salmonids. *Aquac Eng* 7: 147–54, 1988.

22. **Benfey TJ**, **Sutterlin AM**. The haematology of triploid landlocked Atlantic salmon, Salmo solar L. *J Fish Biol* 24: 333–338, 1984.

23. **Berge GE**, **Goodman M**, **Espe M**, **Lied B**. Intestinal absorption of amino acids in fish: Kinetics and interaction of the in vitro uptake of L-methionine in Atlantic salmon (Salmo salar L.). *Aquaculture* 229: 265–273, 2004.

24. **Bergersen L**, **Rafiki A**, **Ottersen OP**. Immunogold cytochemistry identifies specialized membrane domains for monocarboxylate transport in the central nervous system. *Neurochem Res* 27: 89–96, 2002.

25. **Bin P**, **Huang R**, **Zhou X**. Oxidation resistance of the sulfur amino acids: methionine and cysteine. *Biomed Res Int* 2017: 1–6, 2017.

26. **Blikslager AT**, **Moeser AJ**, **Gookin JL**, **Jones SL**, **Odle J**. Restoration of barrier function in injured intestinal mucosa. *Physiol Rev* 87: 545–564, 2007.

27. **Bodoy S**, **Martín L**, **Zorzano A**, **Palacín M**, **Estévez R**, **Bertran J**. Identification of LAT4, a novel amino acid transporter with system L activity. *J Biol Chem* 280: 12002–12011, 2005.

28. **Boebel KP**, **Baker DH**. Efficacy of the calcium salt and free acid forms of methionine hydroxy analog for chicks. *Poult Sci* 61: 1167–1175, 1982.

29. **Böhmer C**, **Bröer A**, **Munzinger M**, **Kowalczuk S**, **Rasko JEJ**, **Lang F**, **Bröer S**. Characterization of mouse amino acid transporter B0AT1 (slc6a19). *Biochem J* 389: 745–751, 2005.

30. **Bonen A**, **Heynen M**, **Hatta H**. Distribution of monocarboxylate transporters MCT1-MCT8 in rat tissues and human skeletal muscle. *Appl Physiol Nutr Metab* 31: 31–39, 2006.

31. **Brachet P**, **Puigserver A**. Transport of methionine hydroxy analog across the brush border membrane of rat jejunum. *J Nutr* 117: 1241–6, 1987.

32. **Brachet P**, **Puigserver A**. Na+-independent and nonstereospecific transport of 2-hydroxy 4-methylthiobutanoic acid by brush border membrane vesicles from chick small intestine. *Comp Biochem Physiol* 94: 157–163, 1989.

33. **Broer A**, **Brookes N**, **Ganapathy V**, **Dimmer KS**, **Wagner CA**, **Lang F**, **Broer S**. The astroglial ASCT2 amino acid transporter as a mediator of Glutamine efflux. *J Neurochem* 73: 2184–2194, 1999.

34. **Bröer A**, **Klingel K**, **Kowalczuk S**, **Rasko JEJ**, **Cavanaugh J**, **Bröer S**. Molecular cloning of mouse amino acid transport system B0, a neutral amino acid transporter related to Hartnup disorder. *J Biol Chem* 279: 24467–24476, 2004.

35. **Bröer A**, **Klingel K**, **Kowalczuk S**, **Rasko JEJ**, **Cavanaugh J**, **Bröer S**. Molecular cloning of mouse amino acid transport system B0, a neutral amino acid transporter related to Hartnup disorder. *J Biol Chem* 279: 24467–24476, 2004.

36. **Bröer A**, **Tietze N**, **Kowalczuk S**, **Chubb S**, **Munzinger M**, **Bak LK**, **Bröer S**. The orphan transporter v7-3 (slc6a15) is a Na+-dependent neutral amino acid transporter (B0AT2). *Biochem J* 393: 421–430, 2006.

37. **Broer A**, **Wagner C**, **Lang F**, **Broer S**. Neutral amino acid transporter ASCT2 displays substrate-induced Na+ exchange and a substrate-gated anion conductance. *Biochem J* 346: 705–710, 2000.

38. **Broer A**, **Wagner CA**, **Lang F**, **Broer S**. The heterodimeric amino acid transporter 4F2hc/y+ LAT2 mediates arginine efflux in exchange with glutamine. *Biochem J* 349: 787–795, 2000.

39. **Bröer S**. Amino acid transport across mammalian intestinal and renal epithelia. *Physiol Rev* 88: 249–286, 2008.

40. **Broer S**, **Broer A**, **Schneider H-P**, **Stegen C**, **Halestrap AP**, **Deitmer JW**. Characterization of the high-affinity monocarboxylate transporter MCT2 in Xenopus laevis oocytes. *Biochem J* 341: 529–535, 1999.

41. **Bröer S**, **Fairweather SJ**. Amino acid transport across the mammalian intestine. *Compr Physiol* 9: 343–373, 2019.

42. **Bröer S**, **Rahman B**, **Pellegri G**, **Pellerin L**, **Martin JL**, **Verleysdonk S**, **Hamprech B**, **Magistretti PJ**. Comparison of lactate transport in astroglial cells and monocarboxylate transporter 1 (MCT 1) expressing Xenopus laevis oocytes. Expression of two different monocarboxylate transporters in astroglial cells and neurons. *J Biol Chem* 272: 30096–30102, 1997.

43. **Broer S**, **Schneider H-P**, **Broer A**, **Rahman B**, **Hamprecht B**, **Deitmer JW**. Characterization of the monocarboxylate transporter 1 expressed in Xenopus laevis oocytes by changes in cytosolic pH. *Biochem J* 333: 167–174, 1998.

44. **Brosnan JT**, **Brosnan ME**, **Bertolo RF**, **Brunton JA**. Methionine: a metabolically unique amino acid. *Livest Sci* 112: 2–7, 2007.

45. **Bucke D**. The anatomy and histology of the alimentary tract of the carnivorous fish the pike Esox lucius L. *J Fish Biol* 3: 421–431, 1971.

46. **Buckingham SD**, **Pym L**, **Sattelle DB**. Oocytes as an expression system for studying receptor/channel targets of drugs and pesticides. In: *Xenopus Protocols. Humana Press.* 2006, p. 331–345.

47. **Buddington RK**, **Diamond JM**. Aristotle revisited : The function of pyloric caeca in fish. *Proc Natl Acad Sci* 83: 8012–8014, 1986.

48. **Buddington RK**, **Diamond JM**. Pyloric ceca of fish: a "new" absorptive organ. *Am J Physiol Liver Physiol* 252: G65-76, 1987.

49. **Bui D**, **Ravasz D**, **Chinopoulos C**. The effect of 2-ketobutyrate on mitochondrial substrate-level phosphorylation. *Neurochem Res* 44: 2301–2306, 2019.

50. **Bunchasak C**. Role of dietary methionine in poultry production. *J Poult Sci* 46: 169–179, 2009.

51. **Burant CF**, **Bell GI**. Mammalian facilitative glucose transporters: evidence for similar substrate recognition sites in functionally monomeric proteins. *Biochemistry* 31: 10414–10420, 1992.

52. **Burnstock G**. The morphology of the gut of the brown trout (Salmo trutta). *Q J Microsc Sci* 100: 183–198, 1959.

53. **Burrells C**, **Williams PD**, **Southgate PJ**, **Crampton VO**. Immunological, physiological and pathological responses of rainbow trout (Oncorhynchus mykiss) to increasing dietary concentrations of soybean proteins. *Vet Immunol Immunopathol* 72: 277–288, 1999.

54. **Busch AE**, **Herzer T**, **Waldegger S**, **Schmidt F**, **Palacin M**, **Biber J**, **Markovich D**, **Murer H**, **Lang F**. Opposite directed currents induced by the transport of dibasic and neutral amino acids in Xenopus oocytes expressing the protein rBAT. *J Biol Chem* 269: 25581–25586, 1994.

55. **Buyse M**, **Sitaraman VS**, **Liu X**, **Bado A**, **Merlin D**. Luminal leptin enhances CD147/MCT-1-mediated uptake of butyrate in the human intestinal cell line Caco2-BBE. *J Biol Chem* 277: 28182–28190, 2002.

56. **Cao XJ**, **Wang WM**, **Song F**. Anatomical and Histological Characteristics of the Intestine of the Topmouth Culter (Culter alburnus). *J Vet Med Ser C Anat Histol Embryol* 40: 292–298, 2011.

57. **Carpenter L**, **Halestrap AP**. The kinetics, substrate and inhibitor specificity of the lactate transporter of Ehrlich-Lettre tumour cells studied with the intracellular pH indicator BCECF. *Biochem J* 304: 751–760, 1994.

58. **Cavet ME**, **Akhter S**, **Murtazina R**, **De Medina FS**, **Chung-Ming TSE**, **Donowitz M**. Half-lives of plasma membrane Na+/H+ exchangers NHE1-3: Plasma membrane NHE2 has a rapid rate of degradation. *Am J Physiol - Cell Physiol* 281: 2039–2048, 2001.

59. **CCAC**. Guidelines On: The Care and Use of Fish in Research, Teaching and Testing. Ottawa, ON, Canada: Canadian Council on Animal Care. 2005.

60. **Chan SY**, **Martín-Santos A**, **Loubière LS**, **González AM**, **Stieger B**, **Logan A**, **Mccabe CJ**, **Franklyn JA**, **Kilby MD**. The expression of thyroid hormone transporters in the human fetal cerebral cortex during early development and in N-Tera-2 neurodifferentiation. *J*

Physiol 589: 2827–2845, 2011.

61. **Cheeseman CI**, **O'Neill D**. Isolation of intestinal brush-border membranes. *Curr Protoc Cell Biol* 30: 3–21, 2006.

62. **Chen J**, **Zhu Y**, **Hu M**. Mechanisms and kinetics of uptake and efflux of L-methionine in an intestinal epithelial model (Caco-2). *J Nutr* 124: 1907–16, 1994.

63. **Chidlow G**, **Wood JPM**, **Graham M**, **Osborne NN**. Expression of monocarboxylate transporters in rat ocular tissues. *Am J Physiol - Cell Physiol* 288: 416–428, 2005.

64. **Chillarón J**, **Estévez R**, **Mora C**, **Wagner CA**, **Suessbrich H**, **Lang F**, **Gelpí JL**, **Testar X**, **Busch AE**, **Zorzano A**, **Palacín M**. Obligatory amino acid exchange via systems b(o,+)-like and y+L-like. A tertiary active transport mechanism for renal reabsorption of cystine and dibasic amino acids. *J Biol Chem* 271: 17761–17770, 1996.

65. **Chillarón J**, **Estévez R**, **Mora C**, **Wagner CA**, **Suessbrich H**, **Lang F**, **Gelpí JL**, **Testar X**, **Busch AE**, **Zorzano A**, **Palacín M**. Obligatory amino acid exchange via systems b o,+ -like and y + L-like. *J Biol Chem* 271: 17761–17770, 1996.

66. **Choct M**. Managing gut health through nutrition. *Br Poult Sci* 50: 9–15, 2009.

67. **Christense HN**. A transport system serving for mono- and diamino acids. *Proc Natl Acad Sci U S A* 51: 337–344, 1964.

68. **Christensen H**, **Oxender DL**, **Liang M**, **Vatz KA**. The use of N-Methylation to direct the route of mediated transport of amino acids. *J Biol Chem* 240: 3609–3616, 1965.

69. **Christensen HN**, **Antonioli JA**. Cationic amino acid transport in the rabbit reticulocyte. *J Biol Chem* 244: 1497–1504, 1969.

70. **Christensen HN**, **Liang M**. Transport of diamino acids into the Ehrlich cell. *J Biol Chem* 241: 5542–5551, 1966.

71. **Christensen HN**, **Liang M**, **Archer EG**. A distinct Na+-requiring transport system for alanine, serine, cysteine, and similar amino acids. *J Biol Chem* 242: 5237–5246, 1967.

72. **Clarke LL**. A guide to Ussing chamber studies of mouse intestine. *Am J Physiol Liver Physiol* 296: G1151–G1166, 2009.

73. **Cleal JK**, **Glazier JD**, **Ntani G**, **Crozier SR**, **Day PE**, **Harvey NC**, **Robinson SM**, **Cooper C**, **Godfrey KM**, **Hanson MA**, **Lewis RM**. Facilitated transporters mediate net efflux of amino acids to the fetus across the basal membrane of the placental syncytiotrophoblast. *J Physiol* 589: 987–997, 2011.

74. **Cleveland BM**, **Weber GM**. Ploidy effects on genes regulating growth mechanisms during fasting and refeeding in juvenile rainbow trout (Oncorhynchus mykiss). *Mol Cell Endocrinol* 382: 139–149, 2014.

75. **Closs EI**, **Gräf P**, **Habermeier A**, **Cunningham JM**, **Förstermann U**. Human cationic amino acid transporters hCAT-1, hCAT-2A, and hCAT-2B: Three related carriers with distinct transport properties. *Biochemistry* 36: 6462–6468, 1997.

76. **Coady MJ**, **Chang MH**, **Charron FM**, **Plata C**, **Wallendorff B**, **Sah JF**, **Markowitz SD**, **Romero MF**, **Lapointe JY**. The human tumour suppressor gene SLC5A8 expresses a Na+ -monocarboxylate cotransporter. *J Physiol* 557: 719–731, 2004.

77. **Collie NL**. Intestinal nutrient transport in coho salmon (Oncorhynchus kisutch) and the effects of development, starvation, and seawater adaptation. *J Comp Physiol B* 156: 163–174, 1985.

78. **Cotter D**, **O'Donovan V**, **O'Maoiléidigh N**, **Rogan G**, **Roche N**, **Wilkins NP**. An evaluation of the use of triploid Atlantic salmon (Salmo salar L.) in minimising the impact of escaped farmed salmon on wild populations. *Aquaculture* 186: 61–75, 2000.

79. **Craig PM**, **Moon TW**. Methionine restriction affects the phenotypic and transcriptional response of rainbow trout (Oncorhynchus mykiss) to carbohydrate-enriched diets. *Br J Nutr* 109: 402–412, 2013.

80. **Curran PF**, **Solomon AK**. Ion and water fluxes in the ileum of rats. *J Genera* 41: 143–168, 1957.

81. **Dabrowski K**, **Rinchard J**, **Lee K-J**, **Blom JH**, **Ciereszko A**, **Ottobre J**. Effects of diets containing gossypol on reproductive capacity of rainbow trout (Oncorhynchus mykiss). *Biol Reprod* 62: 227–234, 2000.

82. **Dahan A**, **West BT**, **Amidon GL**. Segmental-dependent membrane permeability along the intestine following oral drug administration: Evaluation of a triple single-pass intestinal perfusion (TSPIP) approach in the rat. *Eur J Pharm Sci* 36: 320–329, 2009.

83. **Dänner E**, **Bessei W**. Effectiveness of liquid DL-methionine hydroxy analogue-free acid (DL-MHA-FA) compared to DL-methionine on performance of laying hens. *Arch für Geflügelkd* 66: 97–101, 2002.

84. **Day PE**, **Cleal JK**, **Lofthouse EM**, **Hanson MA**, **Lewis RM**. What factors determine placental glucose transfer kinetics. *Placenta* 34: 953–958, 2013.

85. **Deitmer JW**, **Bröer A**, **Bröer S**. Glutamine efflux from astrocytes is mediated by multiple pathways. *J Neurochem* 87: 127–135, 2003.

86. **Deuticke B**, **Rickert I**, **Beyer E**. Stereoselective, SH-dependent transfer of lactate in mammalian erythrocytes. *Biochim Biophys Acta - Biomembr* 507: 137–55, 1978.

87. **Devés R**, **Boyd CAR**. Transporters for cationic amino acids in animal cells: Discovery, structure, and function. *Physiol Rev* 78: 487–545, 1998.

88. **Deves R**, **Chavez P**, **Boyd CA**. Identification of a new transport system (y+ L) in human erythrocytes that recognizes lysine and leucine with high affinity. *J Physiol* 454: 491–501, 1992.

89. **Devlin RH**, **Sakhrani D**, **Biagi CA**, **Eom KW**. Occurrence of incomplete paternal-chromosome retention in GH-transgenic coho salmon being assessed for reproductive containment by pressure-shock-induced triploidy. *Aquaculture* 304: 66–78, 2010.

90. **Dibner JJ**, **Knight CD**. Conversion of 2-Hydroxy-4-(Methylthio)butanoic Acid to L-Methionine in the Chick: A Stereospecific Pathway. *J Nutr* 114: 1716–1723, 1984.

91. **Dimmer KS**, **Friedrich B**, **Lang F**, **Deitmer JW**, **Broer S**. The low-affinity monocarboxylate transporter MCT4 is adapted to the export of lactate in highly glycolytic cells. *Biochem J* 350: 219–227, 2000.

92. **Doluisio JT**, **Billups NF**, **Dittert LW**, **Sugita ET**, **Swintosky J V**. Drug absorption I: An

in situ rat gut technique yielding realistic absorption rates. *J Pharm Sci* 58: 1196–200, 1969.

93. **Doyle FA**, **McGivan JD**. The bovine renal epithelial cell line NBL-1 expresses a broad specificity Na+-dependent neutral amino acid transport system (System B°) similar to that in bovine renal brush border membrane vesicles. *BBA - Biomembr* 1104: 55–62, 1992.

94. **Drew MD**, **Syed NA**, **Goldade BG**, **Laarveld B**, **Van Kessel AG**. Effects of dietary protein source and level on intestinal populations of Clostridium perfringens in broiler chickens. *Poult Sci* 83: 414–420, 2004.

95. **Drew MD**, **Van Kessel AG**, **Maenz DD**. Absorption of methionine and 2-hydroxy-4-methylthiobutoanic acid in conventional and germ-free chickens. *Poult Sci* 82: 1149–1153, 2003.

96. **Dubinsky WP**, **Racker E**. The mechanism of lactate transport in human erythrocytes. *J Membr Biol* 44: 25–36, 1978.

97. **Ducroc R**, **Sakar Y**, **Fanjul C**, **Barber A**, **Bado A**, **Lostao MP**. Luminal leptin inhibits L-glutamine transport in rat small intestine: Involvement of ASCT2 and B0AT1. *Am J Physiol - Gastrointest Liver Physiol* 299: 179–185, 2010.

98. **Ellis E**, **Moffett J**. A genetic approach to the study of neutral amino acid transport in mammalian cells in culture. *J Membr Biol* 91: 199–212, 1986.

99. **Elvert C**, **De Abreu Fernandes E**, **Lemme A**. Biological effectiveness of methionine hydroxy-analogue calcium salt in relation to DL-methionine in broiler chickens. *Asian-Australasian J Anim Sci* 21: 1506–1515, 2008.

100. **Engelhardt W V.**, **Rechkemmer G**. Segmental differences of short-chain fatty acid transport across guinea-pig large intestine. *Exp Physiol* 77: 491–499, 1992.

101. **Englund G**, **Rorsman F**, **Rönnblom A**, **Karlbom U**, **Lazorova L**, **Gråsjö J**, **Kindmark A**, **Artursson P**. Regional levels of drug transporters along the human intestinal tract: Co-expression of ABC and SLC transporters and comparison with Caco-2 cells. *Eur J Pharm Sci* 29: 269–277, 2006.

102. **Erickson RH**, **Gum JR**, **Lindstrom MM**, **McKean D**, **Kim YS**. Regional expression and dietary regulation of rat small intestinal peptide and amino acid transporter mRNAs. *Biochem Biophys Res Commun* 216: 249–57, 1995.

103. **Espe M**, **Andersen SM**, **Holen E**, **Rønnestad I**, **Veiseth-Kent E**, **Zerrahn J-EE**, **Aksnes A**. Methionine deficiency does not increase polyamine turnover through depletion of hepatic S-adenosylmethionine in juvenile Atlantic salmon. *Br J Nutr* 112: 1274–1285, 2014.

104. **Esteve-Garcia E**, **Austic RE**. Intestinal absorption and renal excretion of dietary methionine sources by the growing chicken. *J Nutr Biochem* 4: 576–587, 1993.

105. **Fagerholm U**, **Johansson M**, **Lennernäs H**. Comparison between permeability coefficients in rat and human jejunum. *Pharm Res* 13: 1336–1342, 1996.

106. **Fankhauser BYG**. The effects of changes in chromosome number on amphibian development. *Q Rev Biol* 20: 20–78, 1945.

107. **FAO**. The State of World Fisheries and Aquaculture 2014: opportunities and challenges. *Food Agric. United Nations*.

108. **FAO**. The State of World Fisheries and Aquaculture 2018-Meeting the sustainable development goals. *CC BY-NC-SA 3.0 IGO*.

109. **FAO**. *The State of World Fisheries and Aquaculture. Sustainability in action*. 2020.

110. **Fast AW**, **Pewnim T**, **Keawtabtim R**, **Saijit R**, **Te FT**, **Vejaratpimol R**. Comparative growth of diploid and triploid Asian catfish clarias macrocephalus in Thailand. *J World Aquac Soc* 26: 390–395, 1995.

111. **Feher JJ**. *Quantitative human physiology: an introduction*. Academic press, 2017.

112. **Feng D**, **Zhou X**, **Zuo J**, **Zhang C**, **Yin Y**, **Wang X**, **Wang T**. Segmental distribution and expression of two heterodimeric amino acid transporter mRNAs in the intestine of pigs during different ages. *J Sci Food Agric* 88: 1012–1018, 2008.

113. **Feng Z**, **Ma Y**, **Wang X**, **Li, Xiaojie**, **Thacker P.** Efficacy of methionine hydroxy analog and DL-methionine as methionine sources for growing pigs. *J Anim Vet Adv* 5: 135–142, 2006.

114. **Fernández E**, **Carrascal M**, **Rousaud F**, **Abián J**, **Zorzano A**, **Palacín M**, **Chillarón J**. rBAT-b0,+AT heterodimer is the main apical reabsorption system for cystine in the kidney. *Am J Physiol Physiol* 283: F540–F548, 2002.

115. **Ferraris RP**, **Ahearn GA**. Sugar and amino acid transport in fish intestine. *Comp Biochem Physiol -- Part A Physiol* 77: 397–413, 1984.

116. **Finkelstein JD**. Methionine metabolism in mammals. *J Biol Chem* 1: 228–237, 1990.

117. **Finkelstein JD**. Pathways and regulation of homocysteine metabolism in mammals. *Semin Thromb Hemost* 26: 219–225, 2000.

118. **Finkelstein JD**, **Martin JJ**. Methionine metabolism in mammals. *J Nutr Biochem* 259: 9508–9513, 1984.

119. **Fishbein WN**, **Merezhinskaya N**, **Foellmer JW**. Relative distribution of three major lactate transporters in frozen human tissues and their localization in unfixed skeletal muscle. *Muscle and Nerve* 26: 101–112, 2002.

120. **Flint HJ**, **Scott KP**, **Louis P**, **Duncan SH**. The role of the gut microbiota in nutrition and health. *Nat Rev Gastroenterol Hepatol* 9: 577–589, 2012.

121. **Forsling BYML**, **Widdas WF**. The effect of temperature on the competitive inhibition of glucose transfer in human erythrocytes by phenolphthalein, phloretin and stilboestrol. 194: 545–554, 1968.

122. **Forster IP**, **Dominy WG**. Efficacy of three methionine sources in diets for Pacific white shrimp, Litopenaeus vannamei. *J World Aquac Soc* 37: 474–480, 2006.

123. **Fotiadis D**, **Kanai Y**, **Palacín M**. The SLC3 and SLC7 families of amino acid transporters. *Mol Aspects Med* 34: 139–158, 2013.

124. **Fraga S**, **Pinho MJ**, **Soares-Da-Silva P**. Expression of LAT1 and LAT2 amino acid transporters in human and rat intestinal epithelial cells. *Amino Acids* 29: 229–233, 2005.

125. **Fraser TWK**, **Hansen T**, **Skjæraasen JE**, **Mayer I**, **Sambraus F**, **Fjelldal PG**. The effect of triploidy on the culture performance, deformity prevalence, and heart morphology in

Atlantic salmon. *Aquaculture* 416–417: 255–264, 2013.

126. **Friesema ECH**, **Ganguly S**, **Abdalla A**, **Manning Fox JE**, **Halestrap AP**, **Visser TJ**. Identification of monocarboxylate transporter 8 as a specific thyroid hormone transporter. *J Biol Chem* 278: 40128–40135, 2003.

127. **Furriols M**, **Chillaron J**, **Mora C**, **Castello A**, **Bertran J**, **Camps M**, **Testar X**, **Vilaro S**, **Zorzano A**, **Palacin M**. rBAT, related to L-cystine transport, is localized to the microvilli of proximal straight tubules, and its expression is regulated in kidney by development. *J Biol Chem* 268: 27060–27068, 1993.

128. **Ganapathy V**, **Ganapathy ME**, **Leibach FH**. Intestinal transport of peptides and amino acids. *Curr Top Membr* 50: 379–412, 2000.

129. **Ganapathy V**, **Gopal E**, **Miyauchi S**, **Prasad PO**. Biological functions of SLC5A8, a candidate tumour suppressor. *Biochem Soc Trans* 33: 237–240, 2005.

130. **Ganapathy V**, **Thangaraju M**, **Gopal E**, **Martin PM**, **Itagaki S**, **Miyauchi S**, **Prasad PD**. Sodium-coupled monocarboxylate transporters in normal tissues and in cancer. *AAPS J* 10: 193, 2008.

131. **Garcia CK**, **Brown MS**, **Pathak RK**, **Goldstein JL**. cDNA cloning of MCT2, a second monocarboxylate transporter expressed in different cells than MCT1. *J. Biol. Chem.* 270: 1843–1849, 1995.

132. **Garcia CK**, **Goldstein JL**, **Pathak RK**, **Anderson RGW**, **Brown MS**. Molecular characterization of a membrane transporter for lactate, pyruvate, and other monocarboxylates: Implications for the Cori cycle. *Cell* 76: 865–873, 1994.

133. **Gazzola GC**, **Dall'Asta V**, **Guidotti GG**. The transport of neutral amino acids in cultured human fibroblasts. *J Biol Chem* 255: 929–936, 1980.

134. **Gill RK**, **Saksena S**, **Alrefai WA**, **Sarwar Z**, **Goldstein JL**, **Carroll RE**, **Ramaswamy K**, **Dudeja PK**. Expression and membrane localization of MCT isoforms along the length of the human intestine. *Am J Physiol - Cell Physiol* 289: 846–852, 2005.

135. **Gliddon CM**, **Shao Z**, **LeMaistre JL**, **Anderson CM**. Cellular distribution of the neutral amino acid transporter subtype ASCT2 in mouse brain. *J Neurochem* 108: 372–383, 2009.

136. **Goff JB**, **Gatlin DM**. Evaluation of different sulfur amino acid compounds in the diet of red drum, Sciaenops ocellatus, and sparing value of cystine for methionine. *Aquaculture* 241: 465–477, 2004.

137. **Goldin AL**. Expression of ion channels by injection of mRNA into Xenopus oocytes. In: *Methods in Cell Biology. Academic Press*. 1991, p. 487–509.

138. **Gonçalves P**, **Martel F**. Regulation of colonic epithelial butyrate transport: Focus on colorectal cancer. *Porto Biomed J* 1: 83–91, 2016.

139. **Gopal E**, **Fei Y-J**, **Miyauchi S**, **Zhuang L**, **Prasad PD**, **Ganaopathy V**. Sodium-coupled and electrogenic transport of B-complex vitamin nicotinic acid by slc5a8, a member of the Na/glucose co-transporter gene family. *Biochem J* 388: 309–316, 2005.

140. **Gopal E**, **Fei YJ**, **Sugawara M**, **Miyauchi S**, **Zhuang L**, **Martin P**, **Smith SB**, **Prasad PD**, **Ganapathy V**. Expression of slc5a8 in kidney and its role in Na+-coupled transport of

lactate. *J Biol Chem* 279: 44522–44532, 2004.

141. **Gopal E**, **Miyauchi S**, **Martin PM**, **Ananth S**, **Roon P**, **Smith SB**, **Ganapathy V**. Transport of nicotinate and structurally related compounds by human SMCT1 (SLC5A8) and its relevance to drug transport in the mammalian intestinal tract. *Pharm Res* 24: 575–584, 2007.

142. **Gopal E**, **Umapathy NS**, **Martin PM**, **Ananth S**, **Gnana-Prakasam JP**, **Becker H**, **Wagner CA**, **Ganapathy V**, **Prasad PD**. Cloning and functional characterization of human SMCT2 (SLC5A12) and expression pattern of the transporter in kidney. *Biochim Biophys Acta - Biomembr* 1768: 2690–2697, 2007.

143. **Gould GW**, **Thomas HM**, **Jess TJ**, **Bell GI**. Expression of human glucose transporters in Xenopus oocytes: Kinetic characterization and substrate specificities of the erythrocyte, liver, and brain isoforms. *Biochemistry* 30: 5139–5145, 1991.

144. **Gray GM**, **Ingelfinger FJ**. Intestinal absorption of sucrose in man : Interrelation of hydrolysis and monosaccharide product absorption. *J Clin Invest* 45: 388–398, 1966.

145. **Grollman EF**, **Philp NJ**, **McPhie P**, **Ward RD**, **Sauer B**. Determination of transport kinetics of chick MCT3 monocarboxylate transporter from retinal pigment epithelium by expression in genetically modified yeast. *Biochemistry* 39: 9351–9357, 2000.

146. **Grosell M**, **Gilmour KM**, **Perry SF**. Intestinal carbonic anhydrase, bicarbonate, and proton carriers play a role in the acclimation of rainbow trout to seawater. *Am J Physiol - Regul Integr Comp Physiol* 293: 2099–2111, 2007.

147. **Gu S**, **Adan-Rice D**, **Leach RJ**, **Jiang JX**. A novel human amino acid transporter, hNAT3: cDNA cloning, chromosomal mapping, genomic structure, expression, and functional characterization. *Genomics* 74: 262–272, 2001.

148. **Guetg A**, **Mariotta L**, **Bock L**, **Herzog B**, **Fingerhut R**, **Camargo SMR**, **Verrey F**. Essential amino acid transporter Lat4 (Slc43a2) is required for mouse development. *J Physiol* 593: 1273–1289, 2015.

149. **Guo X**, **Allen SK**. Sex determination and polyploid gigantism in the Dwarf Surfclam. *Genetics* 138: 1199–206, 1994.

150. **Hägglund MGA**, **Roshanbin S**, **Löfqvist E**, **Hellsten S V.**, **Nilsson VCO**, **Todkar A**, **Zhu Y**, **Stephansson O**, **Drgonova J**, **Uhl GR**, **Schiöth HB**, **Fredriksson R**. B0AT2 (SLC6A15) Is Localized to Neurons and Astrocytes, and Is Involved in Mediating the Effect of Leucine in the Brain. *PLoS One* 8: 1–15, 2013.

151. **Hahn T**, **Barth S**, **Weiss U**, **Mosgoeller W**, **Desoye G**. Sustained hyperglycemia in vitro down-regulates the GLUT1 glucose transport system of cultured human term placental trophoblast: a mechanism to protect fetal development? *FASEB J* 12: 1221–31, 1998.

152. **Halestrap AP**. The monocarboxylate transporter family-Structure and functional characterization. *IUBMB Life* 64: 1–9, 2012.

153. **Halestrap AP**. Monocarboxylic acid transporters. *Compr Physiol* 3: 1611–1643, 2013.

154. **Halestrap AP**. The SLC16 gene family-structure, role and regulation in health and disease [Online]. *Mol Aspects Med* 34: 337–349, 2013.

155. **Halestrap AP**, **Meredith D**. The SLC16 gene family - From monocarboxylate transporters (MCTs) to aromatic amino acid transporters and beyond. *Pflugers Arch* 447: 619–628, 2004.

156. **Halestrap AP**, **Price NT**. The proton-linked monocarboxylate transporter (MCT) family structure, function and regulation. *Biochem J* 343: 281–299, 1999.

157. **Halestrap AP**, **Wilson MC**. The monocarboxylate transporter family-role and regulation. *IUBMB Life* 64: 109–119, 2012.

158. **Hand RE**, **Nell JA**, **Thompson PA**. Studies on triploid oysters in Australia: XIII. Performance of diploid and triploid Sydney rock oyster, Saccostrea glomerata (Gould, 1850), progeny from a third generation breeding line. *Aquaculture* 233: 93–107, 2004.

159. **Hansen TJ**, **Olsen RE**, **Stien L**, **Oppedal F**, **Torgersen T**, **Breck O**, **Remen M**, **Vågseth T**, **Fjelldal PG**. Effect of water oxygen level on performance of diploid and triploid Atlantic salmon post-smolts reared at high temperature. *Aquaculture* 435: 354–360, 2015.

160. **Happe A**, **Quillet E**, **Chevassus B**. Early life history of triploid rainbow trout (Salmo gairdneri Richardson). *Aquaculture* 71: 107–118, 1988.

161. **Harris T**, **Eliyahu G**, **Frydman L**, **Degani H**. Kinetics of hyperpolarized 13C1-pyruvate transport and metabolism in living human breast cancer cells. *Proc Natl Acad Sci U S A* 106: 18131–18136, 2009.

162. **Hashimoto Y**, **Sadamoto Y**, **Konno A**, **Kon Y**, **Iwanaga T**. Distribution of neutral amino acid transporter ASCT1 in the non-neuronal tissues of mice. *Jpn J Vet Res* 52: 113–124, 2004.

163. **Hatanaka T**, **Haramura M**, **Fei YJ**, **Miyauchi S**, **Bridges CC**, **Ganapathy PS**, **Smith SB**, **Ganapathy V**, **Ganapathy ME**. Transport of Amino Acid-Based Prodrugs by the Na+- and Cl --Coupled Amino Acid Transporter ATB0,+ and Expression of the Transporter in Tissues Amenable for Drug Delivery. *J Pharmacol Exp Ther* 308: 1138–1147, 2004.

164. **Hatanaka T**, **Huang W**, **Ling R**, **Prasad PD**, **Sugawara M**, **Leibach FH**, **Ganapathy V**. Evidence for the transport of neutral as well as cationic amino acids by ATA3, a novel and liver-specific subtype of amino acid transport system A. *Biochim Biophys Acta - Biomembr* 1510: 10–17, 2001.

165. **Hatanaka T**, **Huang W**, **Wang H**, **Sugawara M**, **Prasad PD**, **Leibach FH**, **Ganapathy V**. Primary structure, functional characteristics and tissue expression pattern of human ATA2, a subtype of amino acid transport system A. *Biochim Biophys Acta - Biomembr* 1467: 1–6, 2000.

166. **Hatzoglou M**, **Fernandez J**, **Yaman I**, **Closs E**. Regulation of cationic amino acid transport: the story of the CAT-1 transporter [Online]. *Annu Rev Nutr* : 377–99, 2004.

167. **Hawkins AJS**, **Day AJ**, **Gérard A**, **Naciri Y**, **Ledu C**, **Bayne BL**, **Héral M**. A genetic and metabolic basis for faster growth among triploids induced by blocking meiosis I but not meiosis II in the larviparous European flat oyster, Ostrea edulis L. *J Exp Mar Bio Ecol* 184: 21–40, 1994.

168. **Hibasami H**, **Hoffman JL**, **Pegg AE**. Decarboxylated S-adenosylmethionine in mammalian cells. *J Biol Chem* 255: 6675–6678, 1980.

169. **Hidalgo IJ**, **Li J**. Carrier-mediated transport and efflux mechanisms of Caco-2 cells. *Adv Drug Deliv Rev* 22: 53–66, 1996.

170. **Hill JE**, **Hemmingsen SM**, **Goldade BG**, **Tim J**, **Klassen J**, **Zijlstra RT**, **Goh H**, **Kessel AG Van**, **Dumonceaux TJ**, **Goh SH**. Comparison of Ileum Microflora of Pigs Fed Corn- , Wheat- , or Barley-Based Diets by Chaperonin-60 Sequencing and Quantitative PCR Comparison of Ileum Microflora of Pigs Fed Corn- , Wheat- , or Barley-Based Diets by Chaperonin-60 Sequencing and Quantitati. 71: 867–875, 2005.

171. **Hoehler D**, **Lemme A**, **Jensen SK**, **Vieira SL**. Relative effectiveness of methionine sources in diets for broiler chickens. *J Appl Poult Res* 14: 679–93, 2005.

172. **Hoehler D**, **Lemme A**, **Roberson K**, **Turner K**. Impact of methionine sources on performance in turkeys. *J Appl Poult Res* 14: 296–305, 2005.

173. **Hoffer LJ**. Homocysteine remethylation and trans-sulfuration. *Metabolism* 53: 1480–3, 2004.

174. **Hong C**, **Maunakea A**, **Jun P**, **Bollen AW**, **Hodgson JG**, **Goldenberg DD**, **Weiss WA**, **Costello JF**. Shared epigenetic mechanisms in human and mouse gliomas inactivate expression of the growth suppressor SLC5A8. *Cancer Res* 65: 3617–3623, 2005.

175. **Hooper L V.**, **Midtvedt T**, **Gordon JI**. How host-microbial interactions shape the nutrient environment of the mammalian intestine. *Annu Rev Nutr* 22: 283–307, 2002.

176. **Hopfer U**, **Nelson K**, **Perrotto J**, **Isselbacher KJ**. Glucose transport in isolated brush border membrane from rat small intestine. *J Biol Chem* 248: 25–32, 1973.

177. **Hosokawa H**, **Sawamura T**, **Kobayashi S**, **Ninomiya H**, **Miwa S**, **Masaki T**. Cloning and characterization of a brain-specific caionic amino acid transporter. *J Biol Chem* 272: 8717–8722, 1997.

178. **Howard A**, **Goodlad RA**, **Walters JRF**, **Ford D**, **Hirst BH**. Increased expression of specific intestinal amino acid and peptide transporter mRNA in rats fed by TPN is reversed by GLP-2. *J Nutr* 134: 2957–2964, 2004.

179. **Howard A**, **Gray PA**, **Ford D**, **Hirst BH**. System ASC activity and expression of the amino acid transporter ASCT1 in human intestinal Caco-2 cells. *J Physiol* 527: 21P-22P, 2000.

180. **Hugo SE**, **Cruz-Garcia L**, **Karanth S**, **Anderson RM**, **Stainier DYR**, **Schlegel A**. A monocarboxylate transporter required for hepatocyte secretion of ketone bodies during fasting. *Genes Dev* 26: 282–293, 2012.

181. **Ideno M**, **Kobayashi M**, **Sasaki S**, **Futagi Y**, **Narumi K**, **Furugen A**, **Iseki K**. Involvement of monocarboxylate transporter 1 (SLC16A1) in the uptake of L-lactate in human astrocytes. *Life Sci* 192: 110–114, 2018.

182. **Ingham L**, **Arme C**. Intestinal absorption of amino acids by rainbow trout, Salmo gairdneri (Richardson). *J Comp Physiol* 117: 323–334, 1977.

183. **Ito K**, **Groudine M**. A new member of the cationic amino acid transporter family is preferentially expressed in adult mouse brain. *J Biol Chem* 272: 26780–26786, 1997.

184. **Iwanaga T**, **Takebe K**, **Kato I**, **Karaki SI**, **Kuwahara A**. Cellular expression of monocarboxylate transporters (MCT) in the digestive tract of the mouse, rat, and humans,

with special reference to slc5a8. *Biomed Res* 27: 243–254, 2006.

185. **Johnson OW**, **Dickhoff WW**, **Utter FM**. Comparative growth and development of diploid and triploid coho salmon, Oncorhynchus kisutch. *Aquaculture* 57: 329–36, 1986.

186. **Jorgensen K. E**, **Sheikh MI**. Transport of pyruvate by luminal membrane vesicles from pars convoluta and pars recta of rabbit proximal tubule. *Biochim Biophys Acta* 938: 345–352, 1988.

187. **Juel C**. Symmetry and pH dependency of the lactate/proton carrier in skeletal muscle studied with rat sarcolemmal giant vesicles. *Biochim Biophys Acta - Biomembr* 1283: 106–110, 1996.

188. **Juel G**, **Halestrap AP**. Lactate transport in skeletal muscle - Role and regulation of the monocarboxylate transporter. *J Physiol* 517: 633–642, 1999.

189. **Kanai Y**, **Fukasawa Y**, **Cha SH**, **Segawa H**, **Chairoungdua A**, **Kim DK**, **Matsuo H**, **Kim JY**, **Miyamoto KI**, **Takeda E**, **Endou H**. Transport properties of a system y+L neutral and basic amino acid transporter. *J Biol Chem* 275: 20787–20793, 2000.

190. **Kansal V.**, **Sharma R**. Mechanism and regulation of amino acid transport in mammary gland. *Asian-Australasian J Anim Sci* 14: 710–719, 2001.

191. **Keembiyehetty CN**, **Gatlin DM**. Evaluation of different sulfur compounds in the diet of juvenile sunshine bass (Morone chrysops ♀ × M. saxatilis ♂). *Comp Biochem Physiol -- Part A Physiol* 112: 155–159, 1995.

192. **Keembiyehetty CN**, **Gatlin DM**. Performance of sunshine bass fed soybean-meal-based diets supple- mented with different methionine compounds. *Progress Fish-Culturist* 59: 25–30, 1997.

193. **Khojasteh SB**, **Sheikhzadeh F**, **Mohammadnejad D**, **Azami A**. Histological, histochemical and ultrastructural study of the intestine of rainbow trout (Oncorhynchus mykiss). *World Appl Sci J* 6: 1525–1531, 2009.

194. **Kim BGGB**, **Lindemann MDMD**, **Rademacher M**, **Brennan JJ**, **Cromwell GL**. Efficacy of DL-methionine hydroxy analog free acid and DL-methionine as methionine sources for pigs. *J Anim Sci* 84: 104–111, 2006.

195. **Kim DK**, **Kanai Y**, **Chairoungdua A**, **Matsuo H**, **Cha SH**, **Endou H**. Expression cloning of a Na+-independent aromatic amino acid transporter with structural similarity to H+/monocarboxylate transporters. *J Biol Chem* 276: 17221–17228, 2001.

196. **Kim DK**, **Kanai Y**, **Matsuo H**, **Kim JY**, **Chairoungdua A**, **Kobayashi Y**, **Enomoto A**, **Cha SH**, **Goya T**, **Endou H**. The human T-type amino acid transporter-1: Characterization, gene organization, and chromosomal location. *Genomics* 79: 95–103, 2002.

197. **Kim JW**, **Closs EI**, **Albritton LM**, **Cunningham JM**. Transport of cationic amino acids by the mouse ecotropic retrovirus receptor. *Nature* 352: 725–728, 1991.

198. **Kirat D**, **Kato S**. Monocarboxylate transporter 1 (MCT1) mediates transport of short-chain fatty acids in bovine caecum. *Exp Physiol* 91: 835–844, 2006.

199. **Kirchhoff P**, **Dave MH**, **Remy C**, **Kosiek O**, **Busque SM**, **Dufner M**, **Geibel JP**, **Verrey F**, **Wagner CA**. An amino acid transporter involved in gastric acid secretion. *Pflugers Arch*

Eur J Physiol 451: 738–748, 2006.

200. **Kleta R**, **Romeo E**, **Ristic Z**, **Ohura T**, **Stuart C**, **Arcos-Burgos M**, **Dave MH**, **Wagner CA**, **Camargo SRM**, **Inoue S**, **Matsuura N**, **Helip-Wooley A**, **Bockenhauer D**, **Warth R**, **Bernardini I**, **Visser G**, **Eggermann T**, **Lee P**, **Chairoungdua A**, **Jutabha P**, **Babu E**, **Nilwarangkoon S**, **Anzai N**, **Kanai Y**, **Verrey F**, **Gahl WA**, **Koizumi A**. Mutations in SLC6A19, encoding B0AT1, cause Hartnup disorder. *Nat Genet* 36: 999–1002, 2004.

201. **Kluge H**, **Gessner DK**, **Herzog E**, **Eder K**. Efficacy of DL-methionine hydroxy analogue-free acid in comparison to DL-methionine in growing male white Pekin ducks. *Poult Sci* 95: 590–594, 2016.

202. **Kobayashi M**, **Hashimoto F**, **Ohe K**, **Nadamura T**, **Nishi K**, **Shikano N**, **Nishii R**, **Higashi T**, **Okazawa H**, **Kawai K**. Transport mechanism of 11C-labeled L- and D-methionine in human-derived tumor cells. *Nucl Med Biol* 39: 1213–1218, 2012.

203. **Kohyama N**, **Shiokawa H**, **Ohbayashi M**, **Kobayashi Y**, **Yamamoto T**. Characterization of monocarboxylate transporter 6: Expression in human intestine and transport of the antidiabetic drug nateglinide. *Drug Metab Dispos* 41: 1883–1887, 2013.

204. **Krogdahl Å**, **Bakke-McKellep AM**, **Baeverfjord G**. Effects of graded levels of standard soybean meal on intestinal structure, mucosal enzyme activities, and pancreatic response in Atlantic salmon (Salmo solar L.). *Aquac Nutr* 9: 361–371, 2003.

205. **Kuang SY**, **Xiao WW**, **Feng L**, **Liu Y**, **Jiang J**, **Jiang WD**, **Hu K**, **Li SH**, **Tang L**, **Zhou XQ**. Effects of graded levels of dietary methionine hydroxy analogue on immune response and antioxidant status of immune organs in juvenile Jian carp (Cyprinus carpio var. Jian). *Fish Shellfish Immunol* 32: 629–636, 2012.

206. **Lafrenière RG**, **Carrel L**, **Willard HF**. A novel transmembrane transporter encoded by the XPCT gene in xq13.2. *Hum Mol Genet* 3: 1133–1139, 1994.

207. **Lam WK**, **Felmlee MA**, **Morris ME**. Monocarboxylate transporter-mediated transport of γ-hydroxybutyric acid in human intestinal Caco-2 cells. *Drug Metab Dispos* 38: 441–447, 2010.

208. **Leclercq E**, **Taylor JF**, **Fison D**, **Fjelldal PG**, **Diez-Padrisa M**, **Hansen T**, **Migaud H**. Comparative seawater performance and deformity prevalence in out-of-season diploid and triploid Atlantic salmon (Salmo salar) post-smolts. *Comp Biochem Physiol - A Mol Integr Physiol* 158: 116–125, 2011.

209. **Lemme A**, **Hoehler D**, **Brennan JJ**, **Mannion PF**. Relative effectiveness of methionine hydroxy analog compared to DL-methionine in broiler chickens. *Poult Sci* 81: 838–845, 2002.

210. **Levine RR**, **McNary WF**, **Kornguth PJ**, **LeBlanc R**. Histological reevaluation of everted gut technique for studying intestinal absorption. *Eur J Pharmacol* 9: 211–9, 1970.

211. **Li G**, **Li J**, **Tan B**, **Wang J**, **Kong X**, **Guan G**, **Li F**, **Yin Y**. Characterization and Regulation of the amino acid transporter SNAT2 in the small intestine of piglets. *PLoS One* 10: 1–15, 2015.

212. **Li H**, **Myeroff L**, **Smiraglia D**, **Romero MF**, **Pretlow TP**, **Kasturi L**, **Lutterbaugh J**, **Rerko RM**, **Casey G**, **Issa JP**, **Willis J**, **Willson JKV**, **Plass C**, **Markowitz SD**. SLC5A8,

a sodium transporter, is a tumor suppressor gene silenced by methylation in human colon aberrant crypt foci and cancers. *Proc Natl Acad Sci U S A* 100: 8412–8417, 2003.

213. **Lilyestrom CG**, **Wolters WR**, **Bury D**, **Rezk M**, **Dunham RA**. Growth, carcass traits, and oxygen tolerance of diploid and triploid catfish hybrids. *N Am J Aquac* 61: 293–303, 1999.

214. **Lin RY**, **Vera JC**, **Chaganti RSK**, **Golde DW**. Human monocarboxylate transporter 2 (MCT2) is a high affinity pyruvate transporter. *J Biol Chem* 273: 28959–28965, 1998.

215. **Lincoln RF**. Sexual maturation in female triploid plaice, Pleuronectes platessa, and plaice × flounder, Platichthys flesus, hybrids. *J Fish Biol* 19: 499–508, 1981.

216. **Lincoln RF**, **Scott AP**. Production of all-female triploid rainbow trout. *Aquaculture* 30: 375–380, 1983.

217. **Lingens G**, **Molnar S**. Studies on metabolism of broilers by using 14C-labelled DL-methionine and DL-methionine hydroxy analogue Ca-salt. *Arch Anim Nutr* 49: 113–24, 1996.

218. **Liu YL**, **Yi GF**, **Song GL**, **Hou YQ**, **Huang JW**, **Vázquez-Añón M**, **Knight CD**. Impact of feeding 2-hydroxy-4-(methylthio)butanoic acid and DL-methionine supplemented maize-soybean-rapeseed meal diets on growth performance and carcase quality of broilers. *Br Poult Sci* 48: 190–197, 2007.

219. **Liu Z**, **Liu K**. The transporters of intestinal tract and techniques applied to evaluate interactions between drugs and transporters. *Asian J Pharm Sci* 8: 151–158, 2013.

220. **Loewen ME**, **Bekar LE**, **Walz W**, **Forsyth GW**, **Gabriel SE**. pCLCA1 lacks inherent chloride channel activity in an epithelial colon carcinoma cell line. *Am J Physiol Liver Physiol* 287: G33–G41, 2004.

221. **Lorenzo A**, **Cozzi S**, **Badía P**, **Bolaños A**. Intestinal phenylalanine transport in the cultured gilthead bream (Sparus aurata). *Comp Biochem Physiol Part A Physiol* 94: 209–213, 1989.

222. **Lorenzo A**, **Rodriguez A**, **García T**, **Badía P**, **Gómez T**. Intestinal glucose and galactose transport in the cultured gilthead bream (Sparus aurata). *Comp Biochem Physiol -- Part A Physiol* 88: 411–416, 1987.

223. **Lovell T**. *Nutrition and feeding of fish. New York: Van Nostrand Reinhold*. 1989.

224. **Lozoya-Agullo I**, **Gonzalez-Alvarez I**, **Zur M**, **Fine-Shamir N**, **Cohen Y**, **Markovic M**, **Garrigues TM**, **Dahan A**, **Gonzalez-Alvarez M**, **Merino-Sanjuán M**, **Bermejo M**, **Avdeef A**. Closed-loop Doluisio (colon, small intestine) and single-pass intestinal perfusion (colon, jejunum) in rat—Biophysical model and predictions based on Caco-2. *Pharm Res* 35: 2, 2018.

225. **Lozoya-Agullo I**, **Zur M**, **Wolk O**, **Beig A**, **González-Álvarez I**, **González-Álvarez M**, **Merino-Sanjuán M**, **Bermejo M**, **Dahan A**. In-situ intestinal rat perfusions for human Fabs prediction and BCS permeability class determination: Investigation of the single-pass vs. the Doluisio experimental approaches. *Int J Pharm* 480: 1–7, 2015.

226. **Lucia V**, **Vieira P**, **Baldisserotto B**. Amino acids and carbohydrates absorption by Na+ -dependent transporters in the pyloric ceca of Hoplias malabaricus (Erythrinidae). *Ciência Rural* 31: 793–797, 2001.

227. **Mackenzie B**, **Erickson JD**. Sodium-coupled neutral amino acid (System N/A) transporters of the SLC38 gene family. *Pflugers Arch Eur J Physiol* 447: 784–795, 2004.

228. **Mackenzie B**, **Schäfer MKH**, **Erickson JD**, **Hedige MA**, **Weihe E**, **Varoqui H**. Functional properties and cellular distribution of the system A glutamine transporter SNAT1 support specialized roles in central neurons. *J Biol Chem* 278: 23720–23730, 2003.

229. **MacLeod CL**. Regulation of cationic amino acid transporter (CAT) gene expression. *Biochem Soc Trans* 24: 846–52, 1996.

230. **Maenz DD**, **Engele-schaan CM**. Methionine and 2-hydroxy-4-methylthiobutanoic acid are transported by distinct Na + -dependent and H + -dependent systems in the brush border membrane of the chick intestinal epithelium. *J Nutr* 126: 529–536, 1996.

231. **Maenz DD**, **Engele-Schaan CM**. Methionine and 2-hydroxy-4-methylthiobutanoic acid are partially converted to nonabsorbed compounds during passage through the small intestine and heat exposure does not affect small intestinal absorption of methionine sources in broiler chicks. *J Nutr* 126: 1438–1444, 1996.

232. **Maffia M**, **Cassano G**, **Marcucci D**, **Vilella S**, **Storelli C**. The Na+-dependent proline carrier, of eel intestinal brush-border membrane, sequentially binds proline and then Na+. *BBA - Biomembr* 1027: 8–16, 1990.

233. **Majumdar S**, **Gunda S**, **Pal D**, **Mitra AK**. Functional activity of a monocarboxylate transporter, MCT1, in the human retinal pigmented epithelium cell line, ARPE-19. *Mol Pharm* 2: 109–117, 2005.

234. **Malik G**, **Hoehler D**, **Rademacher M**, **Drew MD**, **Van Kessel AG**. Apparent absorption of methionine and 2-hydroxy-4-methylthiobutanoic acid from gastrointestinal tract of conventional and gnotobiotic pigs. *Animal* 3: 1378–1386, 2009.

235. **Malo C**. Multiple pathways for amino acid transport in brush border membrane vesicles isolated from the human fetal small intestine. *Gastroenterology* 100: 1644–52, 1991.

236. **Mandal AB**, **Elangovan A V.**, **Johri TS**. Comparing bio-efficacy of liquid DL-methionine hydroxy analogue free acid with DL-methionine in broiler chickens. *Asian-Australasian J Anim Sci* 17: 102–108, 2004.

237. **Manning Fox JE**, **Meredith D**, **Halestrap AP**. Characterisation of human monocarboxylate transporter 4 substantiates its role in lactic acid efflux from skeletal muscle. *J Physiol* 529: 285–293, 2000.

238. **Manor ML**, **Cleveland BM**, **Weber GM**, **Kenney PB**. Effects of sexual maturation and feeding level on fatty acid metabolism gene expression in muscle, liver, and visceral adipose tissue of diploid and triploid rainbow trout, Oncorhynchus mykiss. *Comp Biochem Physiol Part - B Biochem Mol Biol* 179: 17–26, 2015.

239. **Manor ML**, **Weber GM**, **Cleveland BM**, **Yao J**, **Kenney PB**. Expression of genes associated with fatty acid metabolism during maturation in diploid and triploid female rainbow trout. *Aquaculture* 435: 178–186, 2015.

240. **Margheritis E**, **Imperiali FG**, **Cinquetti R**, **Vollero A**, **Terova G**, **Rimoldi S**, **Girardello R**, **Bossi E**. Amino acid transporter B0AT1 (slc6a19) and ancillary protein: impact on function. *Pflugers Arch Eur J Physiol* 468: 1363–1374, 2016.

241. **Margheritis E**, **Terova G**, **Cinquetti R**, **Peres A**, **Bossi E**. Functional properties of a newly cloned fish ortholog of the neutral amino acid transporter B0AT1 (SLC6A19). *Comp Biochem Physiol - A Mol Integr Physiol* 166: 285–292, 2013.

242. **Markovich D**. Expression cloning and radiotracer uptakes in xenopus laevis oocytes. *Nat Protoc* 3: 1975–1980, 2008.

243. **Martín-Venegas R**, **Brufau MT**, **Mañas-Cano O**, **Mercier Y**, **Nonis MK**, **Ferrer R**. Monocarboxylate transporter 1 is up-regulated in Caco-2 cells by the methionine precursor DL-2-hydroxy-(4-methylthio)butanoic acid. *Vet J* 202: 555–560, 2014.

244. **Martín-Venegas R**, **Geraert PA**, **Ferrer R**. Partial Na+ dependence of DL-2-hydroxy-4-(methylthio)butanoic acid uptake in the chicken small intestine. *Poult Sci* 87: 1392–1394, 2008.

245. **Martin-Venegas R**, **Rodriguez-Lagunas MJ**, **Geraert P**, **Ferrer R**. Monocarboxylate transporter 1 mediates DL-2-hydroxy- (4-methylthio) butanoic acid transport across the apical membrane of Caco-2 cell monolayers. *J Nutr* 137: 49–54, 2007.

246. **Martin PM**, **Gopal E**, **Ananth S**, **Zhuang L**, **Itagaki S**, **Prasad BM**, **Smith SB**, **Prasad PD**, **Ganapathy V**. Identity of SMCT1 (SLC5A8) as a neuron-specific Na+-coupled transporter for active uptake of L-lactate and ketone bodies in the brain. *J Neurochem* 98: 279–288, 2006.

247. **Mastrototaro L**, **Sponder G**, **Saremi B**, **Aschenbach JR**. Gastrointestinal methionine shuttle: Priority handling of precious goods. *IUBMB Life* 68: 924–934, 2016.

248. **Mato JM**, **Alvarez L**, **Ortiz P**, **Pajares MA**. S-adenosylmethionine synthesis: molecular mechanisms and clinical implications. *Pharmacol Ther* 73: 265–280, 1997.

249. **Maxime V**. The physiology of triploid fish: Current knowledge and comparisons with diploid fish. *Fish Fish* 9: 67–78, 2008.

250. **McGeachy SA**, **Benfey TJ**, **Friars GW**. Freshwater performance of triploid Atlantic salmon (Salmo salar) in New Brunswick aquaculture. *Aquaculture* 137: 333–341, 1995.

251. **McGivan JD**, **Pastor-Anglada M**. Regulatory and molecular aspects of mammalian amino acid transport. *Biochem J* 299: 321–334, 1994.

252. **Meier C**, **Ristic Z**, **Klauser S**, **Verrey F**. Activation of system L heterodimeric amino acid exchangers by intracellular substrates. *EMBO J* 21: 580–589, 2002.

253. **Mengual R**, **Schlageter MH**, **Sudaka P**. Kinetic asymmetry of renal Na + -L-Lactate cotransport. *J Biol Chem* 265: 292–299, 1990.

254. **Mengual R**, **Sudaka P**. The mechanism of Na+-L-lactate cotransport by brush border membrane vesicles from horse kidney: Analysis of rapid equilibrium kinetics in absence of membrane potential. *J Membr Biol* 71: 163–171, 1983.

255. **Mepham TB**, **Smith MW**. Amino acid transport in the gold fish intestine. *J Physiol* 184: 673–684, 1966.

256. **Merezhinskaya N**, **Ogunwuyi SA**, **Mullick FG**, **Fishbein WN**. Presence and localization of three lactic acid transporters (MCT1, -2, and -4) in separated human granulocytes, lymphocytes, and monocytes. *J Histochem Cytochem* 52: 1483–1493, 2004.

257. **Métayer-Coustard S**, **Mameri H**, **Seiliez I**, **Crochet S**, **Crépieux P**, **Mercier Y**, **Geraert P-A**, **Tesseraud S**. Methionine deprivation regulates the S6K1 pathway and protein synthesis in avian QM7 myoblasts without activating the GCN2/eIF2 alpha cascade. *J Nutr* 140: 1539–1545, 2010.

258. **Métayer S**, **Seiliez I**, **Collin A**, **Duchêne S**, **Mercier Y**, **Geraert PA**, **Tesseraud S**. Mechanisms through which sulfur amino acids control protein metabolism and oxidative status. *J Nutr Biochem* 19: 207–215, 2008.

259. **Meunier V**, **Bourrié M**, **Berger Y**, **Fabre G**. The human intestinal epithelial cell line Caco-2; pharmacological and pharmacokinetic applications. *Cell Biol Toxicol* 11: 187–194, 1995.

260. **Michelato M**, **Furuya WM**, **Gatlin DM**. Metabolic responses of Nile tilapia Oreochromis niloticus to methionine and taurine supplementation. *Aquaculture* 485: 66–72, 2018.

261. **Miller AJ**, **Zhou JJ**. Xenopus oocytes as an expression system for plant transporters. *Biochim Biophys Acta - Biomembr* 1465: 343–358, 2000.

262. **Miller DS**, **Kinter WB**. Pathways of cycloleucine transport in killifish small intestine. *Am J Physiol Metab* 237: E567, 1979.

263. **Mitsumoto Y**, **Sato K**, **Ohyashiki T**, **Mohri T**. Leucine-proton cotransport system in Chang liver cell. *J Biol Chem* 261: 4549–4554, 1986.

264. **Miyauchi S**, **Gopal E**, **Fei YJ**, **Ganapathy V**. Functional identification of SLC5A8, a tumor suppressor down-regulated in colon cancer, as a Na+-coupled transporter for short-chain fatty acids. *J Biol Chem* 279: 13293–13296, 2004.

265. **Morris ME**, **Felmlee MA**. Overview of the proton-coupled MCT (SLC16A) family of transporters: Characterization, function and role in the transport of the drug of abuse γ-hydroxybutyric acid. *AAPS J* 10: 311, 2008.

266. **Moschen I**, **Bröer A**, **Galic S**, **Lang F**, **Bröer S**. Significance of short chain fatty acid transport by members of the monocarboxylate transporter family (MCT). *Neurochem Res* 37: 2562–2568, 2012.

267. **Mueckler M**, **Thorens B**. The SLC2 (GLUT) family of membrane transporters. *Mol Aspects Med* 34: 121–138, 2013.

268. **Munck BG**, **Munck LK**. Phenylalanine transport in rabbit small intestine. *J Physiol* 480: 99–107, 1994.

269. **Munck LK**, **Grøndahl ML**, **Thorbøll JE**, **Skadhauge E**, **Munck BG**. Transport of neutral, cationic and anionic amino acids by systems B, bo,+, XAG, and ASC in swine small intestine. *Comp Biochem Physiol Part A Mol Integr Physiol* 126: 527–537, 2000.

270. **Munck LK**, **Munck BG**. Chloride-dependence of amino acid transport in rabbit ileum. *Biochim Biophys Acta* 1027: 17–20, 1990.

271. **Murakami Y**, **Kohyama N**, **Kobayashi Y**, **Ohbayashi M**, **Ohtani H**, **Sawada Y**, **Yamamoto T**. Functional characterization of human monocarboxylate transporter 6 (SLC16A5). *Pharmacology* 33: 1845–1851, 2005.

272. **Nachi AM**, **Hernandez-Blazquez FJ**, **Barbieri RL**, **Leite RG**, **Ferri S**, **Phan MT**. Intestinal histology of a detritivorous (iliophagous) fish Prochilodus scrofa (characiformes,

prochilodontidae). *Ann des Sci Nat - Zool Biol Anim* 19: 81–88, 1998.

273. **Nagai A**, **Takebe K**, **Nio-Kobayashi J**, **Takahashi-Iwanaga H**, **Iwanaga T**. Cellular expression of the monocarboxylate transporter (MCT) family in the placenta of mice. *Placenta* 31: 126–133, 2010.

274. **Nagamori S**, **Wiriyasermkul P**, **Guarch ME**, **Okuyama H**, **Nakagomi S**, **Tadagaki K**, **Nishinaka Y**, **Bodoy S**, **Takafuji K**, **Okuda S**, **Kurokawa J**, **Ohgaki R**, **Nunes V**, **Palacín M**, **Kanai Y**. Novel cystine transporter in renal proximal tubule identified as a missing partner of cystinuria-related plasma membrane protein rBAT/SLC3A1. *Proc Natl Acad Sci U S A* 113: 775–780, 2016.

275. **Nakanishi T**, **Hatanaka T**, **Huang W**, **Prasad PD**, **Leibach FH**, **Ganapathy ME**, **Ganapathy V**. Na+ - and CI- -coupled active transport of carnitine by the amino acid transporter ATB0,+ from mouse colon expressed in HRPE cells and Xenopus oocytes. *J Physiol* 532: 297–304, 2001.

276. **Nickel A**, **Kottra G**, **Schmidt G**, **Danier J**, **Hofmann T**, **Daniel H**. Characteristics of transport of selenoamino acids by epithelial amino acid transporters. *Chem Biol Interact* 177: 234–241, 2009.

277. **Nishimura H**, **Pallardo F V.**, **Seidner GA**, **Vannucci S**, **Simpson IA**, **Birnbaum MJ**. Kinetics of GLUT1 and GLUT4 glucose transporters expressed in Xenopus oocytes. *J Biol Chem* 268: 8514–8520, 1993.

278. **Nitzan T**, **Rozenberg P**, **Cnaani A**. Differential expression of amino-acid transporters along the intestine of Mozambique tilapia (Oreochromis mossambicus) and the effect of water salinity and time after feeding. *Aquaculture* 472: 71–75, 2017.

279. **Nord E**, **Wright SH**, **Kippen I**, **Wright EM**. Pathways for carboxylic acid transport by rabbit renal brush border membrane vesicles. *Physiol Am J Physiol* 243: F456-62, 1982.

280. **Nord EP**, **Wright SH**, **Kippen I**, **Wright EM**. Specificity of the Na +-dependent monocarboxylic acid transport pathway in rabbit renal brush border membranes. *J Membr Biol* 72: 213–221, 1983.

281. **Nordrum S**, **Bakke-McKellep AM**, **Buddington RK**. Effects of soybean meal and salinity on intestinal transport of nutrients in Atlantic salmon (Salmo. *Comp Biochem Physiol* 125: 317–335, 2000.

282. **Novak DA**, **Beveridge MJ**, **Malandro M**, **Seo J**. Ontogeny of amino acid transport system A in rat placenta. *Placenta* 17: 643–51, 1996.

283. **NRC**. *National Research Council. Nutrient requirements of fish and shrimp*. National academies press, 2011.

284. **Nuez-Ortín WG**, **Carter CG**, **Wilson R**, **Cooke IR**, **Amoroso G**, **Cobcroft JM**, **Nichols PD**. Triploid Atlantic salmon shows similar performance, fatty acid composition and proteome response to diploids during early freshwater rearing. *Comp Biochem Physiol - Part D Genomics Proteomics* 22: 67–77, 2017.

285. **O'Flynn FM**, **Mcgeachy SA**, **Friars GW**, **Benfey TJ**, **Bailey JK**. Comparisions of cultured triploid and diploid Atlantic salmon (Salmo solar L.). *ICES J Mar Sci* 54: 1160–1165, 1997.

286. **Ochs RS**. Understanding enzyme inhibition. *J Chem Educ* 77: 1453–1456, 2000.

287. **Ohkubo M**, **Ohta K**, **Inoue K**, **Yuasa H**. Nicotinate uptake by two kinetically distinct Na+-dependent carrier-mediated transport systems in the rat small intestine. *Drug Metab Pharmacokinet* 27: 255–262, 2012.

288. **Opapeju FO**, **Htoo JK**, **Dapoza C**, **Nyachoti CM**. Bioavailability of methionine hydroxy analog-calcium salt relative to dl-methionine to support nitrogen retention and growth in starter pigs. *Animal* 6: 1750–1756, 2012.

289. **Oppedal F**, **Taranger GL**, **Hansen T**. Growth performance and sexual maturation in diploid and triploid Atlantic salmon (Salmo salar L.) in seawater tanks exposed to continuous light or simulated natural photoperiod. *Aquaculture* 215: 145–162, 2003.

290. **Opstad I**, **Fjelldal PG**, **Karlsen Ø**, **Thorsen A**, **Hansen TJ**, **Taranger GL**. The effect of triploidization of Atlantic cod (Gadus morhua L.) on survival, growth and deformities during early life stages. *Aquaculture* 388–391: 54–59, 2013.

291. **Orsenigo MN**, **Tosco M**, **Bazzini C**, **Laforenza U**, **Faelli A**. A monocarboxylate transporter MCT1 is located at the basolateral pole of rat jejunum. *Exp Physiol* 84: 1033–1042, 1999.

292. **Orsenigo MN**, **Tosco M**, **Laforenza U**, **Faelli A**. Facilitated transport of lactate by rat jejunal enterocyte. *J Membr Biol* 158: 257–264, 1997.

293. **Oxender DL**, **Christensen HN**. Evidence for two types of mediation of neutral amino-acid transport in Ehrlich cells. *Nature* 197: 765–7, 1963.

294. **Ozerov MY**, **Lumme J**, **Päkk P**, **Rintamäki P**, **Ziętara MS**, **Barskaya Y**, **Lebedeva D**, **Saadre E**, **Gross R**, **Primmer CR**, **Vasemägi A**. High Gyrodactylus salaris infection rate in triploid Atlantic salmon Salmo salar. *Dis Aquat Organ* 91: 129–136, 2010.

295. **Pace N**, editor. *Basic and advanced sciences for anaesthetic practice: Prepare for the FRCA: Key articles from the anaesthesia and intensive care medicine journal*. Elsevier Health Sciences, 2015.

296. **Palacin M**. A new family of proteins (rBAT and 4F2hc) involved in cationic and zwitterionic amino acid transport: A tale of two proteins in search of a transport function. *J Exp Biol* 196: 123–137, 1994.

297. **Palacín M**, **Esperanza F**, **Josep C**, **Zorzano A**. The amino acid transport system bo,+ and cystinuria Manuel. *Mol Membr Biol* 18: 21–26, 2001.

298. **Pan Y**, **Wong EA**, **Dibner JJ**, **Vazquez-Anon M**, **Webb KE**. Poly (A)+ RNA encoding proteins capable of transporting L -methionine and / or DL -2-hydroxy-4- (methylthio) butanoic acid are present in the intestinal mucosa of broilers. 132: 382–386, 2002.

299. **Paroder V**, **Spencer SR**, **Paroder M**, **Arango D**, **Schwartz S**, **Mariadason JM**, **Augenlicht LH**, **Eskandari S**, **Carrasco N**. Na+/monocarboxylate transport (SMCT) protein expression correlates with survival in colon cancer: Molecular characterization of SMCT. *Proc Natl Acad Sci U S A* 103: 7270–7275, 2006.

300. **Payne RL**, **Lemme A**, **Seko H**, **Hashimoto Y**, **Fujisaki H**, **Koreleski J**, **Swiatkiewicz S**, **Szczurek W**, **Rostagno H**. Bioavailability of methionine hydroxy analog-free acid relative

to DL-methionine in broilers. *Anim Sci J* 77: 427–439, 2006.

301. **Pegg AE**. Mammalian polyamine metabolism and function. *IUBMB Life* 61: 880–894, 2009.

302. **Pegg AE**. Functions of polyamines in mammals. *J Biol Chem* 291: 14904–14912, 2016.

303. **Peña AA**, **Bols NC**, **Marshall SH**. An evaluation of potential reference genes for stability of expression in two salmonid cell lines after infection with either Piscirickettsia salmonis or IPNV. *BMC Res Notes* 3: 101, 2010.

304. **Peruzzi S**, **Hagen Ø**, **Jobling M**. Gut morphology of diploid and triploid Atlantic salmon (Salmo salar L.). *Aquac Int* 23: 1105–1108, 2015.

305. **Peruzzi S**, **Puvanendran V**, **Riesen G**, **Seim RR**, **Hagen Ø**, **Martínez-Llorens S**, **Falk-Petersen IB**, **Fernandes JMO**, **Jobling M**. Growth and development of skeletal anomalies in diploid and triploid Atlantic salmon (Salmo salar) fed phosphorus-rich diets with fish meal and hydrolyzed fish protein. *PLoS One* 13: 1–16, 2018.

306. **Pfeiffer R**, **Loffing J**, **Rossier G**, **Bauch C**, **Meier C**, **Eggermann T**, **Loffing-cueni D**, **Kuhn LC**, **Verrey F**. Luminal heterodimeric amino acid transporter defective in Cystinuria. *Mol Biol Cell* 10: 4135–4147, 1999.

307. **Pfeiffer R**, **Rossier G**, **Spindler B**, **Meier C**, **Kühn L**, **Verrey F**. Amino acid transport of y+L-type by heterodimers of 4F2hc/CD98 and members of the glycoprotein-associated amino acid transporter family. *EMBO J* 18: 49–57, 1999.

308. **Philp NJ**, **Yoon H**, **Grollma E**. Monocarboxylate transporter MCT1 is located in the apical membrane and MCT3 in the basal membrane of rat RPE. *Am J Physiol Integr Comp Physiol* 274: R1824–R1828, 1998.

309. **Philp NJ**, **Yoon H**, **Lombardi L**. Mouse MCT3 gene is expressed preferentially in retinal pigment and choroid plexus epithelia. *Am J Physiol - Cell Physiol* 280: 1319–1326, 2001.

310. **Pickel VM**, **Nirenberg MJ**, **Chan J**, **Mosckovitz R**, **Udenfriend S**, **Tate SS**. Ultrastructural localization of a neutral and basic amino acid transporter in rat kidney and intestine. *Proc Natl Acad Sci U S A* 90: 7779–7783, 1993.

311. **Pilegaard H**, **Terzis G**, **Halestrap A**, **Juel G**. Distribution of the lactate/H+ transporter isoforms MCT1 and MCT4 in human skeletal muscle. *Am J Physiol - Endocrinol Metab* 276: 843–848, 1999.

312. **Pingitore P**, **Pochini L**, **Scalise M**, **Galluccio M**, **Hedfalk K**, **Indiveri C**. Large scale production of the active human ASCT2 (SLC1A5) transporter in Pichia pastoris - functional and kinetic asymmetry revealed in proteoliposomes. *Biochim Biophys Acta - Biomembr* 1828: 2238–2246, 2013.

313. **Pinho MJ**, **Pinto V**, **Serrão MP**, **Jose PA**, **Soares-da-Silva P**. Underexpression of the Na + -dependent neutral amino acid transporter ASCT2 in the spontaneously hypertensive rat kidney. *Am J Physiol Integr Comp Physiol* 293: R538–R547, 2007.

314. **Pinto M**, **Robine-Leon S**, **Appay M.**, **Kedinger M**, **Triadou N**, **Dussaulx E**, **Lacroix B**, **Simon-Assmann P**, **Haffen K**, **Fogh J**, **Zweibaum**. Enterocytic-like differentiation and polarization of the human colon adenocarcinoma cell line Caco-2 in culture. *Bio Cell* 47:

323–330, 1983.

315. **Plata C**, **Sussman CR**, **Sindić A**, **Liang JO**, **Mount DB**, **Josephs ZM**, **Chang MH**, **Romero MF**. Zebrafish Slc5a12 encodes an electroneutral sodium monocarboxylate transporter (SMCTn): A comparison with the electrogenic SMCT (SMCTe/Slc5a8). *J Biol Chem* 282: 11996–12009, 2007.

316. **Pongtippatee P**, **Laburee K**, **Thaweethamsewee P**, **Hiranphan R**, **Asuvapongpatana S**, **Weerachatyanukul W**, **Srisawat T**, **Withyachumnarnkul B**. Triploid Penaeus monodon: Sex ratio and growth rate. *Aquaculture* 356–357: 7–13, 2012.

317. **Poston HA**. Response of rainbow trout to source and dietary methionine. *Comp Biochem Physiol* 83: 739–744, 1986.

318. **Poston HA**, **Riis RC**, **Rumsey GL**, **Ketola HG**. The effect of supplemental dietary amino acids, minerals and vitamins on salmonids fed cataractogenic diets. *Cornell Vet* 67: 472–509, 1977.

319. **Powell CD**, **Chowdhury MAK**, **Bureau DP**. Assessing the bioavailability of L-methionine and a methionine hydroxy analogue (MHA-Ca) compared to DL-methionine in rainbow trout (Oncorhynchus mykiss). *Aquac Res* 48: 332–346, 2017.

320. **Pradeep PJ**, **Srijaya TC**, **Hassan A**, **Chatterji AK**, **Raghavan R**, **Withyachumnarnkul B**, **Jeffs A**. Growth performance of triploid red tilapia reared under laboratory conditions. *J Appl Aquac* 25: 176–189, 2013.

321. **Prasad PD**, **Wang H**, **Huang W**, **Kekuda R**, **Rajan DP**, **Leibach FH**, **Ganapathy V**. Human LAT1, a subunit of system L amino acid transporter: Molecular cloning and transport function. *Biochem Biophys Res Commun* 255: 283–288, 1999.

322. **Preston RL**, **Schaeffer JF**, **Curran PF**. Structure-affinity relationships of substrates for the neutral amino acid transport system in rabbit ileum. *J Gen Physiol* 64: 443–467, 1974.

323. **Price NT**, **Jackson VN**, **Halestrap AP**. Cloning and sequencing of four new mammalian monocarboxylate transporter (MCT) homologues confirms the existence of a transporter family with an ancient past. *Biochem Biophys Res Commun* 329: 321–328, 1998.

324. **Quast C**, **Cuboni S**, **Bader D**, **Altmann A**, **Weber P**, **Arloth J**, **Röh S**, **Brückl T**, **Ising M**, **Kopczak A**, **Erhardt A**, **Hausch F**, **Lucae S**, **Binder EB**. Functional coding variants in SLC6A15, a possible risk gene for major depression. *PLoS One* 8: e68645, 2013.

325. **Rasch I**, **Görs S**, **Tuchscherer A**, **Htoo JK**, **Kuhla B**, **Metges CC**. Substitution of dietary sulfur amino acids by DL-2-hydroxy-4-methylthiobutyric acid increases remethylation and decreases transsulfuration in weaned piglets. *J Nutr* 149: 432–440, 2019.

326. **Rechkemmer G**, **von Engelhardt W**. Concentration- and pH-dependence of short-chain fatty acid absorption in the proximal and distal colon of guinea pig (Cavia porcellus). *Comp Biochem Physiol -- Part A Physiol* 91: 659–663, 1988.

327. **Regina A**, **Roux F**, **Revest PA**. Glucose transport in immortalized rat brain capillary endothelial cells in vitro: transport activity and GLUT1 expression. *Biochim Biophys Acta - Gen Subj* 1335: 135–143, 1997.

328. **Richards JD**, **Atwell CA**, **Vázquez-Añón M**, **Dibner JJ**. Comparative in vitro and in vivo

absorption of 2-hydroxy-4(methylthio) butanoic acid and methionine in the broiler chicken. *Poult Sci* 84: 1397–1405, 2005.

329. **Riedijk MA**, **Stoll B**, **Chacko S**, **Schierbeek H**, **Sunehag AL**, **Van Goudoever JB**, **Burrin DG**. Methionine transmethylation and transsulfuration in the piglet gastrointestinal tract. *Proc Natl Acad Sci U S A* 104: 3408–3413, 2007.

330. **Ritzhaupt A**, **Wood IS**, **Ellis A**, **Hosie KB**, **Shirazi-Beechey SP**. Identification and characterization of a monocarboxylate transporter (MCT1) in pig and human colon: Its potential to transport L-lactate as well as butyrate. *J Physiol* 513: 719–732, 1998.

331. **Robinson EH**, **Otis W. Allen J**, **Poe WE**, **Wilson RP**. Utilization of dietary sulfur compounds by fingerling channel catfish: L-methionine, DL-methionine, methionine hydroxy analogue, taurine and inorganic sulfate. *J Nutr* 108: 1932–1936, 1978.

332. **Robinson EH**, **Otis W. Allen J**, **Poe WEWE**, **Wilson RPRP**, **Robinson E.H.**, **Otis WA**, **Poe WEWE**, **Wilson RPRP**, **Robinson EH**, **Otis W. Allen J**, **Poe WEWE**, **Wilson RPRP**. Utilization of dietary sulfur compounds by fingerling channel catfish: L-methionine, DL-methionine, methionine hydroxy analogue, taurine and inorganic sulfate. *J Nutr* 108: 1932–1936, 1978.

333. **Rodriguez AM**, **Perron B**, **Lacroix L**, **Caillou B**, **Leblanc G**, **Schlumberger M**, **Bidart JM**, **Pourcher T**. Identification and characterization of a putative human iodide transporter located at the apical membrane of thyrocytes. The Journal of Clinical Endocrinology. *J Clin Endocr Metab* 87: 3500–3503, 2002.

334. **Römer A**, **Abel H**. Effects of DL-methionine hydroxyanalogue (MHA) or DL-methionine (DL-met) on N-retention in broiler chickens and pigs. *Anim Feed Sci Technol* 81: 193–203, 1999.

335. **Rumsey GL**, **Siwicki AK**, **Anderson DP**, **Bowser PR**. Effect of soybean protein on serological response, non-specific defense mechanisms, growth, and protein utilization in rainbow trout. *Vet Immunol Immunopathol* 41: 323–339, 1994.

336. **Sadler J**, **Pankhurst PM**, **King HR**. High prevalence of skeletal deformity and reduced gill surface area in triploid Atlantic salmon (Salmo salar L.). *Aquaculture* 198: 369–386, 2001.

337. **Sangali CP**, **Bruno LD**, **Nunes R**, **de Oliveira Neto AR**, **Pozza PC**, **Henz JR**, **Giacobbo FC**, **Berwanger E**. Bioavailability of different methionine sources for broilers from 1 to 21 days old. *Cienc e Investig Agrar* 42: 35–43, 2015.

338. **Santos ML**, **Arantes FP**, **Santiago KB**, **Dos Santos JE**. Morphological characteristics of the digestive tract of schizodon knerii (Steindachner, 1875), (characiformes: Anostomidae): An anatomical, histological and histochemical study. *An Acad Bras Cienc* 87: 867–878, 2015.

339. **Sauer N**, **Emrich K**, **Piepho HP**, **Lemme A**, **Redshaw MS**, **Mosenthin R**. Meta-analysis of the relative efficiency of methionine-hydroxy-analogue- free-acid compared with DL-methionine in broilers using nonlinear mixed models. *Poult Sci* 87: 2023–2031, 2008.

340. **Scalise M**, **Pochini L**, **Panni S**, **Pingitore P**, **Hedfalk K**, **Indiveri C**. Transport mechanism and regulatory properties of the human amino acid transporter ASCT2 (SLC1A5). *Amino*

Acids 46: 2463–2475, 2014.

341. **Schanker LS**, **Tocco DJ**, **Brodie BB**, **Hogben CA**. Absorption of drugs from the rat small intestine. *ournal Pharmacol Exp Ther* 123: 81–8, 1958.

342. **Schedl BHP**, **Clifton JA**. Solute and water absorption by the human small intestine. *Nature* 199: 1264–1267, 1963.

343. **Schell BYRE**, **Stevens BR**, **Wright EM**. Kinetics of sodium-dependent solute transport by rabbit renal and jejunal brush-border vesicles using a fluorescent dye. *J Physiol* 335: 307–318, 1983.

344. **Schep LJ**, **Tucker IG**, **Young G**, **Butt AG**. Regional permeability differences between the proximal and distal portions of the isolated salmonid posterior intestine. *J Comp Physiol - B Biochem Syst Environ Physiol* 167: 370–377, 1997.

345. **Schmitt JMG**, **Soergel KH**, **Wood CM**. Absorption of short chain fatty acids from the human jejunum. *Gastroenterology* 70: 211–5, 1976.

346. **Schnackenberg LK**, **Chen M**, **Sun J**, **Holland RD**, **Dragan Y**, **Tong W**, **Welsh W**, **Beger RD**. Evaluations of the trans-sulfuration pathway in multiple liver toxicity studies. *Toxicol Appl Pharmacol* 235: 25–32, 2009.

347. **Schultz SG**, **Zalusky R**. Ion transport in isolated rabbit Ileum: I. short-circuit current and Na fluxes. *J Gen Physiol* 47: 567–584, 1964.

348. **Schurgers N**, **Bijdendijk J**, **Tukker JJ**, **Crommelin DJ**. Comparison of four experimental techniques for studying drug absorption kinetics in the anesthetized rat in situ. *J Pharm Sci* 75: 117–9, 1986.

349. **Schweikhard ES**, **Ziegler CM**. Amino acid secondary transporters: toward a common transport mechanism. *Curr Top Membr* 70: 1–28, 2012.

350. **Scopelliti AJ**, **Font J**, **Vandenberg RJ**, **Boudker O**, **Ryan RM**. Structural characterisation reveals insights into substrate recognition by the glutamine transporter ASCT2/SLC1A5. *Nat Commun* 9: 1–12, 2018.

351. **Segawa H**, **Fukasawa Y**, **Miyamoto K**, **Takeda E**, **Endou H**, **Kanai Y**. Identification and functional characterization of a Na + -independent neutral amino acid transporter with broad substrate selectivity. *J Biol Chem* 274: 19745–19751, 1999.

352. **Séité S**, **Mourier A**, **Camougrand N**, **Salin B**, **Figueiredo-Silva AC**, **Fontagné-Dicharry S**, **Panserat S**, **Seiliez I**. Dietary methionine deficiency affects oxidative status, mitochondrial integrity and mitophagy in the liver of rainbow trout (Oncorhynchus mykiss). *Sci Rep* 8: 10151, 2018.

353. **Sellin JH**, **Desoignie R**, **Burlingame S**. Segmental differences in short-chain fatty acid transport in rabbit colon: effect of pH and Na. *Membr Biol* 136: 147–158, 1993.

354. **Sepponen K**, **Koho N**, **Puolanne E**, **Ruusunen M**, **Pösö AR**. Distribution of monocarboxylate transporter isoforms MCT1, MCT2 and MCT4 in porcine muscles. *Acta Physiol Scand* 177: 79–86, 2003.

355. **Shafgat S**, **Tamarappoo BK**, **Kilberg MS**, **Puranam RS**, **McNamara JO**, **Guadano-Ferraz A**, **Fremeau RT**. Cloning and expression of a novel Na+-dependent neutral amino

acid transporter structurally related to mammalian Na+/glutamate cotransporters. *J Biol Chem* 268: 15351–15355, 1993.

356. **Shen YB**, **Ferket P**, **Park I**, **Malheiros RD**, **Kim SW**. Effects of feed grade L-methionine on intestinal redox status, intestinal development, and growth performance of young chickens compared with conventional DL-methionine. *J Anim Sci* 93: 2977–2986, 2015.

357. **Shotwell MA**, **Jayme DW**, **Kilberg MS**, **Oxender DL**. Neutral amino acid transport systems in Chinese hamsetr ovary cells. *J Biol Chem* 256: 5422–5427, 1981.

358. **Shoveller AK**, **Moehn S**, **Rademacher M**, **Htoo JK**, **Ball RO**. Methionine-hydroxy analogue was found to be significantly less bioavailable compared to dl-methionine for protein deposition in growing pigs. *Animal* 4: 61–66, 2010.

359. **Sivaprakasam S**, **Bhutia YD**, **Yang S**, **Ganapathy V**. Short-chain fatty acid transporters: Role in colonic homeostasis. *Compr Physiol* 8: 299–314, 2018.

360. **Skiba-Cassy S**, **Geurden I**, **Panserat S**, **Seiliez I**. Dietary methionine imbalance alters the transcriptional regulation of genes involved in glucose, lipid and amino acid metabolism in the liver of rainbow trout (Oncorhynchus mykiss). *Aquaculture* 454: 56–65, 2016.

361. **Škovierová H**, **Vidomanová E**, **Mahmood S**, **Sopková J**, **Drgová A**, **Červeňová T**, **Halašová E**, **Lehotský J**. The molecular and cellular effect of homocysteine metabolism imbalance on human health. *Int J Mol Sci* 17: 1–18, 2016.

362. **Sloan JL**, **Mager S**. Cloning and functional expression of a human Na+ and Cl--dependent neutral and cationic amino acid transporter B0+. *J Biol Chem* 274: 23740–23745, 1999.

363. **Small SA**, **MacDonald C**, **Farrell AP**. Vascular reactivity of the coronary artery in rainbow trout (Oncorhynchus mykiss). *Am J Physiol Integr Comp Physiol* 258: R1402–R1410, 1990.

364. **Smith RL**. Intestinal amino-acid transport in the marine teleost, Haemulon plumieri. *Comp Biochem Physiol* 30: 1115–1123, 1969.

365. **Smith TB**, **Wahl DH**, **Mackie RI**. Volatile fatty acids and anaerobic fermentation in temperate piscivorous and omnivorous freshwater fish. *J Fish Biol* 48: 829–841, 1996.

366. **Smyth DH**, **Taylor CB**. Intestinal transfer of short-cahin fatty acids in vitro. *J Physiol* 141: 73–80, 1958.

367. **Soriano-García JF**, **Torras-Llort M**, **Ferrer R**, **Moretó M**. Multiple pathways for L-methionine transport in brush-border membrane vesicles from chicken jejunum. *J Physiol* 509: 527–539, 1998.

368. **Souba WW**, **Pan M**, **Stevens BR**. Kinetics of the sodium-dependent glutamine transporter in human intestinal cell confluent monolayers. *Biochem Biophys Res Commun* 188: 746–753, 1992.

369. **Sperandeo MP**, **Paladino S**, **Maiuri L**, **Maroupulos GD**, **Zurzolo C**, **Taglialatela M**, **Andria G**, **Sebastio G**. A y+ LAT-1 mutant protein interferes with y+ LAT-2 activity: Implications for the molecular pathogenesis of lysinuric protein intolerance. *Eur J Hum Genet* 13: 628–634, 2005.

370. **Sperandio B**, **Gautier C**, **McGovern S**, **Ehrlich DS**, **Renault P**, **Martin-Verstraete I**, **Guédon E**. Control of methionine synthesis and uptake by MetR and homocysteine in

Streptococcus mutans. *J Bacteriol* 189: 7032–7044, 2007.

371. **Srinivas SR**, **Gopal E**, **Zhuang L**, **Itagaki S**, **Martin PM**, **Fei Y-J**, **Ganapathy V**, **Prasad PD**. Cloning and functional identification of slc5a12 as a sodium-coupled low-affinity transporter for monocarboxylates (SMCT2). *Biochem J* 392: 655–664, 2005.

372. **Stanley JG**, **Hidu H**, **Allen SK**. Growth of American oysters increased by polyploidy induced by blocking meiosis I but not meiosis II. *Aquaculture* 37: 147–155, 1984.

373. **Stappaerts J**, **Brouwers J**, **Annaert P**, **Augustijns P**. In situ perfusion in rodents to explore intestinal drug absorption : Challenges and opportunities. *Int J Pharm* 478: 665–681, 2015.

374. **Stevens BR**, **Wright EM**. Kinetic model of the brush-border proline/sodium (IMINO) cotransport. *Ann N Y Acad Sci* 456: 115–7, 1985.

375. **Stevens BR**, **Wright EM**. Kinetics of the intestinal brush border proline (Imino) carrier. *J Biol Chem* 262: 6546–6551, 1987.

376. **Subramaniam M**, **Weber LP**, **Loewen ME**. Intestinal electrogenic sodium-dependent glucose absorption in tilapia and trout reveal species differences in SLC5A-associated kinetic segmental segregation. *Am J Physiol Integr Comp Physiol* 316: 222–234, 2019.

377. **Sugawara M**, **Nakanishi T**, **Fei YJ**, **Huang W**, **Ganapathy ME**, **Leibach FH**, **Ganapathy V**. Cloning of an amino acid transporter with functional characteristics and tissue expression pattern identical to that of system A. *J Biol Chem* 275: 16473–16477, 2000.

378. **Sugawara M**, **Nakanishi T**, **Fei YJ**, **Martindale RG**, **Ganapathy ME**, **Leibach FH**, **Ganapathy V**. Structure and function of ATA3, a new subtype of amino acid transport system A, primarily expressed in the liver and skeletal muscle. *Biochim Biophys Acta - Biomembr* 1509: 7–13, 2000.

379. **Suhre K**, **Shin SY**, **Petersen AK**, **Mohney RP**, **Meredith D**, **Wägele B**, **Altmaier E**, **Deloukas P**, **Erdmann J**, **Grundberg E**, **Hammond CJ**, **De Angelis MH**, **Kastenmüller G**, **Köttgen A**, **Kronenberg F**, **Mangino M**, **Meisinger C**, **Meitinger T**, **Mewes HW**, **Milburn M V.**, **Prehn C**, **Raffler J**, **Ried JS**, **Römisch-Margl W**, **Samani NJ**, **Small KS**, **-Erich Wichmann H**, **Zhai G**, **Illig T**, **Spector TD**, **Adamski J**, **Soranzo N**, **Gieger C**. Human metabolic individuality in biomedical and pharmaceutical research. *Nature* 477: 54–62, 2011.

380. **Sutterlin AM**, **Holder J**, **Benfey TJ**. Early survival rates and subsequent morphological abnormalities in landlocked, anadromous and hybrid (landlocked × anadromous) diploid and triploid Atlantic salmon. *Aquaculture* 64: 157–164, 1987.

381. **Takahashi-Iñiguez T**, **García-Hernandez E**, **Arreguín-Espinosa R**, **Flores ME**. Role of Vitamin B12 on methylmalonyl-CoA mutase activity. *J Zhejiang Univ Sci B* 13: 423–437, 2012.

382. **Takanaga H**, **Mackenzie B**, **Peng J Bin**, **Hediger MA**. Characterization of a branched-chain amino-acid transporter SBAT1 (SLC6A15) that is expressed in human brain. *Biochem Biophys Res Commun* 337: 892–900, 2005.

383. **Takanaga H**, **Mackenzie B**, **Suzuki Y**, **Hediger MA**. Identification of mammalian proline

transporter SIT1 (SLC6A20) with characteristics of classical system imino. *J Biol Chem* 280: 8974–8984, 2005.

384. **Tamai I**, **Sai Y**, **Ono A**, **Kido Y**, **Yabuuchi H**, **Takanga H**, **Satoh E**, **Ogihara T**, **Amano O**, **Izeki S**, **Tsuji A**. Immunohistochemical and functional characterization of pH-dependent intestinal absorption of weak organic acids by the monocarboxylic acid transporter MCT1. *J Pharm Pharmacol* 51: 1113–1121, 1999.

385. **Taylor JF**, **Bozzolla P**, **Frenzl B**, **Matthew C**, **Hunter D**, **Migaud H**. Triploid Atlantic salmon growth is negatively affected by communal ploidy rearing during seawater grow-out in tanks. *Aquaculture* 432: 163–174, 2014.

386. **Taylor JFF**, **Leclercq E**, **Preston ACC**, **Guy D**, **Migaud H**. Parr–smolt transformation in out-of-season triploid Atlantic salmon (Salmo salar L.). *Aquaculture* 362: 255–263, 2012.

387. **Teerijoki H**, **Krasnov A**, **Gorodilov Y**, **Krishna S**, **Mölsä H**. Rainbow trout glucose transporter (OnmyGLUT1): functional assessment in Xenopus laevis oocytes and expression in fish embryos. *J Exp Biol* 204: 2667–2673, 2001.

388. **Teramae H**, **Yoshikawa T**, **Inoue R**, **Ushida K**, **Takebe K**, **Nio-Kobayashi J**, **Iwanaga T**. The cellular expression of SMCT2 and its comparison with other transporters for monocarboxylates in the mouse digestive tract. *Biomed Res* 31: 239–249, 2010.

389. **Tesseraud S**, **Métayer Coustard S**, **Collin A**, **Seiliez I**. Role of sulfur amino acids in controlling nutrient metabolism and cell functions: implications for nutrition. *Br J Nutr* 101: 1132–1139, 2009.

390. **Thomas OP**, **Tamplin C**, **Crissey SD**, **Bossard E**, **Zuckerman A**. An evaluation of methionine hydroxy analog free acid using a nonlinear (exponential) bioassay. *Poult Sci* 70: 605–610, 1991.

391. **Tian J**, **He G**, **Mai K**, **Liu C**. Effects of postprandial starvation on mRNA expression of endocrine-, amino acid and peptide transporter-, and metabolic enzyme-related genes in zebrafish (Danio rerio). *Fish Physiol Biochem* 41: 773–787, 2015.

392. **Titus E**, **Ahearn GA**. Short-chain fatty acid transport in the intestine of a herbivorous teleost. *J Exp Biol* 135: 77–94, 1988.

393. **To VPTH**, **Masagounder K**, **Loewen ME**. SLC transporters ASCT2, B0 AT1-like, y+ LAT1, and LAT4-like associate with methionine electrogenic and radio-isotope flux kinetics in rainbow trout intestine. *Physiol Rep* 7: e14274, 2019.

394. **Topping DL**, **Clifton PM**. Short-chain fatty acids and human colonic function: Roles of resistant starch and nonstarch polysaccharides. *Physiol Rev* 81: 1031–1064, 2001.

395. **Torras-Llort M**, **Torrents D**, **Soriano-García JF**, **Gelpí JL**, **Estévez R**, **Ferrer R**, **Palacín M**, **Moretó M**. Sequential amino acid exchange across b0,+-like system in chicken brush border jejunum. *J Membr Biol* 180: 213–220, 2001.

396. **Torrents D**, **Estévez R**, **Pineda M**, **Fernández E**, **Lloberas J**, **Shi Y-BB**, **Zorzano A**, **Palacín M**, **Palacín M**, **Palacín M**. Identification and characterization of a membrane protein (y+L amino acid transporter-1) that associates with 4F2hc to encode the amino acid transport activity y+L. A candidate gene for lysinuric protein intolerance. *J Biol Chem* 273: 32437–32445, 1998.

397. **Tulli F**, **Messina M**, **Calligaris M**, **Tibaldi E**. Response of European sea bass (Dicentrarchus labrax) to graded levels of methionine (total sulfur amino acids) in soya protein-based semi-purified diets. *Br J Nutr* 104: 664–673, 2010.

398. **Tulli F**, **Messina M**, **Calligaris M**, **Tibaldi E**. Response of European sea bass (Dicentrarchus labrax) to graded levels of methionine (total sulfur amino acids) in soya protein-based semi-purified diets. *Br J Nutr* 104: 664–673, 2010.

399. **Turner RJ**. Quantitative studies of cotransport systems: model and vesicles. *J Membr Biol* 76: 1–5, 1983.

400. **Uhing MR**, **Kimura RE**. The effect of surgical bowel manipulation and anesthesia on intestinal glucose absorption in rats. *J Clin Invest* 95: 2790–2798, 1995.

401. **Ussing HH**, **Zerahn K**. Active transport of sodium as the source of electric current in the short-circuited isolated frog skin. *Acta Physiol Scand* 23: 110–127, 1951.

402. **Utsunomiya-Tate N**, **Endou H**, **Kanai Y**. Cloning and functional characterization of a system ASC-like Na+-dependent neutral amino acid transporter. *J Biol Chem* 271: 14883–14890, 1996.

403. **Van Der Flier LG**, **Clevers H**. Stem cells, self-renewal, and differentiation in the intestinal epithelium. *Annu Rev Physiol* 71: 241–260, 2009.

404. **Van Herck SLJ**, **Delbaere J**, **Bourgeois NMA**, **McAllan BM**, **Richardson SJ**, **Darras VM**. Expression of thyroid hormone transporters and deiodinases at the brain barriers in the embryonic chicken: Insights into the regulation of thyroid hormone availability during neurodevelopment. *Gen Comp Endocrinol* 214: 30–39, 2015.

405. **van Weerden EJ**, **Schutte JB**, **Bertram HL**. DL-methionine and DL-methionine hydroxy analogue free acid in broiler diets. *Poult Sci* 62: 1269–1274, 1983.

406. **Van Winkle LJ**, **Campione AL**, **Gorman JM**. Na+-independent transport of basic and zwitterionic amino acids in mouse blastocysts by a shared system and by processes which distinguish between these substrates. *J Biol Chem* 263: 3150–3163, 1988.

407. **Vargas CP**, **Hagen Ø**, **Solberg C**, **Jobling M**, **Peruzzi S**. Growth and gut morphology of diploid and triploid juvenile Atlantic cod (Gadus morhua). *Aquac Res* 47: 1459–1471, 2016.

408. **Varoqui H**, **Zhu H**, **Yao D**, **Ming H**, **Erickson JD**. Cloning and functional identification of a neuronal glutamine transporter. *J Biol Chem* 275: 4049–4054, 2000.

409. **Vázquez-Añón M**, **Bertin G**, **Mercier Y**, **Reznik G**, **Roberton JL**. Review of the chemistry, metabolism, and dose response of two supplemental methionine sources and the implications in their relative bioefficacy. *Worlds Poult Sci J* 73: 725–736, 2017.

410. **Vazquez-Anon M**, **Gonzales-Esquerra R**, **Saleh E**, **Hampton T**, **Ritcher S**, **Firman J**, **Knight CD**. Evidence for 2-hydroxy-4 (methylthio) butanoic acid and dl -methionine having different dose responses in growing broilers. *Poult Sci* 85: 1409:1420, 2006.

411. **Veillette PA**, **White RJ**, **Specker JL**, **Young G**. Osmoregulatory physiology of pyloric ceca: Regulated and adaptive changes in chinook salmon. *J Exp Zool Part A Comp Exp Biol* 303: 608–613, 2005.

412. **Verhille C**, **Anttila K**, **Farrell AP**. A heart to heart on temperature: Impaired temperature

tolerance of triploid rainbow trout (Oncorhynchus mykiss) due to early onset of cardiac arrhythmia. *Comp Biochem Physiol - A Mol Integr Physiol* 164: 653–657, 2013.

413. **Verma NE**, **Kansal VK**. Characterisation of the routes of methionine transport in mouse mammary glands. The Indian journal of medical research. *Indian J Med Res* 98: 297–304, 1993.

414. **Verrey F**. System L: Heteromeric exchangers of large, neutral amino acids involved in directional transport. *Pflugers Arch Eur J Physiol* 445: 529–533, 2003.

415. **Verrey F**, **Closs EI**, **Wagner CA**, **Palacin M**, **Endou H**, **Kanai Y**. CATs and HATs: The SLC7 family of amino acid transporters. *Pflugers Arch Eur J Physiol* 447: 532–542, 2004.

416. **Vickery HB**, **Schmidt CLA**. The history of the discovery of the amino acids. *Chem Rev* 9: 169–318, 1931.

417. **Vilella S**, **Ahearn GA**, **Cassano G**, **Storelli C**. Na-dependent L-proline transport by eel intestinal brush-border membrane vesicles. *Am J Physiol Integr Comp Physiol* 255: R648–R653, 1988.

418. **Villodre Tudela C**, **Boudry C**, **Stumpff F**, **Aschenbach JR**, **Vahjen W**, **Zentek J**, **Pieper R**. Down-regulation of monocarboxylate transporter 1 (MCT1) gene expression in the colon of piglets is linked to bacterial protein fermentation and pro-inflammatory cytokine-mediated signalling. *Br J Nutr* 113: 610–617, 2015.

419. **von Engelhardt W**, **Rechkemmer G**. Segmental differences of short-chain fatty acid transport across guinea-pig large intestine. *Exp Physiol* 77: 491–499, 1992.

420. **Wallace KN**, **Akhter S**, **Smith EM**, **Lorent K**, **Pack M**. Intestinal growth and differentiation in zebrafish. *Mech Dev* 122: 157–173, 2005.

421. **Walton MJ**, **Cowey CB**, **Adron JW**. Methionine metabolism in rainbow trout fed diets of differing methionine and cystine content. *J Nutr* 112: 1525–1535, 1982.

422. **Wang H**, **Huang W**, **Sugawara M**, **Devoe LD**, **Leibach FH**, **Prasad PD**, **Ganapathy V**. Cloning and functional expression of ATA1, a subtype of amino acid transporter A, from human placenta. *Biochem Biophys Res Commun* 273: 1175–1179, 2000.

423. **Wang H**, **Kavanaugh MP**, **North RA**, **Kabat D**. Cell-surface receptors for ecotropic murine retroviruses is a basic amino-acid transporter. *Nature* 352: 729–731, 1991.

424. **Wang W**, **Gu W**, **Tang X**, **Geng M**, **Fan M**, **Li T**, **Chu W**, **Shi C**, **Huang R**, **Zhang H**, **Yin Y**. Molecular cloning, tissue distribution and ontogenetic expression of the amino acid transporter b0,+ cDNA in the small intestine of Tibetan suckling piglets. *Comp Biochem Physiol - B Biochem Mol Biol* 154: 157–164, 2009.

425. **Wang Z**, **Allen SK**, **Wang R**. Heterozygosity and body size in triploid Pacific oysters, Crassostrea gigas Thunberg, produced from meiosis II inhibition and tetraploids. *Aquaculture* 204: 337–348, 2002.

426. **Weiss MD**, **Donnelly WH**, **Rossignol C**, **Varoqui H**, **Erickson JD**, **Anderson KJ**. Ontogeny of the neutral amino acid transporter SNAT1 in the developing rat. *J Mol Histol* 36: 301–309, 2005.

427. **White MF**, **Gazzola GC**, **Christensen HN**. Cationic amino acid transport into cultured

animal cells. I. Influx into cultured human fibroblast. *J Biol Chem* 257: 4443–4449, 1982.

428. **Wilson BYTH**, **Wiseman G**. The use of sacs of everted small intestine for the study of the transference of substances from the mucosal to the serosal surface. *J Physiol* 123: 116–125, 1954.

429. **Wilson MC**, **Jackson VN**, **Heddle C**, **Price NT**, **Pilegaard H**, **Juel C**, **Bonen A**, **Montgomery I**, **Hutter OF**, **Halestrap AP**. Lactic acid efflux from white skeletal muscle is catalyzed by the monocarboxylate transporter isoform MCT3. *J Biol Chem* 273: 15920–15926, 1998.

430. **Wongkittichote P**, **Ah Mew N**, **Chapman KA**. Propionyl-CoA carboxylase – A review. *Mol Genet Metab* 122: 145–152, 2017.

431. **Woodrow CJ**, **Burchmore RJ**, **Krishna S**. Hexose permeation pathways in Plasmodium falciparum-infected erythrocytes. *Proc Natl Acad Sci* 97: 9931–9936, 2000.

432. **Woodward AD**, **Holcombe SJ**, **Steibel JP**, **Staniar WB**, **Colvin C**, **Trottier NL**. Cationic and neutral amino acid transporter transcript abundances are differentially expressed in the equine intestinal tract. *J Anim Sci* 88: 1028–1033, 2010.

433. **Yabuta Y**, **Kamei Y**, **Bito T**, **Arima J**, **Yoneda K**, **Sakuraba H**, **Ohshima T**, **Nakano Y**, **Watanabe F**. Functional and structural characteristics of methylmalonyl-CoA mutase from Pyrococcus horikoshii. *Biosci Biotechnol Biochem* 79: 710–717, 2015.

434. **Yanagida O**, **Kanai Y**, **Chairoungdua A**, **Kim DK**, **Segawa H**, **Nii T**, **Cha SH**, **Matsuo H**, **Fukushima J ichi**, **Fukasawa Y**, **Tani Y**, **Taketani Y**, **Uchino H**, **Kim JY**, **Inatomi J**, **Okayasu I**, **Miyamoto K ichi**, **Takeda E**, **Goya T**, **Endou H**. Human L-type amino acid transporter 1 (LAT1): characterization of function and expression in tumor cell lines. *Biochim Biophys Acta - Biomembr* 1514: 291–302, 2001.

435. **Yanase H**, **Takebe K**, **Nio-Kobayashi J**, **Takahashi-Iwanaga H**, **Iwanaga T**. Cellular expression of a sodium-dependent monocarboxylate transporter (Slc5a8) and the MCT family in the mouse kidney. *Histochem Cell Biol* 130: 957–966, 2008.

436. **Yang NJ**, **Hinner MJ**. Getting across the cell membrane: an overview for small molecules, peptides, and proteins. In: *Site-Specific Protein Labeling. Humana Press, New York, NY*. 2015, p. 29–53.

437. **Yao D**, **Mackenzie B**, **Ming H**, **Varoqui H**, **Zhu H**, **Hediger MA**, **Erickson JD**. A novel system A isoform mediating Na+/neutral amino acid cotransport. *J Biol Chem* 275: 22790–22797, 2000.

438. **Ye C**, **Sutter BM**, **Wang Y**, **Kuang Z**, **Tu BP**. A metabolic function for phospholipid and histone methylation Cunqi. *Mol Cell* 66: 180–193, 2017.

439. **Yokota H**, **Coates ME**. The uptake of nutrients from the small intestine of gnotobiotic and conventional chicks. *Br J Nutr* 47: 349–356, 1982.

440. **Yoon H**, **Fanelli A**, **Grollman EF**, **Philp NJ**. Identification of a unique monocarboxylate transporter (MCT3) in retinal pigment epithelium. *Biochem Biophys Res Commun* 234: 90–94, 1997.

441. **Young JD**, **Jones SEM**, **Ellory JC**. Amino acid transport in human and in sheep

erythrocytes. *Proc R Soc London - Biol Sci* 209: 355–375, 1980.

442. **Zerangue N**, **Kavanaugh MP**. ASCT-1 is a neutral amino acid exchanger with chloride channel activity. *J Biol Chem* 271: 27991–27994, 1996.

443. **Zhang N**. Role of methionine on epigenetic modification of DNA methylation and gene expression in animals. *Anim Nutr* 4: 11–16, 2018.

444. **Zhang S**, **Saremi B**, **Gilbert ER**, **Wong EA**. Physiological and biochemical aspects of methionine isomers and precursors in broilers. *Poult Sci* 96: 425–439, 2016.

445. **Zhang S**, **Wong EA**, **Gilbert ER**. Bioavailability of different dietary supplemental methionine sources in animals. *Front Biosci* 7: 478–490, 2015.

446. **Zhi AM**, **Feng DY**, **Zhou XY**, **Zou SG**, **Huang ZY**, **Zuo JJ**, **Ye H**, **Zhang CM**, **Dong ZM**, **Liu Z**. Molecular cloning, tissue distribution and segmental ontogenetic regulation of b0,+ amino acid transporter Lantang pigs. *Asian-Australasian J Anim Sci* 21: 1134–1143, 2008.

447. **Zhou QC**, **Mai KS**, **Tan BP**, **Liu YJ**. Partial replacement of fishmeal by soybean meal in diets for juvenile cobia (Rachycentron canadum). *Aquac Nutr* 11: 175–182, 2005.

448. **Zimmermann B**, **Mosenthin R**, **Rademacher M**, **Lynch PB**, **Esteve-Garcia E**. Comparative studies on the relative efficacy of DL-methionine and liquid mechionine hydroxy analogue in growing pigs. *Asian-Aust J Anim Sci* 18: 1003–1010, 2005.

449. **Zou SG**, **Zhi AM**, **Zhou XY**, **Zuo JJ**, **Zhang Y**, **Huang ZY**, **Xu PW**, **Feng DY**. Molecular cloning, segmental distribution and ontogenetic regulation of cationic amino acid transporter 2 in pigs. *Asian-Australasian J Anim Sci* 22: 712–720, 2009.